UNIVERSITY OF SOUTHERN QUEENSLAND

BEHAVIOUR OF SHEAR DAMAGED REINFORCED CONCRETE BEAMS STRENGTHENED WITH EXTERNAL POST-TENSIONING AND CLAMPING

A Dissertation Submitted by

Thuraichamy Guganesan Suntharavadivel
B.Sc.Eng. (*Peradeniya*), M.Eng. (*Tokyo*)

for the award of

Doctor of Philosophy

2008

To my father who only carried a dream of
his loving children's future with him.

ABSTRACT

Over the last few decades, there has been a rapid increase in the volume and weight of heavy vehicles using national road networks. More than half of the bridges around the world are over forty years old. The deterioration of these existing bridges due to increased traffic loading, progressive structural aging, and reinforcement corrosion from severe environmental conditions has become a major problem in most countries. Several techniques have been used to strengthen these structures around the world. External post-tensioning is one of the widely used strengthening techniques in many countries due to its advantages over other methods. Furthermore, flexural strengthening using external post-tensioning has become a well established technique over the past few decades. However, when external post-tensioning is used to strengthen shear damaged reinforced concrete members, unlike flexural damage, the efficiency is significantly reduced by existing shear cracks.

This research study was carried out to investigate the behaviour of reinforced concrete beams with existing shear cracks when strengthened by external means. The study consists of two parts: experimental investigations of reinforced concrete beams with different parameters and numerical analysis of reinforced concrete beams using simplified theoretical formulation and finite element modelling.

To study the behaviour of shear damaged concrete beams, two different strengthening techniques, namely external post-tensioning and external clamping, were used. In addition to the strengthening, the effect of cracks on the behaviour of reinforced concrete beams was investigated by repairing such cracks using epoxy resin injection. Experimental results showed that existing shear cracks have a substantial effect on the member capacity when strengthened by external post-tensioning. Although there are concerns about the practical applications of external clamping, the experimental results suggest that external clamping could be a more effective technique than external post-tensioning to reduce the effect of existing shear cracks on the behaviour of concrete beams. Furthermore, proper repair of the shear cracks could significantly reduce their impact.

In the numerical analysis, a simplified mathematical approach was developed to estimate the capacity of shear damaged reinforced concrete beam by expanding the modified compression field theory (MCFT). In addition to the simplified theoretical formulation, a finite element model was developed using the commercial finite element package, Abaqus. Comparison between the predicted behaviour using finite element analysis (FEA) and the experimental data illustrated that the developed finite element model could be used as a reliable tool to estimate the capacity of shear damaged reinforced concrete beams. A parametric study was conducted to investigate the effect of different parameters such as concrete strength, amount of shear reinforcement and crack width, using the developed finite element model. From the numerical study, it was concluded that the simplified approach developed in this study can be used as a reliable and conservative technique to predict the member capacity of a cracked reinforced concrete beam strengthened by external means. Furthermore, the parametric study showed that crack width is the most sensitive parameter that affects the capacity of a cracked beam strengthened by external post-tensioning.

Based on this research study it can be concluded that existing shear cracks have a substantial effect on the behaviour of reinforced concrete beams strengthened by external post-tensioning. The simplified mathematical approach developed in this study can be used to estimate the capacity of such beams.

CERTIFICATION OF DISSERTATION

I certify that the ideas, experimental work, results, analysis, software and conclusions reported in this dissertation are entirely my own effort, except where otherwise acknowledged. I also certify that the work is original and has not been previously submitted for any other award, except where otherwise acknowledged.

_____ _____

Signature of Candidate Date

ENDORSEMENT:

_____ _____

Signature of Supervisor(s) Date

_____ _____

Signature of Supervisor(s) Date

_____ _____

Signature of Supervisor(s) Date

ACKNOWLEDGEMENTS

Completion of this dissertation would not be possible without genuine support and help from a number of people to whom I wish to express my sincere gratitude.

I would like to acknowledge the advice, guidance and support given by my supervisors Associate Professor Karu Karunasena, Associate Professor Thiru Aravinthan and Dr Santhi S Santhikumar during this research project.

I would like to express my special thanks to my supervisors Associate Professor Karu Karunasena and Dr Santhi S Santhikumar for their invaluable patience and persistence in helping me complete this dissertation. Without your support it may not have been possible for me to complete this research project. – Thank you very much. I am also thankful for the financial support provided by Associate Professor Thiru Aravinthan through a University of Southern Queensland research grant to conduct experimental work during this research project.

I would like to also acknowledge the contribution and support of Dr. David Rogers and Dr. Stephen Liang during various stages of this research project. I thank Associate Professor David Buttsworth for his genuine support to help me to complete this dissertation in time.

Without the financial support of the Australian Government and the University of Southern Queensland who offered me the International Postgraduate Research Scholarship (IPRS) I would not have been able to undertake this study.

Sincere thanks are also due to the Engineering technical staff Glen Bartkowski, Mohan Trada, Daniel Eising, Wayne Crowell, Adrian Blokland and Martin Geach for their kind support while I was to conducting experiments during this project. I extend my thanks to the former undergraduate students Steven Luther, Paul Bolger and Todd Whittaker for their support during the experimental program.

Ms. Ruth Hilton helped me with my written English language expression. I am grateful for her time and support.

My thanks go to all the staff and research students of the Faculty of Engineering & Surveying who helped me in various ways during my stay at the University of

Southern Queensland. I also cannot forget my friends and their families, who are outside the university, for their kindness and support during my stay in Toowoomba.

I would like to thank my mother and other family members for their encouragement and support during my studies. Finally, my sincere thanks go to my wife, Mathura, and our little daughter, Abenaya, for their love, patience and support throughout this study.

TABLE OF CONTENTS

LIST OF FIGURES

LIST OF TABLES

NOTATIONS

A	=	Cross section area of the section
A_g	=	Gross area of a concrete cross section
A_p	=	Cross sectional area of prestressing steel
A_{pt}	=	Cross sectional area of prestressed tendons
A_{st}	=	Cross sectional area of tension reinforcement
A_{sx}	=	Cross sectional area of longitudinal reinforcement steel
A_{sv}	=	Cross sectional area of shear reinforcement (AS3600: 2001)
A_v	=	Cross section area of shear reinforcement (ACI 318-02)
a	=	Maximum aggregate size
b	=	Width of the cross section
b_v	=	Effective width of web for shear (equal to width, b, for rectangular cross section) (AS3600: 2001)
b_w	=	Effective width of web for shear (equal to width, b, for rectangular cross section) (ACI 318-02)
d	=	Distance from the extreme compressive concrete fibre to the centroid of the outer most layer of tensile reinforcement (ACI 318-02)
d_o	=	Distance from the extreme compressive concrete fibre to the centroid of the outer most layer of tensile reinforcement (AS3600: 2001)
E_c	=	Modulus of elasticity of the concrete
f_{c1}	=	Average principal tensile stress in concrete
f_{c2}	=	Average principal compressive stress in concrete
f_{cr}	=	Cracking strength of the concrete
f_{co}	=	Elastic range (compressive stress) of the concrete (Abaqus input)
f_{ct}	=	Elastic range (tensile stress) of the concrete (Abaqus input)
f_{cu}	=	Ultimate compressive stress of the concrete (Abaqus input)
$f_{c,allowable}$	=	Permissible compressive stress in concrete
f_c'	=	Characteristic compressive strength of the concrete
f_l	=	Average stress in the longitudinal reinforcing bar
f_p	=	Average stress in the prestressing steel
$f_{t,allowable}$	=	Permissible tensile stress in concrete
f_v	=	Average stress in the stirrups (shear reinforcement)
f_{sy}	=	Yield strength of shear reinforcing steel

f_y	=	Yield strength of longitudinal reinforcing steel
G	=	Reduced shear modulus of cracked concrete
G_c	=	Elastic shear modulus of uncracked concrete
jd	=	Flexural lever arm (the distance between the compressive reinforcement and tensile reinforcement)
k_w	=	Multiplying factor for average crack width
M	=	Applied moment
M_u	=	Ultimate moment capacity
N_u	=	Ultimate axial force
P	=	Prestressing force
P_{cr}	=	Cracking load
P_u	=	Ultimate load
P_v	=	Vertical component of prestressing force
$P_{v,ext}$	=	Force in the external clamping rods within the crack zone
s	=	Centre -to-centre spacing of shear reinforcement
V	=	Shear capacity of the section
V_c	=	Nominal shear strength provided by concrete
V_{dec}	=	Shear force at the decompression moment
V_s	=	Nominal shear strength provided by shear reinforcement
V_u	=	Ultimate shear force
V_{uc}	=	Ultimate shear strength of the concrete
V_{us}	=	Contribution by shear reinforcement to the ultimate shear strength
v	=	Shear stress action along the section
v_{ci}	=	Shear stress along the shear crack plane
w	=	Shear crack width
w_{max}	=	Maximum crack width
Z	=	Elastic section modulus
$\left.\begin{array}{l}\beta_1\\\beta_2\\\beta_3\end{array}\right\}$	=	Multiplying factors for determining V_{uc}
γ	=	Multiplying factor
ε_o	=	Strain at the peak stress in a uniaxial compression test
ε_1	=	Average principal tensile strain in concrete
ε_2	=	Average principal compressive strain in concrete
ε_c	=	Strain in concrete

ε_c	=	Direct strain across the crack (Equation 5.19)
ε_{max}	=	Maximum strain in concrete
ε_{sy}	=	Yielding strain of steel
ε_{to}	=	Linear range tensile strain of steel
ε_{tu}	=	Ultimate (tensile) strain in concrete
$\varepsilon_c{'}$	=	Strain corresponding to $f_c{'}$
θ	=	Angle between the concrete compression strut and the longitudinal axis of the member
θ_v	=	Angle between the concrete compression strut and the longitudinal axis of the member
ρ_{sx}	=	Reinforcement ratios in the X direction
ρ_{sy}	=	Reinforcement ratios in the Y direction
ρ_w	=	Flexural steel reinforcement ratio
σ_c	=	Compressive stress in concrete
σ_{ci}	=	Compressive stress acting on the crack
σ_{cx}	=	Axial stresses in the concrete in the X direction
σ_{cy}	=	Axial stresses in the concrete in the Y direction
σ_{sx}	=	Axial stresses in the steel in the X direction
σ_{sxcr}	=	Axial stresses in the steel in the X direction at the crack face
σ_{sy}	=	Axial stresses in the steel in the Y direction
σ_{sycr}	=	Axial stresses in the steel in the Y direction at the crack face
σ_x	=	Average stresses in the X direction calculated at a material point in reinforced concrete
σ_{xy}	=	Average shear stress calculated at a material point in reinforced concrete
σ_y	=	Average stresses in the Y direction calculated at a material point in reinforced concrete
σ_{yx}^{yield}	=	Yield stress in the X direction
σ_{yy}^{yield}	=	Yield stress in the Y direction
φ	=	Reduction factor

ABBREVIATIONS

ACI   -   American Concrete Institute

AS   -   Australian Standard

ASCE   -   American Society of Civil Engineers

FEA   -   Finite Element Analysis

FEM   -   Finite Element Method

FRP   -   Fibre Reinforced Plastic

HLA   -   High-performance Lightweight Aggregate

MCFT   -   Modified Compression Field Theory

RC   -   Reinforced Concrete

R/F   -   Reinforcement

USQ   -   University of Southern Queensland

Chapter 1
INTRODUCTION

1.1   General

The concrete repair, protection, and strengthening industry is driven by deterioration of, damage to, and defects in concrete structures along with changes in the use of concrete and the development and enhancement of code requirements. Each year large amounts of concrete are used in every country around the world. Much of the concrete is custom-made for each job, using local materials of varying quality. Designs that are not standard and accelerated construction processes sometimes result in quality being sacrificed in the interest of meeting a schedule. Such factors, in addition to general causes such as increase in loads and environmental conditions, may also increase or accelerate the deterioration of concrete structures.

The annual cost to owners for repair, protection, and strengthening is estimated to be between $18 to $21 billion in the U.S. alone (Emmons and Sordyl 2006). The explosive growth of the repair industry in the past 25 years has resulted in the need for many improvements in areas such as materials, design practices, installation procedures and education. These improvements are needed to increase service life and reduce costs and conflicts. They are of considerable importance when a damaged concrete structure needs to be strengthened to increase its capacity to meet current loading requirements.

1.2   Nature of Cracks in Reinforced Concrete Members

A crack will form in concrete when the principal tensile stress at a location reaches the cracking strength of the concrete. In general the crack direction and orientation will depend on the loading and support condition. Cracks are generally classified as flexural cracks or shear cracks depending on their orientation and direction. When loading is applied to a member, flexural cracks are, in general, generated perpendicular to the axis of bending (or parallel to the loading direction) while shear cracks are generated with an inclination to the loading direction (Figure 1.1).

(a) Flexural cracks
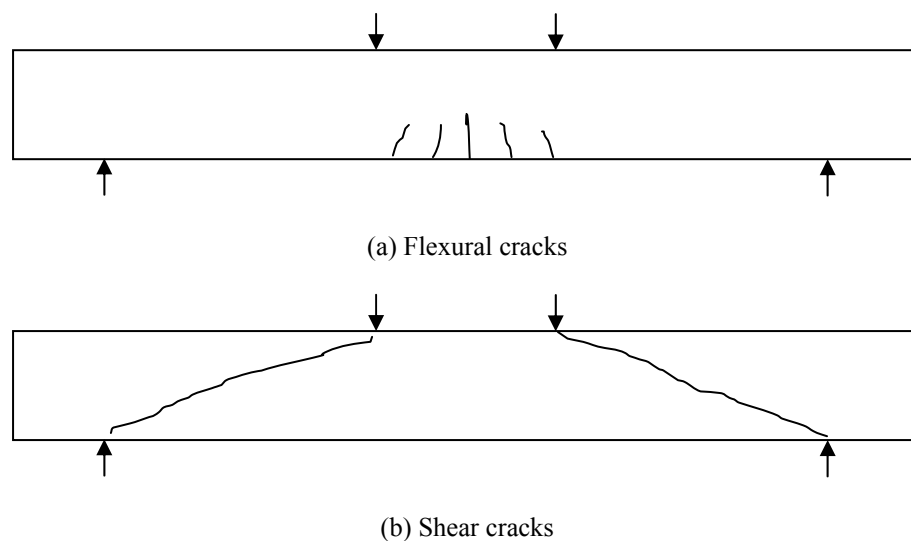
(b) Shear cracks

Figure 1.1. Flexural and shear cracks in a member

This PhD research project aims to investigate the effect of existing shear cracks in a reinforced concrete member when strengthened by external means such as post-tensioning or external clamping and the effectiveness of repairing such cracks.

1.3   Background

Over the last few decades, there has been a rapid increase in the volume and weight of heavy vehicles using road networks. Coupled with this is the fact that more than 50% of the bridges worldwide are over forty years old (Aravinthan and Suntharavadivel 2007). The deterioration of these existing bridges due to increased traffic loading, progressive structural aging, and reinforcement corrosion from severe

environmental conditions has become a major problem in most countries. Furthermore, the number of heavy trucks and the traffic volume on these bridges have resulted in extreme loading conditions that exceed their original design parameters. In some cases, such extreme loading has resulted in cracks that require urgent repair and rehabilitation.

There are number of strengthening techniques in use around the world including external post-tensioning and the use of fibre composites. External post-tensioning is considered to be one of the most appropriate techniques for strengthening or rehabilitating existing structures. Over many years, extensive research has been conducted on the flexural behaviour of reinforced concrete members strengthened by external post-tensioning (Harajli 1993; Moon and Burns 1997a; Moon and Burns 1997b; Naaman and Alkhairi 1991; Tan et al. 2001). However, there has been relatively limited research on the shear strengthening of concrete members using external post-tensioning (Tan and Ng 1998). While some studies claim that the shear capacity of reinforced concrete beams could be improved by external post-tensioning, the effects of existing cracks have not been evaluated in most of the previous studies (Tan and Ng 1998; Tan and Tjandra 2003).

Some of the previous studies conducted at the University of Southern Queensland suggested that existing shear cracks may have a substantial effect on the member capacity of a reinforced concrete member especially when it is strengthened by external post-tensioning (Aravinthan et al. 2004; Snelling 2003; Woods 2004). Preliminary investigation by these researchers revealed that repair of cracks by epoxy injection could potentially enhance the shear strength of structures when strengthened by external post-tensioning. Even though shear crack repair prior to strengthening of reinforced concrete beams was recommended by some recommendations in the literature (American Concrete Institute 2003), there was no clear definition on the criteria for repair or the technique for repair. It was not specified which cracks (width) need to be repaired and the gain of member capacity with and without repair was not detailed. The knowledge gap that exists in

understanding the behaviour of structures with existing shear cracks forms the motivation for this research.

1.4 Objective of the Research

1.4.1 Main Objective of the Research

The main objective of this research was to investigate the effect of existing shear cracks in a reinforced concrete member when strengthened by external means such as post-tensioning or external clamping. The effectiveness of epoxy injection for repairing existing shear cracks is also further investigated.

The project was conducted with a view to proposing a simplified approach to estimate the capacity of shear damaged reinforced concrete members strengthened by external means. It also aimed to investigate the influence of various parameters such as concrete strength, post-tensioning force and crack width on the capacity of cracked beams strengthened by external post-tensioning.

1.4.2 Specific Objectives

In order to achieve the main objective, the following specific objectives were established:

- Contribute to the understanding of the mechanism of shear cracks and how they affect the behaviour of reinforced concrete member strengthened by external post-tensioning.

- Review the current state-of-art experimental and theoretical developments related to existing shear cracks in a reinforced concrete member.

- Investigate the behaviour of existing shear crack in a reinforced concrete member through experiments. Conduct a set of large scale experiments with various test parameters including amount of shear reinforcement and concrete strength.

- Study the efficiency of epoxy resin repairs in eliminating the effect of existing shear cracks in a reinforced concrete member.

- Propose simplified approach to estimate the capacity of shear damaged reinforced concrete members strengthened by external means.

- Model the behaviour of such cracks using finite element method. Use the model to perform a parametric study to gain a better understanding of the contribution of various parameters in eliminating the effect of existing shear crack.

1.4.3 Research Significance

To determine the retrofitting technique for a shear damaged reinforced concrete beam, the effect of existing shear cracks must be known. However, the influence of existing shear cracks on the behaviour of externally post-tensioned (or clamped) members has not been adequately investigated. Therefore, an experimental and finite element study was conducted to study the influence of existing shear cracks on the behaviour of the reinforced concrete beams strengthened by external post-tensioning. Moreover, the effect of epoxy injection in the repair of existing cracks when strengthened by external post-tensioning or clamping done through a systematic approach contributes significantly to the knowledge gap that exist in this area.

1.5   Research Limitations

Due to the complexity and magnitude of this project, a number of constraints were applied to this study in order to retain appropriate focus. These constraints are as follows:

- The dimensions of the experimental specimens were chosen to suit the capacity of available testing infrastructure in the civil engineering laboratory of the University of Southern Queensland. Only one beam geometry was investigated.

- Testing was limited to four-point bending with simple support at each end and two equal point loads applied at third points of the span. All experiments were performed at ambient temperature.

- Only straight tendons were used for post-tensioning in the experiments due to the limitation of laboratory resources.

- Loading was limited to a monotonically increasing load with a constant loading rate. The effect of cyclic loading and other long-term effects of the beam were not investigated.

- For numerical modelling, an epoxy resin with a higher compressive and tensile strength than concrete was used.

- Epoxy resin was modelled as a fully elastic material during loading.

- No temperature effect on the epoxy resin was considered in the numerical modelling.

1.6   Structure of the Thesis

This thesis is divided into seven chapters including the introduction chapter. A brief summary of each chapter is outlined below.

Chapter 1, the current chapter, gives a brief outline of the background and significance of the research project. It also gives the objective of the research followed by the structure of the dissertation.

In **Chapter 2**, a comprehensive literature review related to this research study is presented. A brief introduction to the application of external post-tensioning, different conceptual models and shear design procedures including methods to evaluate the shear failure, cracks in a reinforced concrete member are summarised in this chapter. In addition, a brief background and history of the development of theoretical and experimental investigations are presented. Moreover, a brief

overview of current standards related to predicting shear capacity of a reinforced concrete member and its shortcomings are also discussed in the chapter.

To study the behaviour of existing shear cracks in a reinforced concrete member, sixteen beams were tested in the civil engineering laboratory of the University of Southern Queensland. Details of the experimental program methodology are given in **Chapter 3**. Details of test specimens, material properties, instrumentation, and testing procedures are briefly explained in this chapter.

Results obtained from the experimental program are presented in **Chapter 4**. Brief discussions on the effect of existing shear cracks in a reinforced concrete member, the influence of various parameters including quantity of shear reinforcement and concrete strength on the behaviour of such cracks are also presented in the Chapter 4. A comparison of experimental results with Australian (Standards Australia 2001) and American (American Concrete Institute 2002) code predicted values are also given in this chapter.

Chapter 5 details the theoretical background and modelling of existing shear crack behaviour in a reinforced concrete member that is strengthened by external prestressing. A simplified mathematical approach to estimate the shear capacity of a shear damaged reinforced concrete beam is explained. This is followed by the techniques and material constitutive models used in the finite element modelling using the commercial finite element software, Abaqus (Abaqus Inc. 2006).

Results from the numerical analysis including the simplified mathematical approach and the parametric study are presented in **Chapter 6** together with discussion based on the comparison of experimental and numerical results.

Finally, **Chapter 7** presents the general and specific conclusions of this research study followed by recommendations for future research in this area.

Further information on the experimental results, material data and other relevant information are given in Appendices.

Some of this research has been published or is being published in journals and peer-reviewed conferences. Details are provided below:

1. Thiru Aravinthan and **T.G Suntharavadivel** (2007), "Effect of Existing Shear Damage on Externally Post Tensioned Repair of bent Caps" *ASCE Journal of Structural Engineering*, vol. 133 no. 11, pp. 1662-1669

2. **T.G. Suntharavadivel** and Thiru Aravinthan (2007), "Analytical Studies on Externally Post Tensioned Concrete Girders with Existing Shear Cracks" Concrete Institute of Australia 23rd Biennial Conference, Adelaide Australia (peer-reviewed)

3. **T.G. Suntharavadivel** and Thiru Aravinthan (2007), "Strengthening of Shear Damaged RC Beam with External Clamping" 4th International Structural Engineering and Construction Conference (ISEC-4), Melbourne Australia (peer-reviewed)

4. **T.G. Suntharavadivel**, Thiru Aravinthan and Steven Luther (2006), "Shear Strengthening of Cracked RC Beam Using External Post-Tensioning" 19th Australasian Conference on the Mechanics of Structures and Materials (ACMSM19)*,* Christchurch New Zealand (peer-reviewed)

5. **T.G. Suntharavadivel** and Thiru Aravinthan (2006), "Effect of Existing Cracks in Concrete Bridge Members Strengthened by External Post-Tensioning" Second International fib Conference*,* Naples Italy (peer-reviewed)

6. **T.G. Suntharavadivel** and Thiru Aravinthan (2005), "Overview of External Post-Tensioning in Bridges" Southern Engineering Conference 2005, Toowoomba Australia (peer-reviewed)

Most of above publications are freely available through the *ePrints* collection (http://eprints.usq.edu.au/) of the University of Southern Queensland.

Chapter 2
LITERATURE REVIEW

This chapter outlines the state-of-art of the research project. It gives a brief overview of external post-tensioning and its applications in structural systems. It also provides a basic explanation of shear cracks in a reinforced concrete member and the mechanism of shear transfer across shear cracks. Some discussion on the application of external post-tensioning as a strengthening technique for reinforced concrete members with un-repaired shear cracks is presented.

2.1   Introduction to External Post-Tensioning

External post-tensioning is one of the latest developments in prestressed concrete technology. It refers to a prestressing technique where the prestressing tendons are placed outside the concrete section and the prestressing force is transferred to the concrete by means of end anchorages, deviators (see Figure 2.1) and saddles. The application of the external post-tensioning in strengthening leads to a new structural system where the behaviour is different from the original structural member (Tan and Ng 1998). Because of its practical advantages, external post-tensioning is becoming popular in the construction industry.

External post-tensioning and plate bonding are the two methods that proving to be very useful in increasing the capacity of short and medium span bridges. However,

external post-tensioning has many advantages over other strengthening techniques. Some of the advantages include:

- economical construction;

- easy monitoring and maintenance;

- easier tendon layout, placement and easier construction and compaction;

- application in wide a range of the bridges (small, medium and long span bridges).

Figure 2.1 shows a typical layout of an externally post-tensioned box girder bridge. Generally, the external tendons are placed in the hollow section of the box girder. The prestressing force is transferred to the beam through end anchorages and deviators.
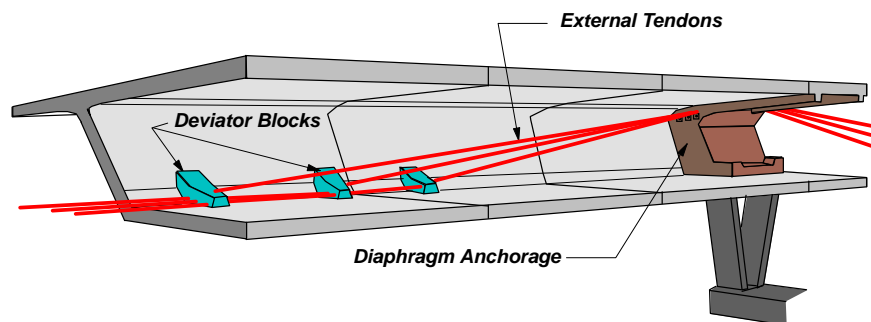
Figure 2.1. Typical layout of an externally post-tensioned box girder bridge
Source: Aravinthan (1999)

Strengthening by external post-tensioning is simply the application of an axial load combined with a hogging bending moment to improve the flexural and/or shear capacity of a structural member. This method can also be used to improve serviceability. For example, the increased stiffness provided by external post-tensioning can reduce in-service deflections and vibrations. The stress range at a critical location can also be reduced, thus improving fatigue performance. The presence of large deflections or sag in a bridge can be reduced or removed. It is also possible to use post-tensioning to increase the strength of a structural member. For example, the objective might be to provide continuity across a support, i.e., change a series of simply supported spans to a continuous one. It can also be used to provide

continuity across an unsupported joint, for example, across the joint between two cantilever spans (Daly and Witarnawan 2000).

Post-tensioning of bridges has been in use since the 1950s and there are many examples throughout the world. In most situations, the load is applied through prestressing cables, either single or grouped strands. In some applications, the stress is applied through high tensile bars. In a few cases, the stress is applied using more unconventional techniques. For example, stress in a tendon can be developed by anchoring a straight tendon in place and imposing a deflection at mid-span. The deflection is then retained by fixing the deflected point. Prestress can also be developed by applying a load to impose a deflection in the deck prior to anchoring the tendons or bars. An extension on the use of external tendons is to place them at large eccentricities. This is possible only when external post-tensioning is used, since the tendons need not be arranged within the concrete section (Figure 2.2).
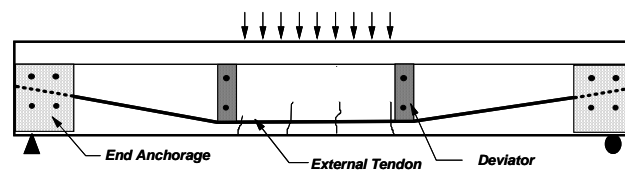
(a) Conventional tendon placement
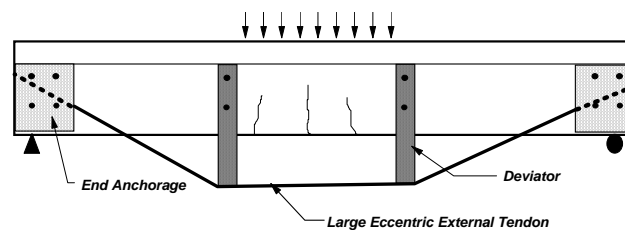
(b) Tendon with large eccentricity

Figure 2.2. Possible tendon placement in external post-tensioning

2.1.1 External Post-Tensioning in New Bridge Construction

External post-tensioning is used in many countries in the construction of new bridges. The world's first externally post-tensioned concrete bridge was built in Germany in 1936 (Virlogeux 1993). The main span of the first bridge was 25.2 m. Since then, the design and application has changed and currently external post-tensioning is used in large span modern bridges. However, the application of external post-tensioning was limited until the late 1970s due to some serious shortcomings with the external tendons. The major issue was the corrosion of the external steel tendons which were inadequately protected.

External post-tensioning was developed and applied in many countries, particularly for new bridges, during the 1980s after the invention of high performance steel with adequate protection against corrosion. The development of fibre reinforced plastic (FRP) tendons led to a remarkable increase in the use of external post-tensioning in bridges. Because an external post-tensioning system is simpler to construct and easier to inspect and maintain than an internal tendon system, it has recently been proposed in the construction of segmental bridges as well (Miyamoto et al. 2000; Rabbat and Sowlat 1987). Some recent applications of external post-tensioning in new bridges are listed below.

- Segmental viaduct (Figure 2.3)
- Girder Bridges with large eccentricity (Figure 2.4)
- Composite bridges (Figure 2.5)
- High-performance lightweight aggregate concrete bridges (Figure 2.6)

(a) Shigenobu river bridge, Japan
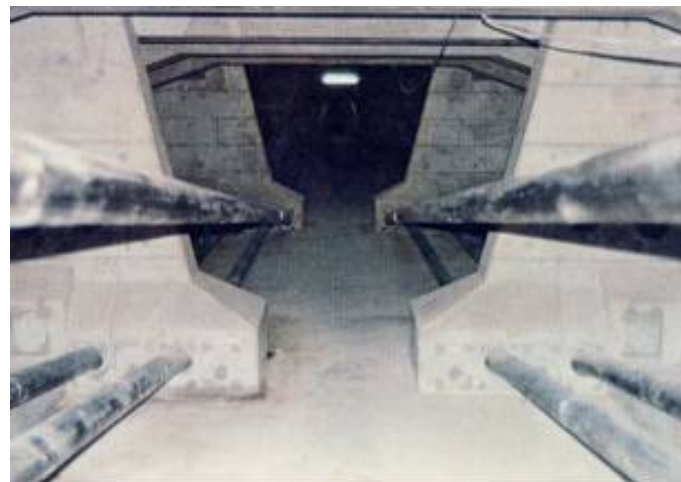
(b) External tendons inside box-girder

Figure 2.3. Segmental viaduct with external post-tensioning
Source: PS Corporation, Japan

Figure 2.4. Pedestrian bridge with large eccentricity post-tensioning tendons
Source: DPS Bridge Works, Tokyo, Japan

(a) Completed view of Shirasawa bridge, Japan
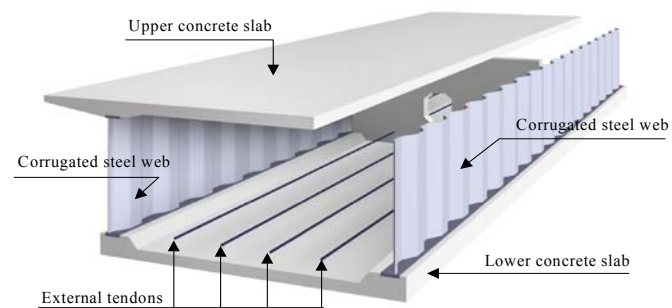
(b) Typical section of a prestressed concrete bridge with corrugated webs

Figure 2.5. Composite bridges
Source: DPS Bridge Works, Tokyo, Japan

(a) Shirarika river bridge made of HLA concrete   (b) Transparent sheaths used for inspection of grouting
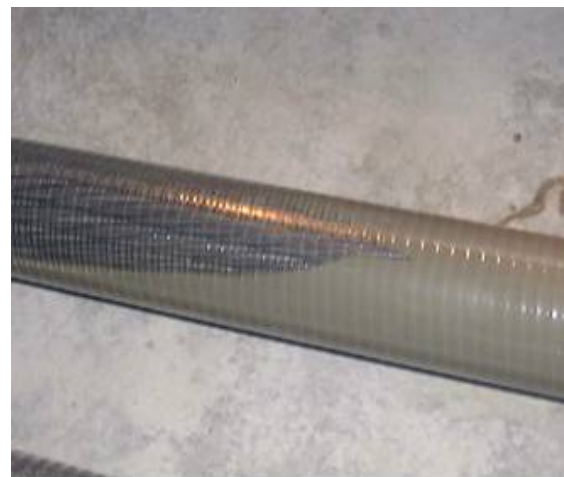
Figure 2.6. High-performance lightweight aggregate (HLA) concrete bridges
Source: DPS Bridge Works, Tokyo, Japan

2.1.2 External Post-Tensioning in Strengthening of Existing Bridges

While new bridges are constructed using external post-tensioning as discussed in the previous section, over the last two decades external post-tensioning has also been considered as one of the most powerful techniques for structural strengthening and rehabilitation. External post-tensioning is preferred for bridge strengthening projects due to its advantages which include:

- minimal disruption to traffic;

- low weight of the additional components;

- speed and short duration of construction;

- low costs involved;

- future re-stressing operations can be carried out quickly and conveniently (if required).

The following projects are some examples of the application of external post-tensioning in strengthening bridges (Figure 2.7, Figure 2.8 and Figure 2.9).

(a) Condet bridge, Indonesia   (b) Kemlaka Gede bridge, Indonesia
Figure 2.7. Flexural strengthening of bridge girders
Source: A method for increasing the capacity of short & medium span bridges (Daly and Witarnawan 2000)

a) Morrison bridges headstock, USA
Source: http://www.co.multnomah.or.us/

(b) Tenthill Creek bridge, QLD

Figure 2.8. Shear strengthening of bridge girders

Figure 2.9. Rehabilitation with lightweight concrete – Puttesund Bridge, Norway
Source: http://gallery.kak.net/

2.2   Application of External Post-Tensioning to Strengthen RC Members

External post-tensioning is a well established strengthening technique for reinforced concrete members in flexure (Harajli et al. 1999; Miyamoto et al. 2000; Moon and Burns 1997a; Moon and Burns 1997b; Pisani 1999). However, the studies on the shear failure and post cracking behaviour of externally prestressed reinforced concrete members are limited. In 1993 Tan and Naaman (1993) developed a strut-and-tie model for externally prestressed concrete members. It simplified the analysis of such concrete members and explained the possible failure modes of the member. This model was widely adopted by many researchers and included in codes of practice (ACI 318-02) to predict the behaviour of externally post-tensioned reinforced concrete members. Even though the strut-and-tie model could be effectively used to analyse reinforced concrete beams strengthened by external post-tensioning, this model could not be directly used to predict the post shear cracking behaviour of a reinforced concrete member strengthened by external post-tensioning.

2.2.1 Flexural Strengthening Using External Post-Tensioning

Flexural strengthening of reinforced concrete members using external post-tensioning has been investigated by many researchers. This section briefly summarises some of the significant investigations carried out on flexural strengthening of reinforced concrete structures using external post-tensioning with a special focus on the effect of existing flexural cracks.

A series of experimental studies were conducted by Harajli to investigate the effect of existing flexural cracks in externally prestressed reinforced concrete beams (Harajli 1993; Harajli et al. 2002). He tested 16 reinforced concrete beams in total. Each specimen had a 127×229 mm rectangular cross section and was simply supported over a 3000 mm span. Two external prestressing profiles were used for each different type of specimen: a straight horizontal tendon profile and a single-point draped tendon profile with a saddle (deviator) at mid span. To simulate actual conditions of flexural members, large fatigue deformations were induced in the beams, prior to the external post-tensioning, by subjecting them to between 5000 and 10000 cycles of large amplitude fatigue loading at constant load range, which varied from 30% to 80% of the calculated ultimate flexural capacity of the specimen. All specimens were loaded in four-point bending using two symmetrical concentrated loads applied at third-points of the span length. To ensure the flexural failure of the beams, enough shear reinforcement was provided to prevent shear cracks. The experimental results showed that the external post-tensioning increased the flexural resistance of the specimens by up to 146%. Harajli also observed that existing cracks were reduced in width or completely closed by the external post-tensioning. Therefore, the existing flexural cracks had no significant effect on the capacity of the reinforced concrete beams strengthened by external post-tensioning.

Aravinthan et al. reported results of another experimental study on the behaviour of flexural cracks in a reinforced concrete member strengthened by external post-tensioning (Aravinthan et al. 2004). Their experimental program consisted of three model cantilever specimens with a rectangular cross section throughout the whole length of 4500 mm. All three specimens were tapered shaped cantilevers with a

rectangular cross section of 300×250 mm at the toe end and 400×250 mm at the heel end. The main variable in their study was the effective prestressing force. Two different prestressing forces of 150 kN and 300 kN were used to strengthen the cracked specimens. From the study they concluded that reinforced concrete members such as headstocks can be effectively strengthened in flexure by external post-tensioning and the strength could be increased by as much as 60%. They also noted that the strength increase was proportional to the amount of post-tensioning force applied and a significant reduction in the ductile behaviour occurred when prestressing was applied.

2.2.2 Shear Strengthening Using External Post-Tensioning

The report published by ACI-ASCE (ASCE-ACI Committee 445 on Shear and Torsion 1998) gives a brief historical background of the research and development related to the shear failure of reinforced concrete members.

In this section, experimental works focussed on shear cracked reinforced concrete beams strengthened by external post-tensioning are reviewed.

Collins and Roper (1990) evaluated various methods for shear repair of reinforced concrete beams by testing twenty beams with dimensions of 75×150×1800 mm, shear span-to-depth ratio equal to 2.8 and without shear reinforcement in critical region. The beams were point-loaded at the mid-span in order to initiate a shear crack (except the control beam). The initial crack on one side was held at a constant width using a clamping plate and loading was continued until a major shear crack developed on the other side. Then the shear cracks were repaired. Repair techniques included epoxy injection, vertical post-tensioning, stitching with 4 mm reinforced steel and bonding external steel shear reinforcement in a 'U-shape' with epoxy resin. In all cases, the strength and ductility were significantly increased compared with the control beam. However, in most cases a brittle shear failure was observed in the beams repaired using the stitching and epoxy injection techniques. The post-tensioning tests resulted in flexural and ductile failure modes.

Teng et al. (1996) reported an experimental study on the performance of strengthened pre-cracked concrete deep beams under shear. They introduced vertical clamping to reduce the effect of the shear cracks in the prestressed concrete and tested a total of 18 prestressed and non-prestressed deep concrete beams to failure, followed by strengthening and re-testing to failure for a second time. The beams had cross sectional dimensions of 150 to 160 mm width and 600 mm depth. Spans of the beams were 1800 and 1200 mm for beams having span-to-depth (a/d) ratios of 3.0 and 2.0 respectively. They found that the vertical clamping technique significantly increased the shear capacity and eliminated the effect of the crack.

A similar technique was tested independently by Khaloo (2000) using 24 reinforced concrete beams with dimensions of 80×150×1800 mm. These beams were tested under different test variables. These included concrete compressive strength, shear span-to-effective depth ratio (a/d), longitudinal tensile reinforcement, level of post-tensioning, presence of shear reinforcement, use of external clamping and presence of shear cracks. Beams were loaded in four-point bending. Test results showed that in the presence of post-compression stress, as low as $0.04\,f'_c$, for strengthening, shear strength increased significantly and the mode of failure of the beams changed from brittle shear to ductile bending (where f'_c denotes the concrete strength). Also, for this level of post-compression, ductile failure was dominant and the impact of all other parameters was limited. Even though Khaloo successfully attempted to identify a technique which could reduce the effect of shear cracks in a reinforced concrete beam, it should be noted that the specimen sizes were notably small. In a shear failure of reinforced concrete beams, size plays a major role in determining the capacity of the beam. Bazant and Yu (2005a, 2005b) reported a number of results on the size effect of a reinforced concrete beam in the shear capacity.

Aravinthan et al. (Aravinthan 2006; Aravinthan and Heldt 2005; Aravinthan and Suntharavadivel 2007; Suntharavadivel and Aravinthan 2007) reported a series of experimental studies on the behaviour of shear cracks in a reinforced concrete member strengthened by external post-tensioning. Their experimental program

consisted of three cantilever specimens, three scaled models of a (Tenthill Creek bridge, QLD) bridge bent cap and six beams. The cantilever specimens had rectangular cross section throughout the whole length of 2500 mm and were of tapered shape with cross sections of 350×250 mm at the toe end and 400×250 mm at the heel end. The main variable in their study was the effective post-tensioning force. Two different post-tensioning forces of 150 kN and 300 kN were used to strengthen the cracked specimens. Specimens were loaded at both ends using active and passive loading. The scaled models of a bridge bent cap had a uniform rectangular cross section of 420×220 mm and each were 2300 mm long. These specimens were tested under asymmetric loading at a distance of about 2/3 of the span from one end. The beam specimens had rectangular cross sections of 300×150 mm throughout the whole length of 2500 mm. The effective span of the beam was set as 2000 mm. Four-point static loading was applied with the shear span 750 mm. External post-tensioning was applied to the beam using two high strength mild steel bars attached to the beam. In the beam specimens and scaled bridge bent cap specimens, they also investigated the effect of injecting epoxy resin to repair existing shear cracks. From the experimental results they concluded that existing shear cracks could have a substantial effect on the member capacity of a reinforced concrete beam strengthened by external post-tensioning and that epoxy resin repair could be a suitable treatment for the shear cracks. They also reported that a 50-70% increase in the member capacity was possible with the proper repair of the shear cracks using epoxy injection before strengthening by external post-tensioning.

Pantelides et al. (2001) reported another experimental study on the effect of shear cracks in bridge bent cap specimens and the efficiency of epoxy repair of such shear cracks before retrofitting with fibre reinforced polymer (FRP) composites. They found that the epoxy repaired specimens performed better than the original specimens without any retrofitting. Even though FRP composites were used to retrofit the reinforced concrete specimen, which may have other practical problems such as separation of the FRP from the specimen due to weaker bonding, it shows the importance of the crack repair prior to the any kind of retrofitting.

It should be noted that while there are several past research done on the shear strengthening of girders with external post-tensioning, the above two are the only research conducted with crack repairs of existing cracks. From their conclusions, it is evident that deeper understanding the behaviour of crack repairs is important to effectively retrofit reinforced concrete girders with external post-tensioning or other means.

2.2.3 Numerical Studies on the Effect of the Cracks in RC Members

The problem of modelling the behaviour of concrete remains one of the most difficult tasks in the field of structural engineering. Ngo and Scordelis identified some of the complexities of using the of finite element method for reinforced concrete members, especially after cracking (Ngo and Scordelis 1967). These are listed below:

- The structural system is three dimensional and is composed of two different materials; concrete and steel.

- The structural system has a continuously changing character due to the cracking of the concrete under increasing load.

- Effects of dowel action in the steel reinforcement, bond between the steel reinforcement and concrete, and bond slip are difficult to incorporate into a general analytical model.

- The stress-strain relationship for concrete is nonlinear and is a function of many variables.

- Concrete deformations are influenced by creep and shrinkage and are time-dependent.

Technological development and on-going research work in this area could resolve some of these issues, but there is still no basic analytical approach that can be used to predict accurately the behaviour of a reinforced concrete member throughout its loading history.

There are a number of constitutive laws proposed by different researchers for reinforced concrete members under different conditions (Bangash 2001; Maekawa et al. 2003). Based on such models, several analyses have been completed on the behaviour of reinforced concrete members strengthened by external post-tensioning. However, there are very limited analytical studies reported on the post cracking behaviour of the reinforced concrete members. The analytical study reported by Pisani considered cracks in concrete members prior to flexural strengthening by external post-tensioning (Pisani 1999). In his study, numerical models were simulated with cyclic loading and compared with the experimental results reported by Harajli (1993). Basically the concrete section was subdivided into layers and the history of stresses and strains in each concrete layer and in each steel bar or cable was recorded. The constitutive laws proposed by Karsan and Jirsa (1969) and Filippou et al. (1983) were used in the computation to describe the behaviours of the concrete and the steel (without bond-slip) respectively.

Flexural cracks are mostly vertical (parallel to the line of loading) and they are able to be closed with the application of horizontal forces such as external post-tensioning. However, this does not apply to shear cracks due to their inclination. Unlike vertical flexural cracks, the application of horizontal external prestressing will not close the inclined shear cracks and may cause a decrease in the shear capacity. Therefore, the modelling of shear crack and the stress transferring mechanism across the crack is a more complex task. Vecchio et al. (2006) modelled reinforced concrete beams to predict the critical shear regions when the beams were strengthened by external post-tensioning. They modelled the concrete beams with different axial compression and identified the critical shear failure regions. However, to the best of the author's knowledge, there is no study reported on the finite element modelling of shear strengthening of concrete members by external post-tensioning in the presence of shear cracks.

2.3   Review of the Current Standards

A number of different methods and equations have been recommended and used to estimate the shear capacity of the reinforced concrete beams worldwide. In this

thesis, the equations given in the American code ACI 318-02 (American Concrete Institute 2002) and Australian code AS3600 (Standards Australia 2001) are reviewed.

2.3.1 ACI Standard (ACI 318-02)

According to ACI 318-02 (American Concrete Institute 2002), the nominal shear strength of reinforced concrete beam, V_n, is given by,

$$V_n = V_c + V_s,$$ (2.1)

where,

V_c = Nominal shear strength provided by concrete, and

V_s = Nominal shear strength provided by shear reinforcement.

The nominal shear strength provided by shear reinforcement, V_s, is calculated as,

$$V_s = \frac{A_v f_{sy} d}{s},$$ (2.2)

where,

A_v = Cross sectional area of shear reinforcement,

f_{sy} = Yield strength of shear reinforcing steel,

d = Distance from the extreme compressive concrete fibre to the centroid of the outer most layer of tensile reinforcement, and

s = Centre -to-centre spacing of shear reinforcement.

The nominal shear strength provided by concrete, V_c, is calculated from following equations:

For non prestressed concrete members subject to shear and flexure only,

$$V_c = \left(1.9\sqrt{f_c^{'}} + 2500\rho_w \frac{V_u d}{M_u} \right) b_w d,$$ (2.3)

For non prestressed concrete members subject to axial compression,

$$V_c = 2\left(1 + \frac{N_u}{2000 A_g}\right)\sqrt{f_c'}\, b_w d \,, \qquad (2.4)$$

where,

f_c'	=	Characteristic compressive cylinder strength of concrete,
ρ_w	=	Flexural steel reinforcement ratio given by Equation 2.5,
V_u	=	Ultimate shear force,
M_u	=	Ultimate moment capacity,
b_w	=	Effective width of web for shear (equal to width, b, for rectangular cross section),
N_u	=	Ultimate axial force, and
A_g	=	Gross area of a concrete cross section.

The flexural steel reinforcement ratio, ρ_w, is given by,

$$\rho_w = \left(\frac{A_{st}}{bd}\right) \qquad (2.5)$$

where,

A_{st}	=	Cross sectional area of tension reinforcement, and
b	=	Width of the section.

2.3.2 *Australian Standard (AS3600: 2001)*

According to Australian Standard AS3600 (Standards Australia 2001), the ultimate shear capacity of a reinforced concrete beam, V_u, is given by,

$$V_u = V_{uc} + V_{us} \,, \qquad (2.6)$$

where,

V_{uc}	=	Ultimate shear strength of the concrete, and
V_{us}	=	Contribution by shear reinforcement to the ultimate shear strength.

Note that V_n, V_c, and V_s in ACI 318-02 denote the same quantities as V_u, V_{uc}, and V_{us} in AS3600 respectively. ACI 318-02 also uses some other parameters with slightly different notations from AS3600. Those parameters are clearly defined in both places as appropriate.

The contribution by shear reinforcement, V_{us}, can be calculated using the following equation:

$$V_{us} = \frac{A_{sv}}{s} f_{sy} d_o \cot\theta_v ,$$ (2.7)

where,

A_{sv}	=	Cross sectional area of shear reinforcement,
f_{sy}	=	Yield strength of shear reinforcing steel,
d_o	=	Distance from the extreme compressive concrete fibre to the centroid of the outer most layer of tensile reinforcement,
θ_v	=	Angle between the concrete compression strut and the longitudinal axis of the member, and
s	=	Centre-to-centre spacing of shear reinforcement.

The value of V_{uc} is given by Equation (2.8) or Equation (2.9) for the reinforced concrete beams without and with external forces respectively.

For reinforced concrete beam without prestress;

$$V_{uc} = \beta_1\beta_2\beta_3 b_v d_0 \left[\frac{A_{st} f_c'}{b_v d_0}\right]^{\frac{1}{3}} ,$$ (2.8)

For reinforced concrete beam with prestress;

$$V_{uc} = \beta_1\beta_2\beta_3 b_v d_o \left[\frac{(A_{st} + A_{pt})f_c'}{b_v d_o}\right]^{\frac{1}{3}} + V_{dec} + P_v ,$$ (2.9)

where,

$\beta_1,$ $\beta_2,$ β_3	=	Multiplying factors for determining V_{uc} as given in AS 3600: 2001 Clause 8.2.7.1,
b_v	=	Effective width of web for shear (equal to width, b, for rectangular cross section),
d_o	=	Distance from the extreme compressive concrete fibre to the centroid of the outer most layer of tensile reinforcement,
A_{pt}	=	Cross sectional area of prestressed tendons,
V_{dec}	=	Shear force at the decompression moment, and
P_v	=	Vertical component of prestressing force.

It should be noted that the there is no special provision to account for existing cracks in the current code of practice AS3600 and ACI 318-02.

2.3.3 Comparison of Test Data with Code Prediction

Values for the shear capacity predicted by the Equations 2.1 and 2.6 are tabulated along with the respective test data in Table 2.1. Three sets of experimental data reported by Aravinthan and Heldt (2005), Aravinthan and Suntharavadivel (2007) and Khaloo (2000) were considered for this comparison purpose (see Appendix C for details of these experimental parameters).

Basically code expressions for the shear strength of reinforced concrete beams are formulated by considering the behaviour of a reinforced concrete beam at the commencement of diagonal cracking (Collins and Mitchell 1991), which is referred to as 'uncracked beam' in this dissertation. Since there is no special provision for existing shear cracks in the beams, the V_{uc} component of the cracked specimen was ignored when calculating the capacity of the cracked specimen. The repaired beam was assumed to be free of cracks and, therefore, treated as an uncracked beam for the purpose of these calculations. For comparison purposes, the calculated and experimental values are plotted as normalized values (dividing by the cross sectional area of the specimens) in Figure 2.10 and Figure 2.11.

Table 2.1: Shear capacity of the RC beams strengthened by external post-tensioning

Specimen	Type of Loading	Maximum Force [kN]			Remarks
		Experimental value	Code prediction		
			AS 3600	ACI 318	
RB1	Asymmetric loading	366	323	321	Bridge bent caps (Aravinthan et al. 2005)
RB2(a)		333	352	348	
RB2(b)		420	338	335	
RB3		546	391	390	
RCB1	Symmetric loading	176.2	176	175	Rectangular beams (Aravinthan et al. 2007)
RCB2		262.2	248	239	
RCB3		278.9	286	284	
RCB4		286	268	258	
1	Loaded equally at two points	31	25	24	The beams strengthened after cracking (Khaloo 2000)
2		32.4	25	24	
3		46	36	36	
4		40	36	36	
5		29	25	24	
6		29	25	24	
7		28	25	24	
8		39	36	36	
9		28.5	25	24	
10		39	36	34	
11		25	25	24	
12		27	36	34	
13		44	37	36	
14		46	37	36	
15		62	54	52	
16		60	54	52	
17		46	37	36	
18		56	54	52	
19		39	37	36	
20		42	54	52	
21		45	37	36	
22		42	37	36	
23		23	37	36	
24		43	37	36	
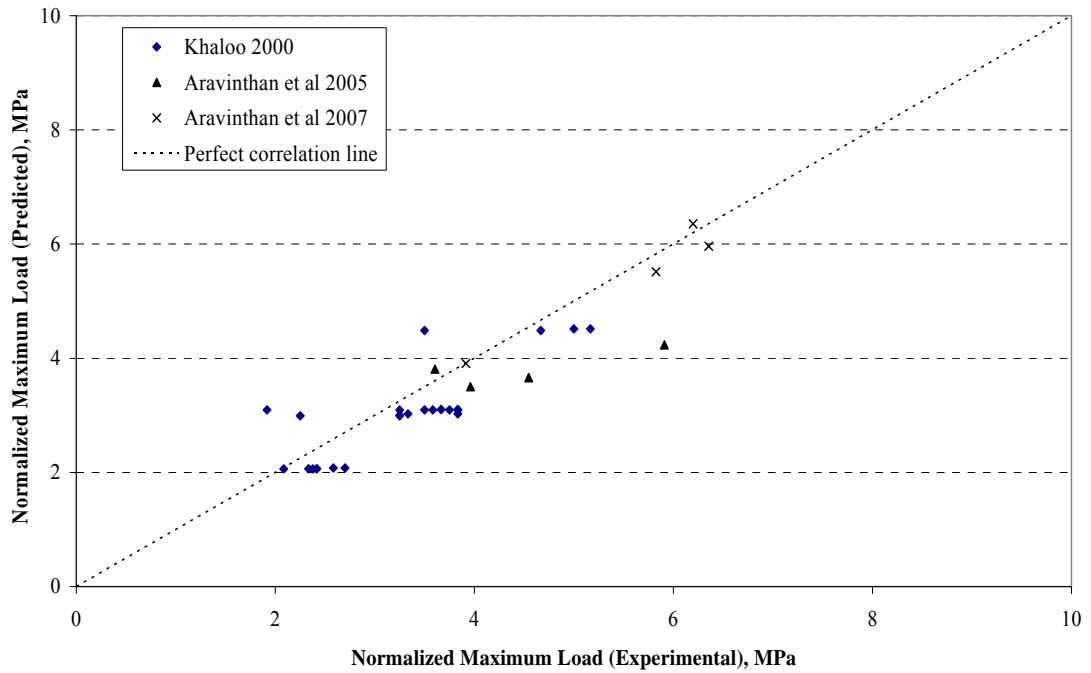
Figure 2.10. Maximum force predicted by ACI 318-02 code vs. experiment
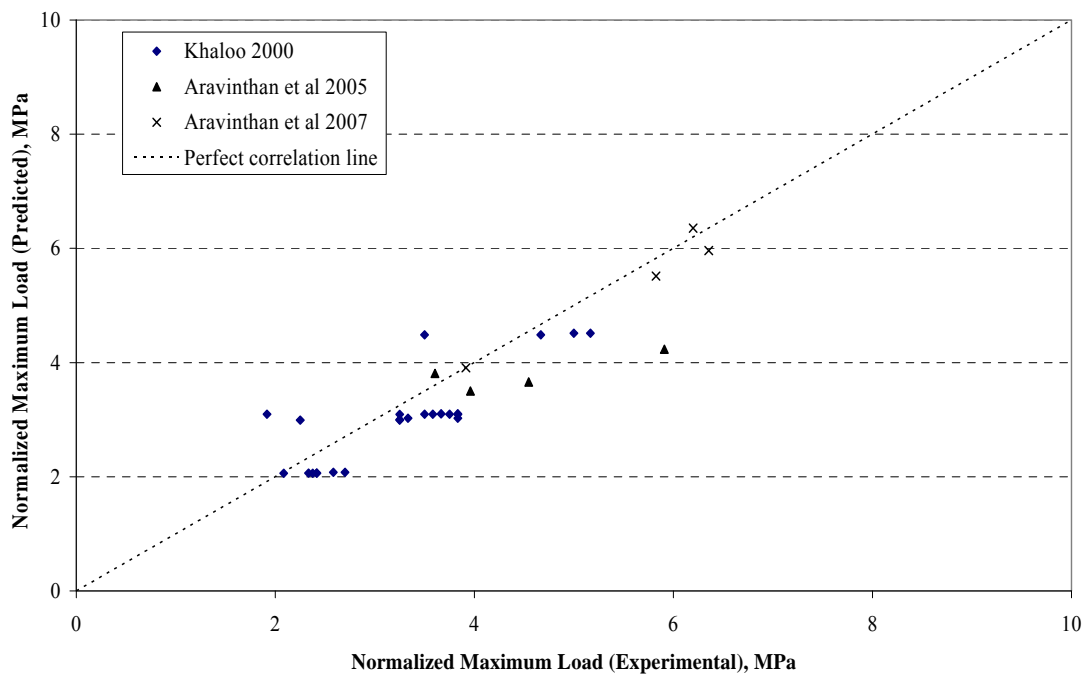
Figure 2.11. Maximum force predicted by AS3600:2001 code vs. experiment

It can be observed from Figure 2.10 that the ACI 318-02 predictions for maximum load show a poor correlation with the test data when an unrepaired shear crack exists. It also noted that the effect of a shear crack is significantly large when the

member was strengthened by conventional external post-tensioning compared with external clamping. In general Figure 2.11 also shows similar behaviour when an unrepaired shear crack exists in a reinforced concrete member. This suggests that the existing codes of practice can effectively predict the shear capacity of reinforced concrete members with no cracks. However, when there is significant shear cracking is present and when the crack is not properly repaired to bring the beam to its original condition, the code equations are not applicable. This is mainly due to the loss of aggregate interlocking factor is lost when large shear cracks are present in a reinforced concrete beam. This indicates that there is need to understand the behaviour of shear damaged beams when strengthened by external post-tensioning.

2.4   Review of the Theoretical Development

2.4.1 General Background

Shear failure mechanism of reinforced concrete members is still the subject of theoretical research after several years of studies. A crack will form in concrete when the principal tensile stress at a location reaches the cracking strength of the concrete. When the member is subjected to a shear force, the directions of the principal stresses are inclined to the longitudinal direction. Hence the shear crack will be inclined to the longitudinal axis. When a concrete member is strengthened by external post-tensioning, the crack inclination will be reduced by the application of axial compression. However, the transfer of axial compression across an existing shear crack is a complex function of many parameters including inclination, crack width and amount of shear reinforcements. As the width of the crack increases, the aggregate interlocking will decrease, which will reduce the capacity of the member. Only a few theoretical models have been developed to explain this phenomenon.

2.4.2 Shear Strength of Reinforced Concrete Members

Many experimental studies have been conducted to investigate the behaviour of shear failure. Even though the estimation of shear capacity of reinforced concrete is still under investigation, many researchers have proposed various methods to estimate shear capacity of reinforced concrete members. The report published by

ACI-ASCE committee 445 (ASCE-ACI Committee 445 on Shear and Torsion 1998) summarised the research and development related to the shear failure of reinforced concrete members until 1998. This section briefly reviews the major developments included in the report and some of the recent studies in this area.

Among the number of proposed models, the strut-and-tie model (Tan and Naaman 1993) is gaining widespread use and respect as a rational method for prediction of shear strength of beams. Provisions for complex beam design such as deep beams using the strut-and-tie model have been included in several codes and guidelines for practice, including AASHTO LRFD (AASHTO 2004) and ACI 318 (American Concrete Institute 2005). Detail of the model is discussed in Chapter 5.

Following the development of the strut-and-tie model, a number of theoretical models have been reported by researchers. In recent times, Choi et al. developed a unified shear strength model for reinforced concrete beams (Choi and Park 2007; Choi et al. 2007). This model was based on the failure mechanism of the compression zone of the specimen which varies according to the span-to-depth ratio (a/d). This model can be applied to both slender and deep beams and describes the failure mechanism of RC beams which changes from a diagonal tension failure to a shear compression failure as a/d decreases. The model was verified by a number of experimental results and it was found that the developed model predicted the shear capacities of a range of beams (both slender and deep beams with and without shear reinforcement) better than current design methods.

A number of different methods have been proposed to predict the shear capacity of reinforced concrete beams under different conditions. These conditions include, but are not limited to, different slenderness ratios, deep beams and beams with and without shear reinforcements. However, these methods cannot be applied directly to a beam with existing shear cracks or a beam with repaired shear cracks. Only a few attempts to determine the shear capacity or behaviour of shear damaged (cracked) beams are reported in the literature. These are outlined in the following section.

2.4.3 Reinforced Concrete Members with Existing Shear Cracks

Wagner treated an analogous problem in his study of the post buckling shear resistance of thin-webbed metal girders (Wagner 1929). He developed the tension field theory to determine the angle of inclination of the diagonal tension. Wagner considered the deformations of the system to determine the angle of the diagonal tension and assumed the angle of the diagonal tensile stresses would coincide with the angle of the principle strain (Collins and Mitchell 1991).

This approach was adopted by Collins and Mitchell (1991) to develop the compression field theory. In the compression field theory it is assumed that, after cracking, the concrete carries no tension and that the shear is carried by a field of diagonal compression.

Later the compression field theory was modified to include the contribution of the tensile stresses in the concrete between cracks. This modification was later referred to as the modified compression field theory (Collins and Mitchell 1991; Vecchio and Collins 1986). Based on the modified compression field theory, the maximum axial force that can be transferred across the shear crack depends on the shear stress along the crack plane, v_{ci}, which depends on the width of the shear crack. This relationship is given by,

$$v_{ci} = \frac{0.18\sqrt{f_c'}}{0.3 + \dfrac{24w}{a+16}},\tag{2.10}$$

where,

w = Shear crack width, and

a = Maximum aggregate size.

This limits the amount of the stress that can transfer across the crack. When the amount of the stress reaches the v_{ci}, additional stress could cause a possible slip along the crack plane which could result in a negative effect (decrease the shear capacity of the member) in some cases.

The modified compression field theory was recognized as a useful approach to determine the behaviour of cracked reinforced concrete beams (Bentz et al. 2006; Stevens 2007; Vecchio and Bucci 1999; Vecchio et al. 2006). The method enables prediction not only of the strength of the cracked member but also the load-deflection characteristic of the member (Bentz 2001). Based on the modified field compression theory, the crack width in a reinforced concrete beam is an important parameter in the analysis of the post cracking behaviour of the member. However, it is a challenging task to determine the crack width in a reinforced concrete member due to various limitations in currently available theory. Therefore, further studies in this area are needed to analyse the actual behaviour of a reinforced concrete member with shear cracks.

Furthermore, to the best of author's knowledge, no mathematical models or significant analytical studies to investigate or study the effect of shear cracks in a reinforced concrete beam strengthened by external post-tensioning have been reported. This dissertation aims to fill or reduce this gap.

2.5   Summary

This chapter has provided some background on the development of theory to enable the prediction of the shear capacity of reinforced concrete beams strengthened by external post-tensioning, including a brief overview of external post-tensioning and its use in civil and structural engineering applications. It is clear that external post-tensioning is a widely used technique for strengthening and that it has significant potential in a wide range of civil engineering applications.

Although external post-tensioning has been used and is increasingly being used in a variety of civil engineering applications, the most significant application in recent years appears to be in the area of rehabilitation of existing structures. The success of external post-tensioning in a rehabilitation project depends on various factors including the effect of existing damage in the structure. Even though it is well proven that existing flexural cracks have no significant effect in the application of

external post-tensioning, there is a lack of experimental investigations relating to the effect of existing shear cracks and current repair techniques in the strengthening of reinforced concrete beams using external post-tensioning.

In addition to the lack of experimental data, shortcomings in current codes of practice has also been well documented as a major inhibitor to the wider usage of this technique in rehabilitation applications especially in shear damaged structures. Current Australian codes of practice for the design of prestressed concrete members (AS3600) do not have any provision to account for the effect of existing shear cracks or to cater for the loss of aggregate interlocking in the shear capacity of a reinforced concrete beam.

Over recent years there have been international efforts to investigate the behaviour of existing shear cracks in reinforced concrete beams (Collins and Roper 1990; Vecchio and Collins 1993). Collins and Vecchio's proposed modified compression field theory can be used to analyse the behavior of cracked reinforced concrete members (Vecchio and Collins 1986). This theory explains the amount of maximum shear transfer across a shear crack in a reinforced concrete beam. Other than this theory, there are no significant research outcomes reported in this area. Furthermore, due to its complexity no significant numerical works incorporating the effect of existing shear cracks in an externally post-tensioned reinforced beam have been reported.

Unlike flexural cracks, existing shear cracks have a substantial effect in the efficiency of externally post-tensioned members (Aravinthan and Suntharavadivel 2007). Thus, there is no doubt that research on the behaviour of existing shear damage in reinforced concrete beams strengthened by external post-tensioning has the potential to bring about far reaching innovations in civil and structural engineering especially in the rehabilitation of existing structures. A good understanding of repairing these cracks by techniques such as epoxy injection further add value not only from a research perspective but also to those who may be envisaging to use such technology in practice.

Chapter 3
EXPERIMENTAL PROGRAM

To gain a better understanding about the behaviour of existing shear cracks in reinforced concrete members, sixteen beams were tested with different variables under monotonically increasing load at the civil engineering laboratory of the University of Southern Queensland. The primary test variables were the concrete strength, the amount of shear reinforcement and the strengthening technique. This chapter describes the objectives of the experimental program, details of the beam specimens, material properties, instrumentation, and test procedures that were used during the experiment. Test results and discussion on the results are presented in Chapter 4.

3.1   Objective of the Experimental Program

The experimental program was designed to achieve the following objectives.

- Investigate the influence of the following parameters on the behaviour of the existing shear cracks in a reinforced concrete member:
  - compressive strength of the concrete;
  - amount of shear reinforcement;
  - orientation of the prestressing force.
- Evaluate the efficiency of an epoxy resin repair technique to existing shear cracks.

- Study the influence of existing shear cracks on the behaviour of a reinforced concrete member strengthened by external post-tensioning.

- Formulate the behaviour of existing shear cracks in a reinforced concrete beam strengthened by external post-tensioning. This formulation may be used to model the shear crack behaviour using finite element method.

3.2   Design of Test Specimen

To achieve the above objectives, the beams were designed mainly in three major groups as follows:

Group 1 – RC beams with minimum shear reinforcement (spaced at 250 mm centres) and externally post-tensioned, some beams repaired with epoxy injection.

Group 2 – RC beams with additional shear reinforcement (spaced at 175 mm centres) and externally post-tensioned, some beams repaired with epoxy injection.

Group 3 – RC beams with minimum shear reinforcement (spaced at 250 mm centres) and strengthened by external clamping (vertical, inclined or combination).

A total of sixteen beams were tested in the above three groups under monotonically increasing load. Test variables of each beam will be explained later in this section. All the beams were designed with a rectangular cross section of 150×300 mm and a length of 2500 mm. These dimensions were selected by considering the facilities available in the civil engineering laboratory at the University of Southern Queensland. These were:

- construction facilities – casting, curing & storage of specimens;

- testing facilities – loading capacity of the testing machine;

- handling facilities – lifting and moving the specimen.

These specimens were tested under a four-point loading arrangement as shown in Figure 3.1. The span of the specimens was selected as 2000 mm with a clearance of

250 mm in each end to prevent any slip from the supports during the testing. The shear span of the specimens was kept at 750 mm during the experiment.
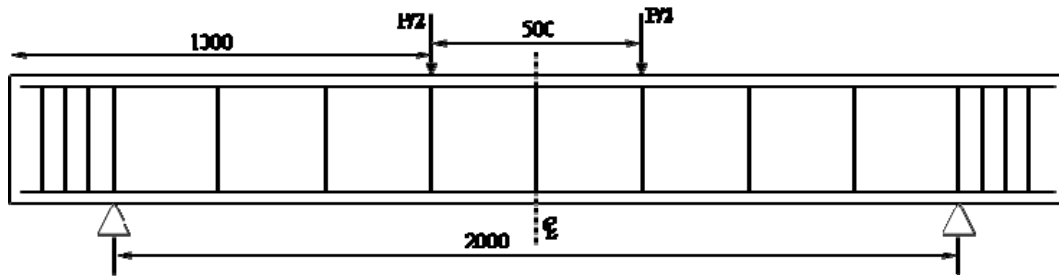
(a) Typical reinforcement arrangement in a specimen
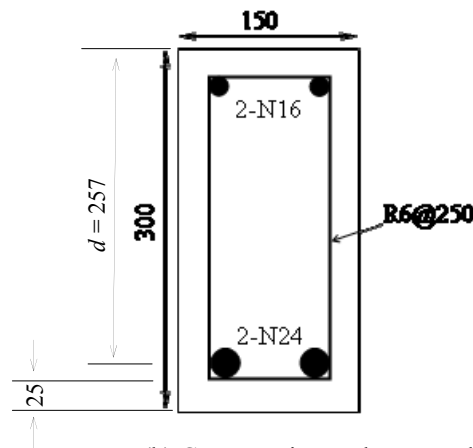
(b) Cross section at the centre line

Figure 3.1. Test set-up and reinforcement arrangements of the specimen

In general, reinforced concrete beams are designed to have flexural failure rather than shear failure. However, in this research, all the specimens were designed such that under loading they would fail in shear. This was achieved by boosting the flexural capacity of each specimen by providing less shear reinforcement than the minimum shear reinforcement recommended in AS 3600 (2001) together with large longitudinal steel areas in the top and the bottom. This type of design (with less shear reinforcement than that specified in code of practices) is a general approach used by many researchers to develop shear cracks in the specimens (Kahloo 2000, Teng et al. 1996).

N-type (hot rolled steel; design yield strength, f_{sy} = 500 MPa) bars were used for longitudinal reinforcement while high strength mild steel bars were used as shear reinforcement.   Two N24 (N-type; diameter = 24 mm) bars were used as tensile reinforcement and two N16 bars were used as compressive reinforcement (Figure 3.2). To change the amount of shear reinforcement, different spacings of 250 mm and 180 mm were selected while keeping the stirrup size constant at 6 mm.

Figure 3.2. Reinforcement arrangement in a specimen

Additional shear reinforcements were provided at both ends of the specimen (Figure 3.2 and Figure 3.3) to carry the transverse tensile force developed by the application of the external post-tensioning. As seen in Figure 3.3, a special arrangement was made to fix the end plate of the external post-tensioning tendons (bars) by using four ferrules (10×45 Zinc Elephant feet) at both ends of each specimen.
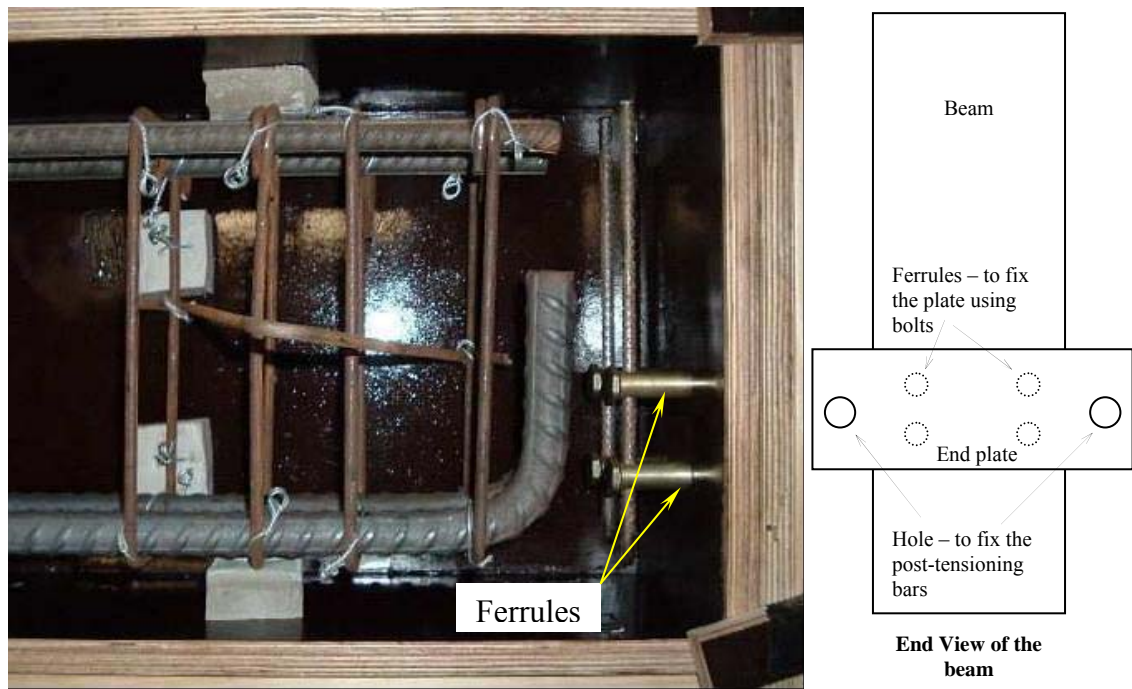
Figure 3.3. Detail of the reinforcement and cage arrangement that was fixed at each end of the specimens

The specimens were prepared in three groups. First and second groups consist of four beams each and there were eight beams in Group 3. The beams in a group were prepared (Figure 3.4) using same batch of concrete (except Group 3, where two batches were used) and allowed to cure under same conditions.

Figure 3.4. Specimens after casting

Test variables are listed in Table 3.1. Specimens are labelled such that they have the strengthening technique identification first followed by the group and then by the individual specimen number. For example ECL21 refers to the external clamped beam from the second group with specimen number identification 1. Details of both external clamping and external post-tensioning techniques will be explained later (Section 3.5) in this chapter.

Basically the specimens in Groups 1 and 2 were designed and tested under the same conditions except that the amount of shear reinforcement in the shear span was varied to investigate the effect of shear reinforcement on the behaviour of the cracked beam. Group 3 specimens were designed with the same specifications as Group 1 and tested with external clamping instead of external post-tensioning as used in Group 1.

Table 3.1: Details of specimen and reinforcements

Group	Detail	Specimen	Dimension b×D [mm]	Shear R/F Spacing [mm]	Longitudinal Reinforcement	
					Tension side	Compression side
1	Minimum shear R/F & External post-tensioned	EPT11	150×300	250	2-N24	2-N16
		EPT12	150×300	250	2-N24	2-N16
		EPT13	150×300	250	2-N24	2-N16
		EPT14	150×300	250	2-N24	2-N16
2	Near minimum shear R/F & External post-tensioned	EPT21	150×300	180	2-N24	2-N16
		EPT22	150×300	180	2-N24	2-N16
		EPT23	150×300	180	2-N24	2-N16
		EPT24	150×300	180	2-N24	2-N16
3	Minimum shear R/F & External clamping (vertical)	ECL31	150×300	250	2-N24	2-N16
		ECL32	150×300	250	2-N24	2-N16
		ECL33	150×300	250	2-N24	2-N16
		ECL34	150×300	250	2-N24	2-N16
	Minimum shear R/F & External clamping (inclined)	ECL35	150×300	250	2-N24	2-N16
		ECL36	150×300	250	2-N24	2-N16
		ECL37	150×300	250	2-N24	2-N16
		ECL38	150×300	250	2-N24	2-N16

Note: EPT = External Post-tensioning
        ECL = External Clamping

3.3   Materials Properties

3.3.1 Concrete

Concrete was ordered from a ready-mix concrete supplier (*Wagner Concrete, Toowoomba*). All of the specimens were prepared with this concrete which had the following properties:

- slump = 80 mm;
- 20 mm nominal size aggregate;
- compressive strength = 32 MPa.

Each batch of concrete was tested for its properties during casting (fresh concrete: slump of the concrete) and during testing of the beams (hardened concrete: compressive and tensile strength of concrete) as specified below:

During casting

- slump of the fresh concrete – to measure the workability of the concrete

During testing of beams

- compressive strength of concrete (Figure 3.5)
- tensile strength of the concrete (Figure 3.6).

All these tests were conducted according to the Australian Standard AS 1012–1981 (Standards Australia 1981). It should be noted that some parts of AS 1012, were revised in later years and the tests were carried out in accordance with the revised versions as follows:

- sampling of fresh concrete: AS 1012.1–1993 (Standards Australia 1993)

- indirect tensile strength of concrete: AS 1012.10–2000 (Standards Australia 2000)

- compressive strength of concrete: AS 1012.14–1991 (Standards Australia 1991).

Figure 3.5. Testing of compressive strength of the concrete

Figure 3.6. Testing of indirect tensile strength of the concrete

The compressive strength of the specimens at the time of tests ranged from 29 MPa to 42 MPa, a significant variation from the ordered specification of 32 MPa. Table 3.2 lists the test results on the concrete strength at the time of test specimens.

Table 3.2: Properties of the fresh and hardened concrete

Specimen	Average Compressive Strength* [MPa]	Slump [mm]
EPT11	39.9	100
EPT12	40.3	100
EPT13	40.4	100
EPT14	40.4	100
EPT21	29.3	120
EPT22	32.3	120
EPT23	35.3	120
EPT24	36.5	120
ECL31	39.4	100
ECL32	37.7	100
ECL33	41.6	100
ECL34	37.7	100
ECL35	41.6	110
ECL36	41.5	110
ECL37	40.0	110
ECL38	39.0	110

* Tested on the same day of the testing of the specimen

It was found that the average tensile strength of the concrete was in the range of 7% to 10% of the average compressive strength in most of the cases. Detailed results can be found in Appendix A.

3.3.2 Reinforcing Steel

N24 and N16 bars were used as bottom (tensile) and top (compressive) reinforcements respectively. The N24 bars were pre-ordered from the manufacturer (*Smorgan steel, Toowoomba*) as they could not be cut and bent on site due to the limitation of the facilities in the laboratory.

Mild steel bars were used as shear reinforcement in the test specimens. Since the yield strength of shear reinforcement is a critical parameter in the shear capacity of the specimens, it is important to determine the actual yield strength of the high strength mild steel bars. For this purpose, a tensile test was performed using four mild steel bar samples at the University of Southern Queensland. Load was applied at a constant rate of 2 mm/min (strain-controlled). Test results are summarised in Table 3.3.

Table 3.3: Yield stress of the shear reinforcement bar

Specimen	Diameter [mm]	Yield Load [kN]	Yield Stress [MPa]
1	6.0	10.4	368
2	6.0	10.3	364
3	6.0	10.4	368
4	6.1	10.5	359
Average			**365**

It can be noted that the yield stress of shear reinforcement bars tested was 365 MPa which is considerably higher than the commonly used nominal strength of shear reinforcement (250 MPa). This higher yield strength was used in the calculation of theoretical capacities of the specimens (in Chapter 4 and Chapter 6) and numerical simulation using Abaqus software.

3.3.3 Prestressing Steel

3.3.3.1 External Post-Tensioning Steel

Two 26.5 mm high tensile Macalloy bars were used to apply the external post-tensioning force to the specimens. Both of the rods were used within their elastic limit during the testing. Further details of these bars are given in Appendix A. The properties of these high strength mild steel bars were not tested separately since the maximum expected stress (< 280 MPa – estimated using the equation proposed by Naaman et al 1991) in these bars was found to be less than their minimum 0.1 % of proof stress (>830 MPa)[*].

3.3.3.2 External Clamping Steel

External clamping was done using six 16 mm mild steel bolts in each side of the specimens. To determine the properties of these mild steel bolts, a tensile test was carried out using six specimens (cut from the mild steel bolts used for external clamping) at the University of Southern Queensland. Load was applied at a constant rate of 2 mm/min (strain-controlled). Summary of the results from the tensile testing of the steel are shown in Table 3.4.

Table 3.4: Properties of external clamping rod

Parameter	Value
Average Load at offset Yield (kN)	65.6
Average Stress at Offset Yield (MPa)	338.4
Average Peak Load (kN)	77.5
Average Peak Stress (MPa)	397.5
Average Breaking Load (kN)	53.7
Average Breaking Stress (MPa)	275.1

---

[*] Also see http://www.structuralsystems.com.au/ssl/tech/docs/broch/2007/2007-BarPT-broch.pdf

3.3.4 Epoxy Resin

In the finite element model, the mechanical properties of the epoxy resin were defined from the values given in the data sheet provided by the manufacturer. However, the Elastic module (E) of the epoxy resin is not given in the provided data sheet. In order to get the Elastic modulus of the resin (Nitofill LV), five standard specimens (Figure 3.7) were prepared and tested using MTS Alliance RT/10 machine (Figure 3.8) at the University of Southern Queensland.

Figure 3.7. Epoxy resin specimens

(a) Specimen fixed in the MTS machine

(b) Failure of the specimen

Figure 3.8. Testing of the epoxy resin in MTS alliance RT/10 machine

Tests were carried out according to the International Standard, ISO 527-2: 1993 (International Organization for Standardization 1993). Important testing specifications are given Table 3.5.

Table 3.5: Specifications of the epoxy tensile testing

Parameter	Value
Clamping Pressure	1 MPa
Test Speed	2 mm/min
Specimen Preparation Method	Specimens Machined to Size on Router Template, Edges Sanded Smooth & Defect Free

A 300×300 mm plate specimen was prepared using the epoxy resin. After 2 weeks of curing, five test specimens were cut from the plate specimen. Sample detail and test results of these specimens are presented in Table 3.6. The stress-strain curves of the specimens are shown in Figure 3.9.

Table 3.6: Material properties of epoxy resin

Specimen	Average dimension [mm]		Peak Load [N]	Peak Stress [MPa]	Peak Strain [%]	Break Strain [%]	Elastic Modulus [MPa]
	Thickness	Width					
1	4.84	10.95	1953	36.88	1.17	1.17	3391
2	4.80	10.14	1847	37.93	1.46	1.46	2679
3	4.85	10.41	1663	32.90	1.08	1.08	3328
4	4.85	10.92	2021	38.18	1.37	1.37	3011
5	4.84	10.74	2269	43.68	1.81	1.81	2763
Mean	**4.84**	**10.63**	**1950**	**37.91**	**1.38**	**1.38**	**3034**
Std Dev	**0.02**	**0.35**	**224**	**3.86**	**0.29**	**0.29**	**321**
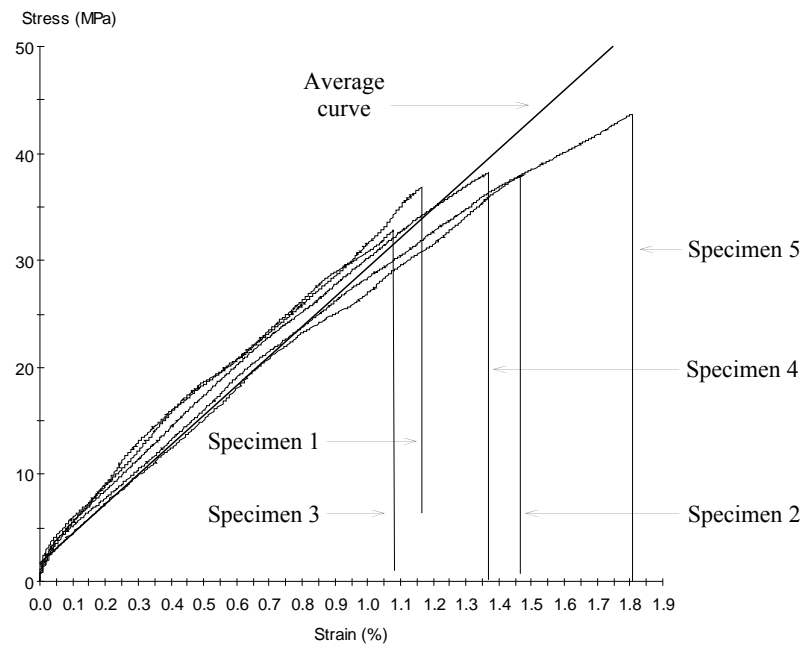
Figure 3.9. Stress-strain curve of the epoxy specimens

The minimum strength of the epoxy resin in compression, tension and flexure are given in Table 3.7 (provided by the manufacturer - *Parbury Technologies Pty Ltd*). It can be noted that the measured tensile strength values (Table 3.6) are significantly higher than the minimum tensile strength value given in Table 3.7. It should be also noted that the minimum compressive and tensile strengths of epoxy resin are significantly higher than those of concrete (more than 200%). As the epoxy took seven days to reach these minimum strengths, it was decided that the epoxy repaired specimens should be cured for at least one week before testing.

Table 3.7: Minimum strength of the epoxy resin

Minimum Strength	Value [MPa]
Compressive Strength	83
Tensile Strength	25
Flexural Strength	50

Source: Data sheet of Nitofill LV, Parbury Technologies Pty Ltd [†]

[†] See Appendix A

3.4   Instrumentation

The behaviour of the specimens, the load, displacement, strain in concrete and reinforcements and the crack width were continuously recorded using various instruments as described below.

3.4.1 Load Measurement

Applied load was measured using load cells. For this research study, LW0-125 type load cells shown in Figure 3.10 were used. Specification of the load cell is given in Table 3.8.

Figure 3.10. LW0-125 type load cell
Source: http://www.transducertechniques.com/

Table 3.8: Specification of LW0-125 load cell

Parameter	Value
Rated Capacity	556 kN [125, 000 lbs]
Accuracy	0.1 kN [25 lbs]
Resolution	Depends on the readout A/D (data Acquisitions system)
Rated Output (R.O.)	2 mV/V nominal
Excitation Voltage	10 VDC

3.4.2 Deflection Measurement

The deflection of the specimen was measured at the mid point of the specimen using LVDT and/or string pot (Figure 3.11). Specifications of the String pot and LVDT are given in Table 3.9.

(a) String pot
Source: http://www.celesco.com/

(b) LVDT
Source: http://www.payab-zamzam.com/LVDT.htm

Figure 3.11. Instruments for deflection measurement

Table 3.9: Specifications of string pot and LVDT

Parameter	Value	
	LVDT	**String Pot**
Linearity Range	50 mm	50 mm
Accuracy	0.01 mm	0.05 mm
Resolution	Depends on the readout A/D	

3.4.3 Strain Measurement

Variation of strain in the reinforcement bar was measured by 2 mm (FLA-2-11 type) strain gauges (Figure 3.12) while 30 mm (PFL-30-11 type) gauges (Figure 3.13) were used to measure the strain in concrete. Both types were 120.4 Ω ($\pm$ 0.5%) linear strain gauges with a gauge factor of 2.11 ($\pm$ 1%). Data sheets of both 2mm and 30 mm strain gauges are attached in Appendix A.

Figure 3.12. Strain gauge attached in shear reinforcement
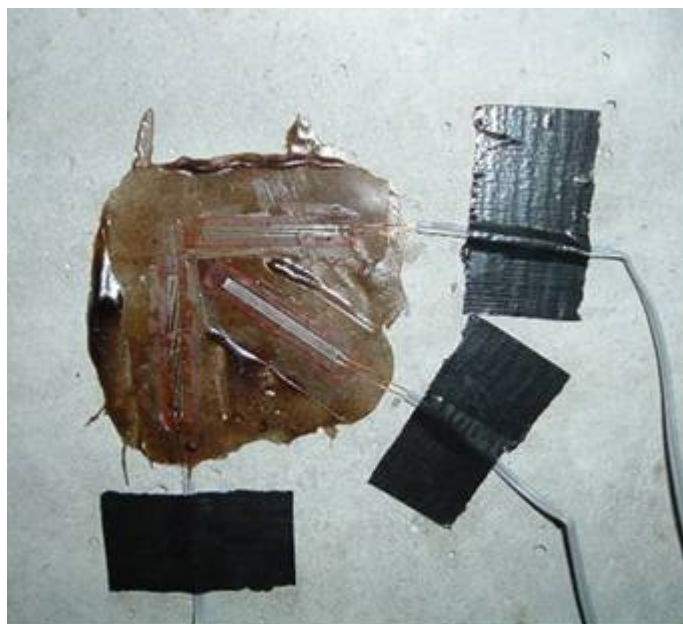
Figure 3.13. Strain gauges attached to concrete

A total of 15 strain gauges were placed in the longitudinal reinforcements, shear reinforcements and on the surface of the concrete. The strain gauge locations are shown in Figure 3.14.
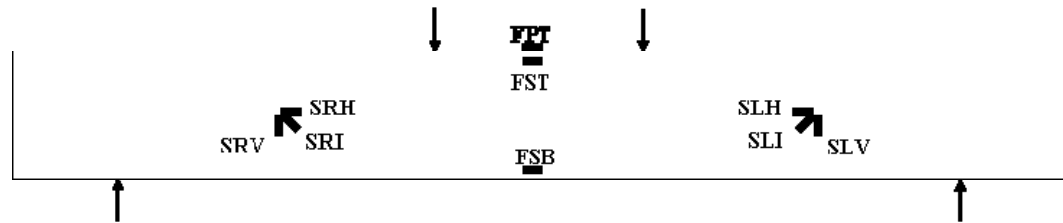
(a) Strain gauge locations in concrete (attached outer surface of the beam)

[**FS** – flexure side; **FP** – flexure plan; **S** – shear; **T** – top; **B** – bottom; **R** – right; **L** – left; **V** – vertical; **H** – horizontal; **I** – inclined]
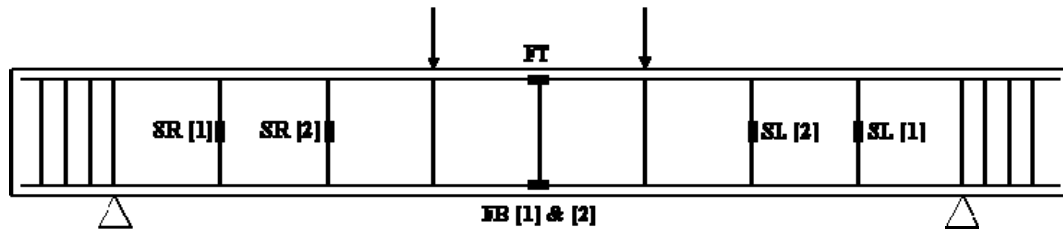
(b) Strain gauge locations in steel bars

[**F** – flexure; **S** – shear; **T** – top; **B** – bottom; **R** – right; **L** – left]

Figure 3.14. Strain gauge locations in the testing specimen

3.4.4 Prestressing Force Measurement

During the study, two types of strengthening techniques were used. Conventional post-tensioning was applied in a horizontal direction and external clamping was applied in a vertical or inclined direction. Due to the limited number of load cells, two different techniques were used to measure the external prestressing force.

1. Measured directly by load cells: this was used to measure the external post-tensioning force.

2. Converted from strain reading: this was used to measure the force in the external clamping rods.

Details of the measurements from the above two techniques are outlined below.

3.4.4.1 Measured Directly From Load Cells

The external post-tensioning force was continuously measured using two load cells attached to the external post-tensioning rod at the 'dead' end (See Figure 3.15). The load cells used were the same as those used to measure the applied load (Figure 3.10).
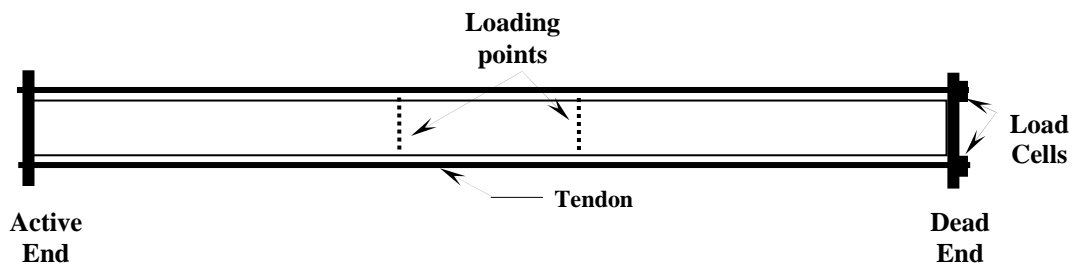
Figure 3.15. Locations of the load cells attached to the post-tensioning rod
(Plan view from top)

3.4.4.2 Converted From Strain Readings

The External clamping force was measured using strain measurement. One 2 mm strain gauge was attached to the mid-length of each of the four clamping rods as shown in Figure 3.16. Then the strain measurements were converted into force using the load-deflection behaviour of the rod.
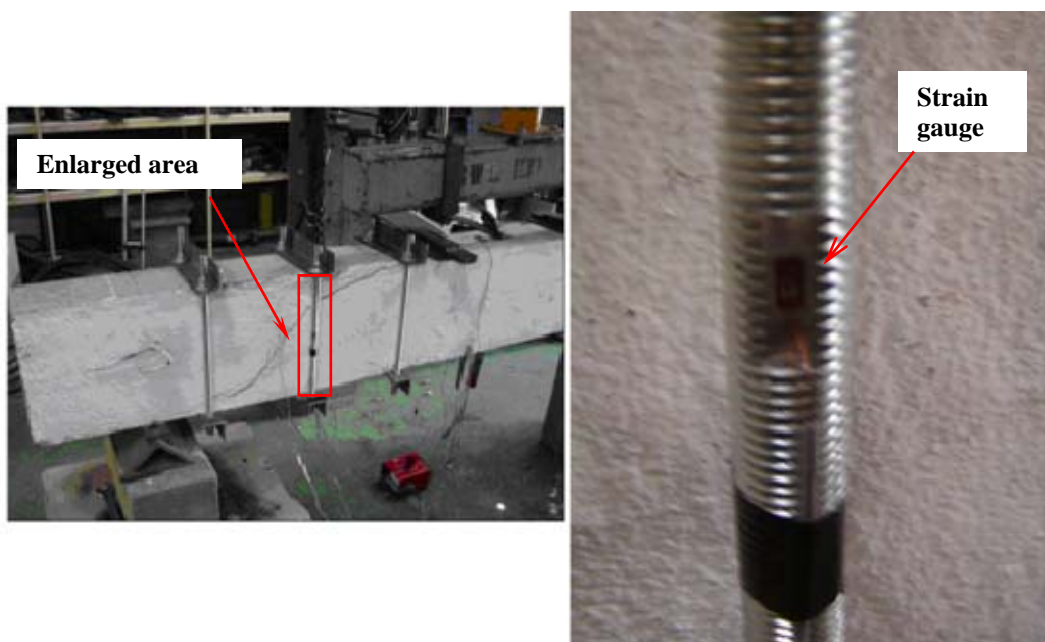
Figure 3.16. Strain measurement in the external clamping rod

3.4.5 Data Acquisition System

The data acquisition system utilised during the experiments was a System 5000 (Model 5100B scanner). This scanner accepts up to four input cards (five channels per card and up to 20 channels per scanner – see Figure 3.17) which can be changed according to the requirement. Each channel can be connected to the gauge through input plugs.
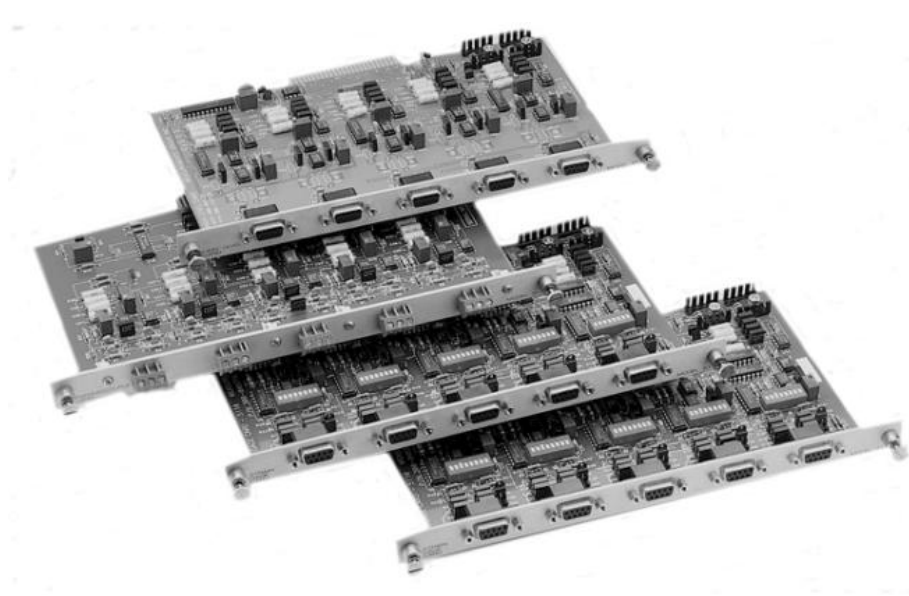
Figure 3.17. Sensor cards used in System 5000 (Model 5100B scanner)
Source: www.vishay.com

Two types of input cards were used for all the experiments conducted during this research project.

1. A high level input card (one card per scanner). Inputs to the strain gauge input card are made through the 9-pin D-sub connectors. LVDT and string pots were connected through this card during all experiments performed for this research project.

2. A strain gauge input card (three cards per scanner). Inputs to the strain gauge input card are also made through the 9-pin D-sub connectors. During all of the experiments performed for this project, strain gauges and load cells were connected to the strain gauge input card using a quarter bridge (with built-in internal dummy) circuit arrangement as shown in Figure 3.18.
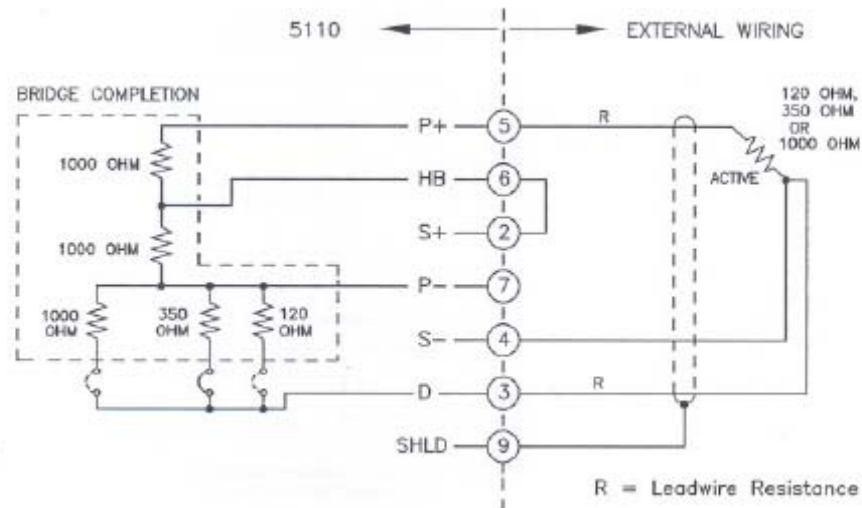
Figure 3.18. Quarter bridge (with internal dummy) circuit arrangement
Source: System 5000 Instruction Manual (Vishay Micro-Measurements 2003)

[**P+**: Positive connection to excitation; **P-**: Negative connection to excitation; **HB**: Half bridge; **S+**: Positive signal input to amplifier; **S-**: Negative signal input to amplifier; **D**: Dummy; **SHLD**: Shield]

All of the measurements, except the crack width measurement which was recorded manually, were transferred to the computer through System5000s (Figure 3.19). During testing two System 5000s were connected in series so that up to 40 channels could be used if required.

Figure 3.19. System5000 (top) attached to the computer (bottom)

3.5   Strengthening Techniques

In this research study, the following two strengthening techniques were used to investigate the effect of existing shear cracks under different conditions:

- external post-tensioning;

- external Clamping.

Details of these techniques are explained below.

3.5.1 External Post-Tensioning

External post-tensioning was applied through two 24 mm mild steel bars attached to the specimens with an eccentricity of 50 mm. Initially about 150 kN force was applied (75 kN at each rods) to the specimens from the 'active' end (see Figure 3.15). A hydraulic jack was used to apply the post-tensioning force to the steel bars as shown in Figure 3.20.

Figure 3.20. Hydraulic jacking system used for post-tensioning at the 'active' end of the specimen

3.5.2 External Clamping

External clamping, using 12 mm high strength mild steel bars, was applied in two ways.

1. Vertical clamping – clamping rods were vertical as shown in Figure 3.21.
2. Inclined clamping – the clamping rods were inclined 45^0 to the vertical and nearly perpendicular to the shear crack (see Figure 3.22).
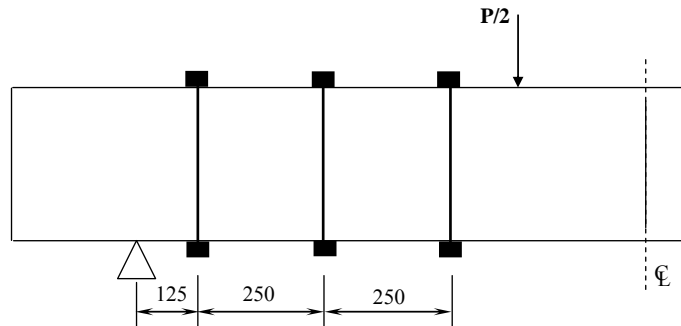
Figure 3.21. Arrangement of vertical clamping rods
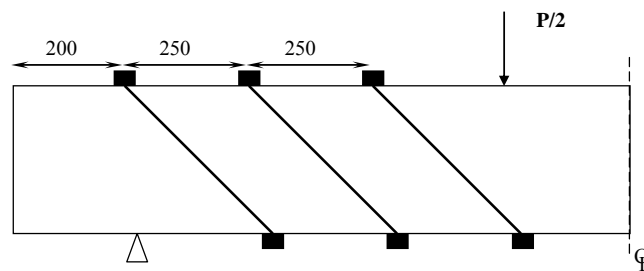
Figure 3.22. Arrangement of inclined clamping rods

As explained under '*Testing Procedure*' (Section 3.7), a combined vertical and inclined clamping technique was also tested. This arrangement is shown in Figure 3.23.
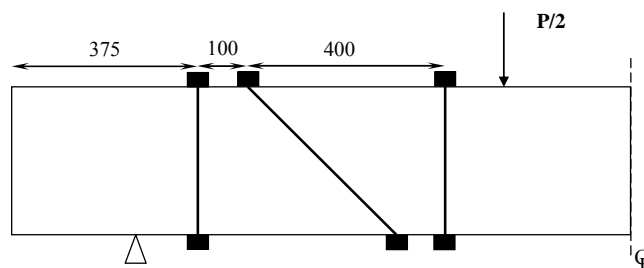
Figure 3.23. Arrangement of combined external clamping

A total of six rods (three rods on each side) were used in each shear span of the specimen and each rod was tightened with a constant torque of 15 Nm. To uniformly distribute stresses, thin wooden pieces were used between the concrete surface and steel angle on the top and bottom surface of the specimen, as shown in Figure 3.24.
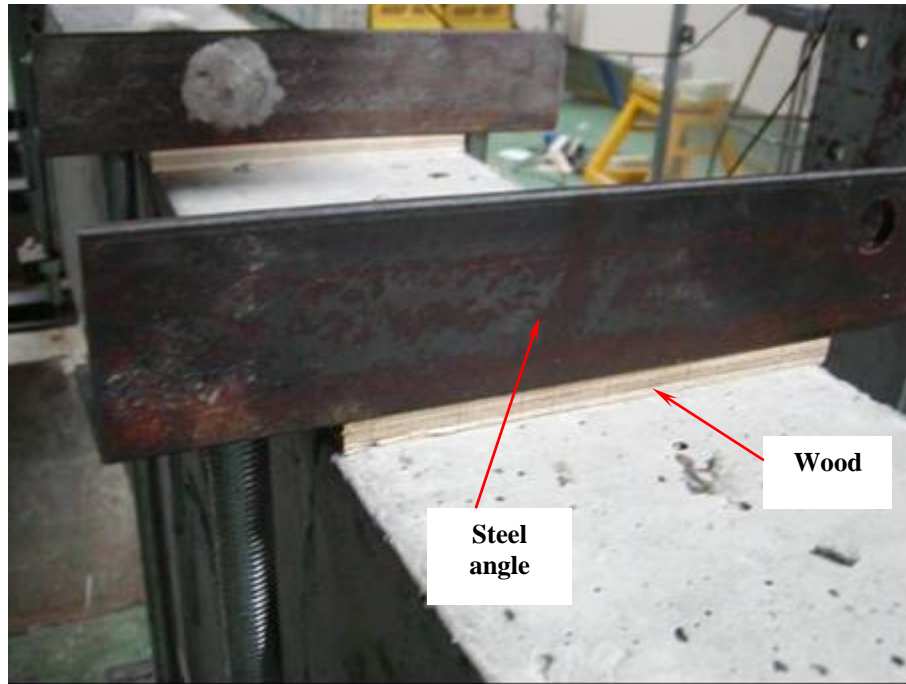
Figure 3.24. Wooden pieces provided in between the concrete and steel

3.6   Repair of Shear Cracks Using Epoxy Resin Injection

Initially, the cracks were sealed using a structural epoxy adhesive paste and filler (Lokset E). After allowing two days for the external seal to cure a low viscosity epoxy (Nitofill LV) was injected through holes at various points along the cracks (see Figure 3.25). The low viscosity epoxy was capable of repairing cracks with width as small as 0.2 mm at the surface and cracking tapering internally down to 0.01 mm. The epoxy was injected from bottom part of the crack to ensure the crack was properly filled with the epoxy. The repaired specimens were kept under normal environmental conditions for curing for a week.
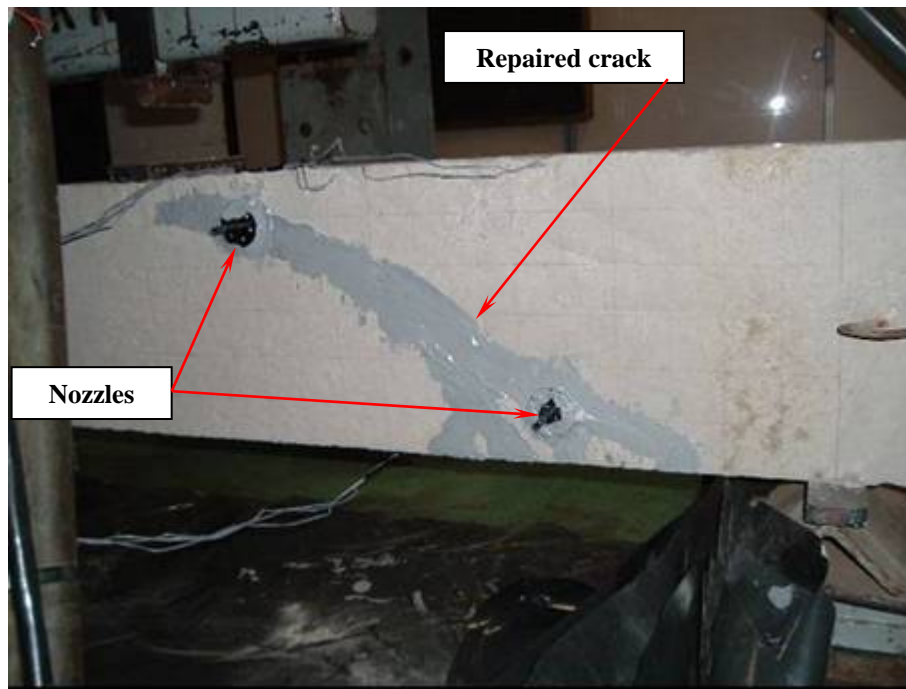
Figure 3.25. Epoxy repaired specimen

3.7   Testing Procedure

All specimens were tested under four-point loading using a monotonically increasing load under a displacement control method. In the test set-up, two wedge type supports were used at both ends of the specimen. The only possible longitudinal force acting in the beam is the friction force. As the beam was designed to have shear failure, the deflection (or curvature) of the beam is small. Therefore, the magnitude of the friction force is also significantly small compared with the applied load. In addition to that, all specimens have same dimensions, tested under same conditions. These will further eliminate the influence of the small friction force on the test results. Therefore, the influence of the longitudinal (friction) force can be ignored. The displacement was applied at a constant rate of 2 mm/min. To generate the shear crack, specimens were loaded up to 90% of their estimated shear capacity.

3.7.1 Testing of Group 1 Specimens

The first specimen EPT11 served as a control beam. A monotonically increasing load was applied to the specimen until its failure. This was loaded without any strengthening.

The second beam EPT12 was pre-loaded to cracking and later strengthened by external post-tensioning and reloaded until failure. Details of the post-tensioning procedure were explained under '*External Post-tensioning*' (Section 3.5.1) in this chapter.

The third specimen, EPT13, was also pre-loaded to cracking and these generated cracks were repaired by epoxy injection. Thereafter EPT13 was strengthened by external post-tensioning and loaded again until failure. Details of the epoxy resin injection can be found under '*Repair of shear cracks using epoxy resin injection*' (Section 3.6) in this chapter.

The last beam, EPT14, was strengthened by external post-tensioning and tested under monotonically increasing loading. This simulated the condition of a new beam with external post-tensioning. These test variables are summarised in Table 3.10.

Table 3.10: Test variables for external post-tensioned specimens

Specimen	Preloading	Epoxy Repair of Cracks	External Post-tensioning	Remarks
EPT11	No	No	No	Control Specimen
EPT12	Yes	No	After preloading	-
EPT13	Yes	Yes	After Repair	-
EPT14	No	No	Yes	Uncracked specimen

3.7.2 *Testing of Group 2 Specimens*

As explained above in this chapter, Group 1 and Group 2 specimens were prepared to investigate the effect of shear reinforcement ratio. Therefore, Group 2 specimens were tested under the same conditions as Group 1.

3.7.3 Testing of Group 3 Specimens

The control beam ECL31 was loaded until failure. Other specimens were strengthened by external clamping.

Specimen ECL32 was initially loaded up to about 90% of the estimated capacity and then unloaded. Then vertical clamping was applied to the specimen (Figure 3.21) which was reloaded until failure. Details of the clamping procedure are explained under '*External Clamping*' (Section 3.5.2) in this chapter.

Specimen ECL33 was initially loaded up to about 90% of the estimated capacity and then unloaded. Then the specimen was repaired using epoxy resin injection before vertical clamping was applied to the specimen. Finally the specimen was reloaded until failure.

Specimen ECL34 was strengthened with vertical clamping without any initial cracks and loaded to failure.

Specimen ECL35 was tested similarly to ECL33. However, the initial loading was applied up to the peak load then unloaded. This means that the specimen was loaded almost to failure before it was repaired using epoxy resin injection.

Specimens ECL36 and ECL37 were also initially loaded up to about 90% of their estimated capacity and then unloaded. Inclined clamping was applied, as shown in Figure 3.22, to both specimens before they were reloaded to failure. Specimen ECL37 was repaired using epoxy resin injection before applying the external clamping.

The last specimen ECL38 was strengthened with combined vertical and inclined clamping as shown in Figure 3.23. This arrangement was chosen to avoid local crushing of the concrete due to a 'wedge' action of the force near to the loading point

(see Figure 3.26) that occurred in the specimens with inclined clamping. The test variables are summarised in Table 3.11.
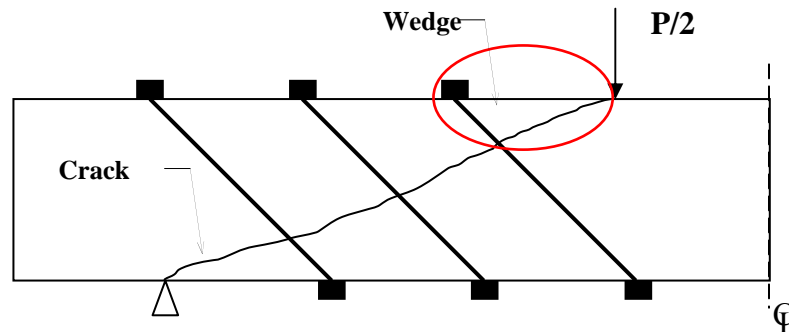
Figure 3.26. Failure area due to 'wedge' action

Table 3.11: Test variables for external clamping specimens

Specimen	Preloading	Epoxy Repair of Cracks	Strengthening Technique
ECL31	No	No	No
ECL32	Yes	No	Vertical clamping after preloading
ECL33	Yes	Yes	Vertical clamping after repair
ECL34	No	No	Vertical clamping
ECL35	Yes	Yes	Vertical clamping after repair
ECL36	Yes	No	Inclined clamping after preloading
ECL37	Yes	Yes	Inclined clamping after repair
ECL38	Yes	No	Combination of vertical and inclined clamping after preloading

3.8   Safety Assessment

Workshop health and safety is emphasized heavily in civil engineering laboratories at the University of Southern Queensland. As this experimental program involved a heavy loading machine, post-tensioning, handling of epoxy resins and construction of significantly heavy reinforced concrete specimens, there were a number of safety issues involved.

Simple safety measures were observed for the construction and loading of the specimens. Steel capped boots were worn at all times and hard hats were worn when the specimens were loaded. Other pieces of personal protective equipment (PPE) were worn for specific activities during the construction. These included safety glasses when cutting reinforcement with a cutting wheel and a dust mask when grinding the sealant off the beam.

During the post-tensioning process the following safety precautions were taken to avoid any possible hazardous incidents. These methods were adopted from guidelines for prestressing and other good practices developed over the years at USQ:

- To avoid possible injures if post-tensioning rods slipped or broke, no-one stood behind the ends of the rods during stressing or loading;

- Additional nuts were placed as 'stoppers' in each post-tensioning rod as shown in Figure 3.27 to prevent possible slipping or breakage of post-tensioning rods during loading and post-tensioning process;

- Warning signs were displayed to advise that stressing was in progress.
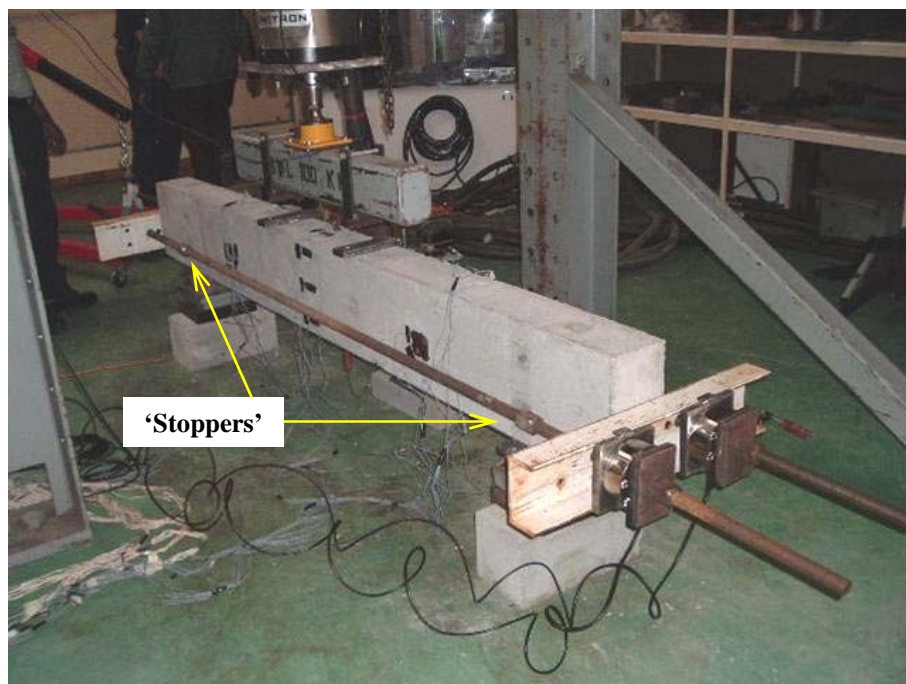
Figure 3.27. 'Stoppers' placed in the external post-tensioning rod

Reference was made to relevant material safety data sheets (MSDS) so that safety issues relating to the use of epoxy resins were known. As the epoxy resins use in these tests are toxic if swallowed and can cause skin and eye irritation, gloves were worn when using the resins and care was taken to avoid contact with the skin.

Furthermore, before starting the experimental program the author undertook the *General Safety Induction Construction Industry* course provided by Downs Group Training (Provider No. 1719), Australia. In addition, the test set-up and loading arrangements were checked and a detailed risk assessment was prepared by the University safety officer. The risk assessment sheet prepared for this research is included in Appendix A.

3.9   Summary

Details of the experimental program carried out in this research study were presented in this chapter. In order to achieve the objectives of the research a total of sixteen beams were tested under three groups, with a monotonically increasing load. The parts of the experimental program explained in this chapter were:

- design and preparation of test specimens;
- testing of material properties;
- measurement and instrumentation;
- testing procedure.

Further details of some of the data and product descriptions explained in this chapter can be found in Appendix A. The results obtained from this experimental program are given and discussed in the following chapter.

Chapter 4
EXPERIMENTAL RESULTS

This chapter presents a summary of experimental results obtained from the sixteen specimens tested in the civil engineering laboratory at the University of Southern Queensland and discussion of these results. Experimental setups including specimen design, construction and instrumentation were explained in Chapter 3.

As explained in Chapter 3, for each specimen data was collected through more than 20 data channels connected to the data acquisition system (System 5000). Since data was collected at a sampling rate of 1 Hz, a large amount of data was obtained. A summary of the data (filtered) is given in Appendix B.

4.1   Overview of the Experimental Results

The experimental results of the sixteen beams tested are summarised in Table 4.1. The table summarises the main features of each specimen including concrete strength, ultimate load and approximate cracking load. Other characteristics are discussed as appropriate.

Table 4.1: Summary of experimental results

Specimen	Average Compressive Strength [MPa]	Ultimate Load^, P_u [kN]	Cracking Load^, P_{cr}* [kN]	Remarks	Failure mode
EPT11	39.9	196	65	Control beam	Shear (ductile)
EPT12	40.3	194	65	Pre-cracked + Post-tensioned	
EPT13	40.4	310	65	Pre-cracked & Repaired + Post-tensioned	Shear (brittle)
EPT14	40.4	354	65	Post-tensioned	
EPT21	29.3	197	55	Control beam	Shear (ductile)
EPT22	32.3	173	55	Pre-cracked + Post-tensioned	
EPT23	40.5	293	65	Pre-cracked & Repaired + Post-tensioned	Shear (brittle)
EPT24	36.5	288	62	Post-tensioned	
ECL31	39.4	176	60	Control beam	Shear (ductile)
ECL32	37.7	262	62	Pre-cracked + Clamped	
ECL33	41.6	279	65	Pre-crack & Repaired + Clamped	
ECL34	37.7	287	65	Clamped	
ECL35	41.6	260	65	Loaded & Repaired + Clamped	
ECL36	41.5	214	65	Failed due to concrete crushing	Concrete crushing
ECL37	40.0	233	65		
ECL38	39.0	243	62		

* Approximate value (load recorded when the first crack was observed)

^ Total load applied to the specimen

It can be noted that the approximate cracking force P_{cr} (force applied when the first flexural crack was observed) is approximately the same in all specimens with a similar concrete strength. The maximum load, P_u, of the specimens varies significantly and this will be discussed in the following sections.

4.2   Failure Mode

As mentioned in Chapter 3 (Section 3.2) all specimens were expected to fail in shear. Nevertheless, some specimens (ECL36, ECL37 and ECL38) failed due to local concrete crushing as shown in Figure 4.1. All other specimens failed in shear as shown in Figure 4.2 and Figure 4.3.

Figure 4.1. Failure due to concrete crushing

The failure mode of Group 1 specimens (with shear reinforcement at 250 mm spacing) is different from that of Group 2 specimens (with shear reinforcement spacing of 180 mm). Group 1 specimens EPT11, EPT12, EPT13 and EPT14 failed with single shear crack appearing in the shear span as shown in Figure 4.2 while specimens in the Group 2 failed with two shear cracks appearing in the shear span as shown in Figure 4.3. It suggests that the additional shear reinforcement in the shear span area supports the load transfer when cracks develop in that section.
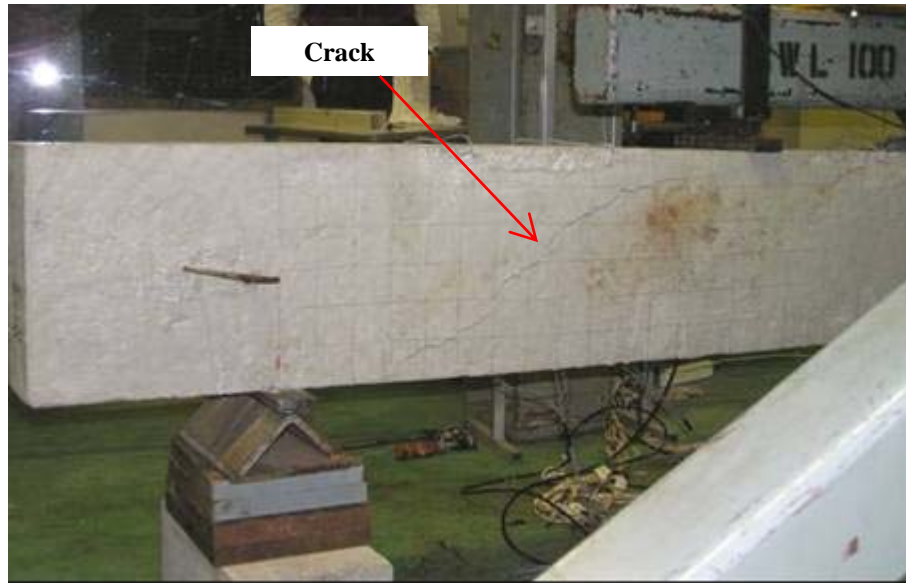
Figure 4.2. Single shear crack appeared in Group 1 specimens
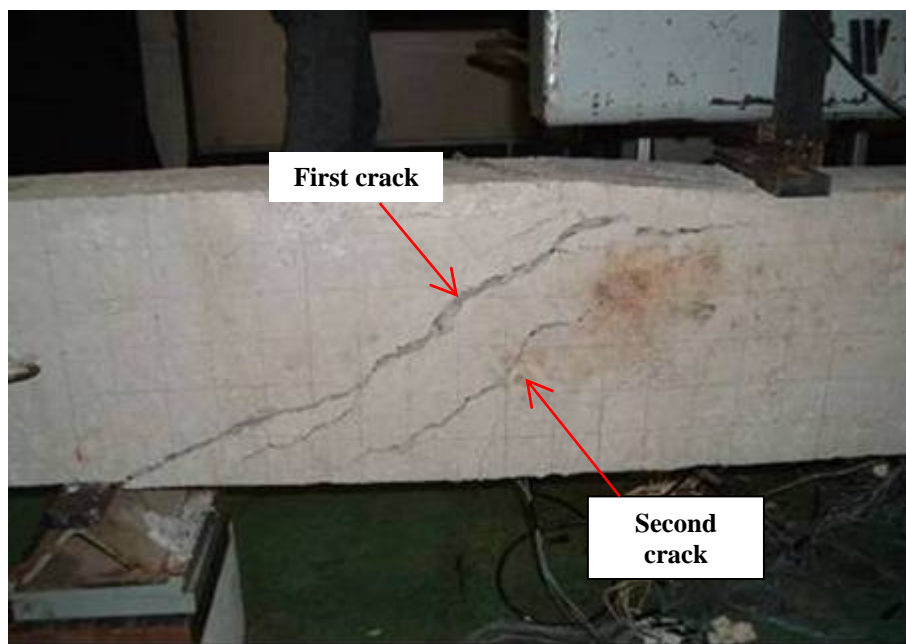
Figure 4.3. Shear failure of Group 2 specimens

The failure mode of specimens with external clamping was much different from the failure mode of specimens with external post-tensioning. As external clamping divided the shear span into a number of segments, many shear cracks developed from the bottom parts of the external clamping as shown in Figure 4.4. This behaviour can be attributed due to "strut-and-tie" action formed by the clamping. More detail about the "strut-and-tie" model is explained in Chapter 5.
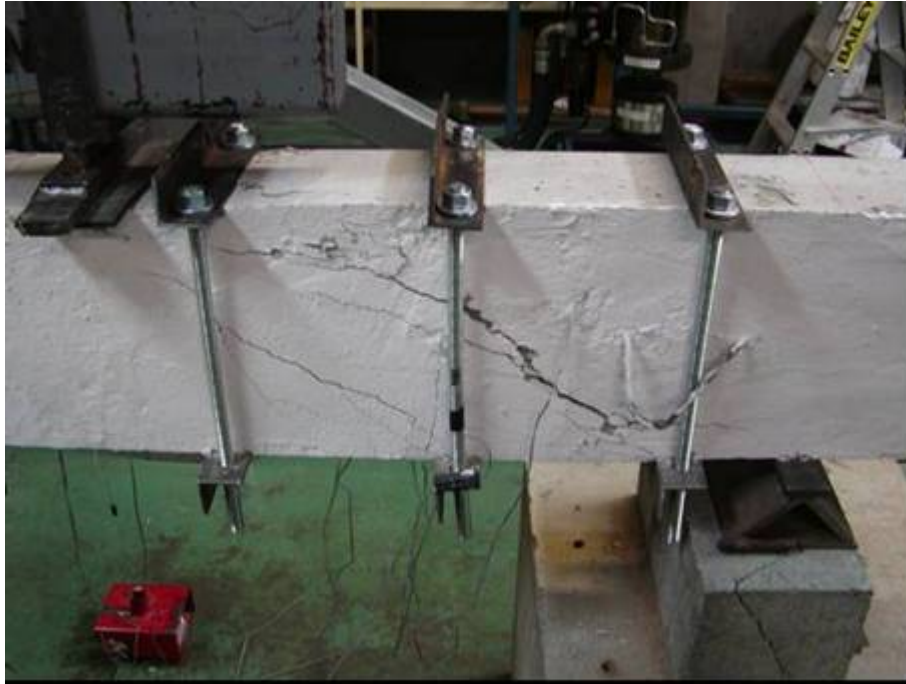
Figure 4.4. Shear cracks appeared in the specimens with external clamping
(Right hand side end of beam is shown)

4.3   Specimens Strengthened By External Post-Tensioning

As mentioned in Chapter 3, there were eight beams tested in two groups to investigate the effect of existing shear cracks in reinforced concrete members strengthened by external post-tensioning. Two different shear reinforcement ratios were used in the specimens.

4.3.1 Behaviour of Specimens during Testing

In this section a brief summary is given on the observed behaviour of the specimens during the experiment. It explains the experimental procedures as well as the effect of shear cracks in the specimens.

4.3.1.1 Group 1 (EPT11, EPT12, EPT13 and EPT14)

Initially, some flexural cracks were observed in the bottom of the mid span section in the control beam EPT11. However, they did not develop further with the increased

load. The first shear crack appeared at 125 kN near the tension side at the support and progressed with further loading. The beam achieved 196 kN before it failed in shear and the load-deflection behaviour is shown in Figure 4.5. The formation of shear cracks reduced its stiffness, as indicated in the figure. The maximum crack width at failure was 2.5 mm (see Figure 4.6).
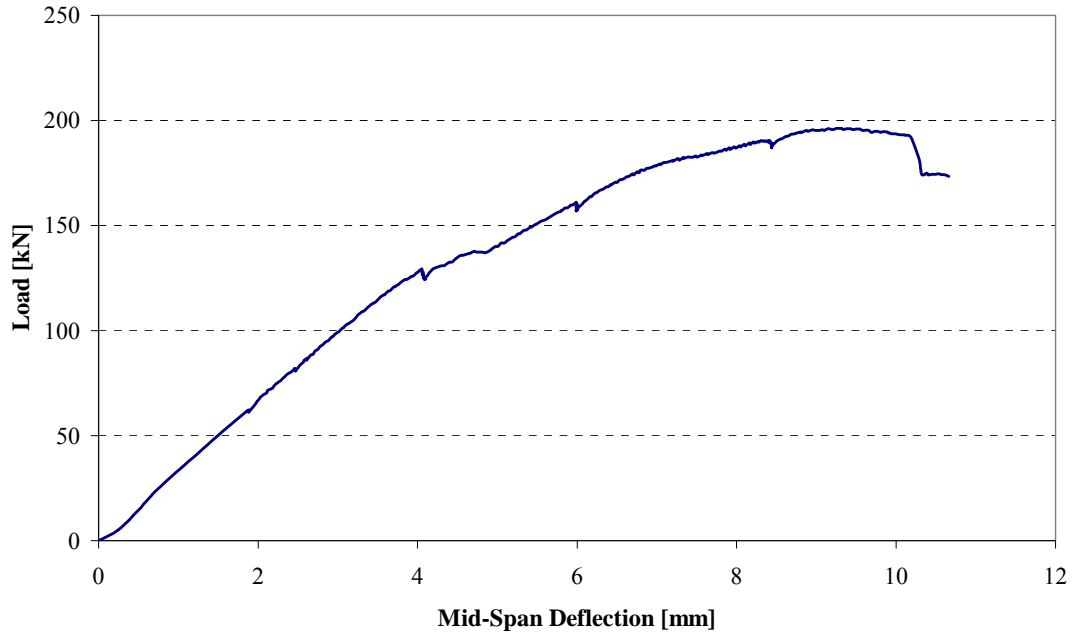
Figure 4.5. Load-deflection behaviour of control specimen EPT11

Figure 4.6. Failure of control specimen EPT11
(Right hand side of the specimen is shown)

The second beam, EPT12, was initially loaded up to 90% (about 180 kN) of its estimated capacity to generate the initial shear cracks. The formation of cracks and the beam's performance (see Figure 4.7) were very similar to EPT11. The applied load was then released and the beam was strengthened. After applying a 152 kN post-tension force using external rods, the specimen was reloaded until failure. Even though high prestress was applied, external post-tensioning did not fully close the initial shear cracks. The same cracks further widened and led to failure during the second stage of loading, as shown in Figure 4.8. The failure occurred at 194 kN, slightly lower than the load on the control beam. The load-deflection curve of EPT12 is shown in Figure 4.9. At the maximum load, the crack width was 3 mm and it increased to 8 mm at failure.
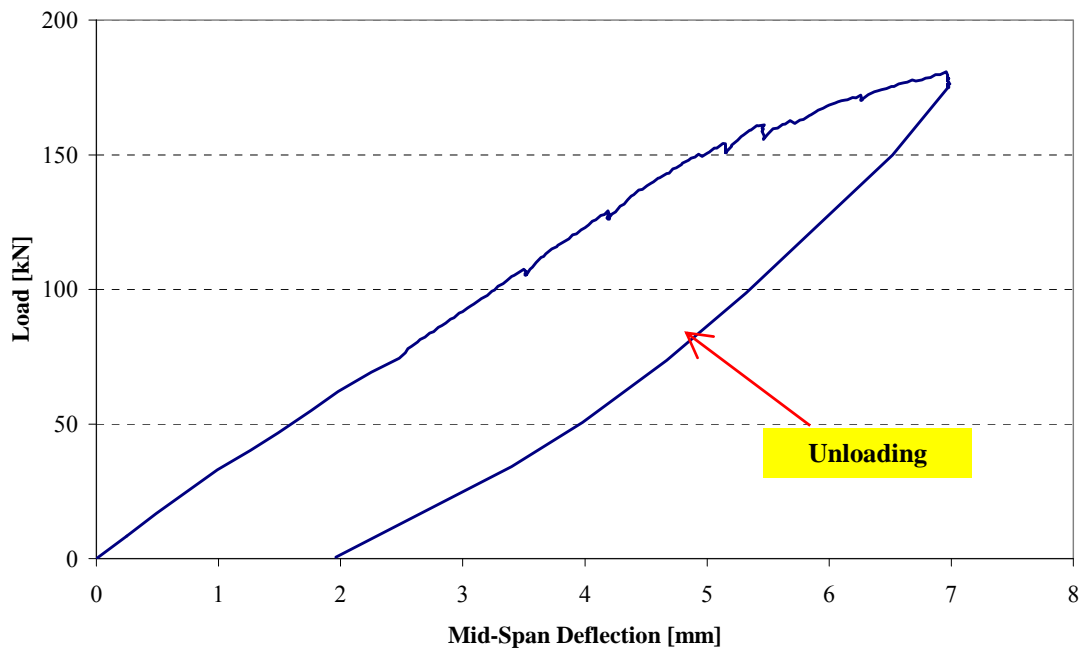
Figure 4.7. Initial loading of EPT12

Figure 4.8. Failure of EPT12 (Post-tensioned without crack repair)
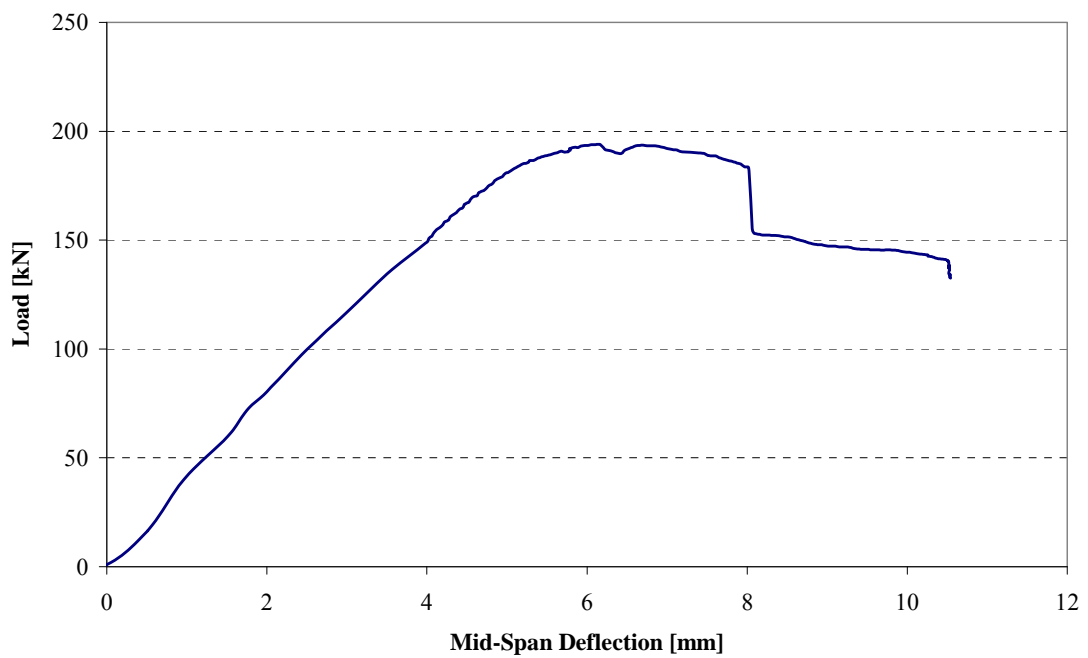
Figure 4.9. Load-deflection behaviour of EPT12

The third specimen, EPT13, was loaded the same way as EPT12 and initial shear crack generated. The cracks were repaired with epoxy injection and left for a week to cure the resin and to develop a good bond. Then the specimen was post-tensioned to 150 kN, similar to EPT12, and reloaded until failure. An interesting result was observed in the crack propagation. A new shear crack developed leading to failure of the beam (Figure 4.10). The repaired cracks did not open-up again during the

subsequent loading. This suggested that the epoxy repair was properly done. Furthermore, it increased the capacity of the member to 310 kN, a 58% increment on the control beam capacity. Brittle failure was observed in specimen EPT13, which was very different from EPT12. The change in failure mode is evident from the sudden drop in the load after the peak in the load-deflection curve (shown in Figure 4.11) for specimen EPT13. At maximum load the crack width was 3 mm and 7 mm at failure.
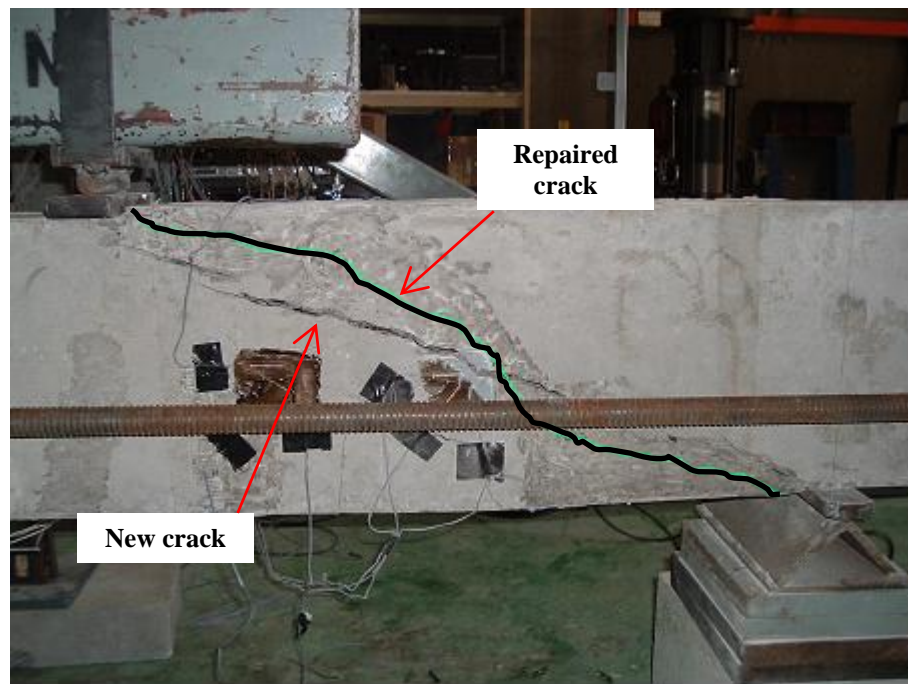
Figure 4.10. Failure of EPT13 (Post-tensioned after epoxy repaired)
* Repaired crack is highlighted
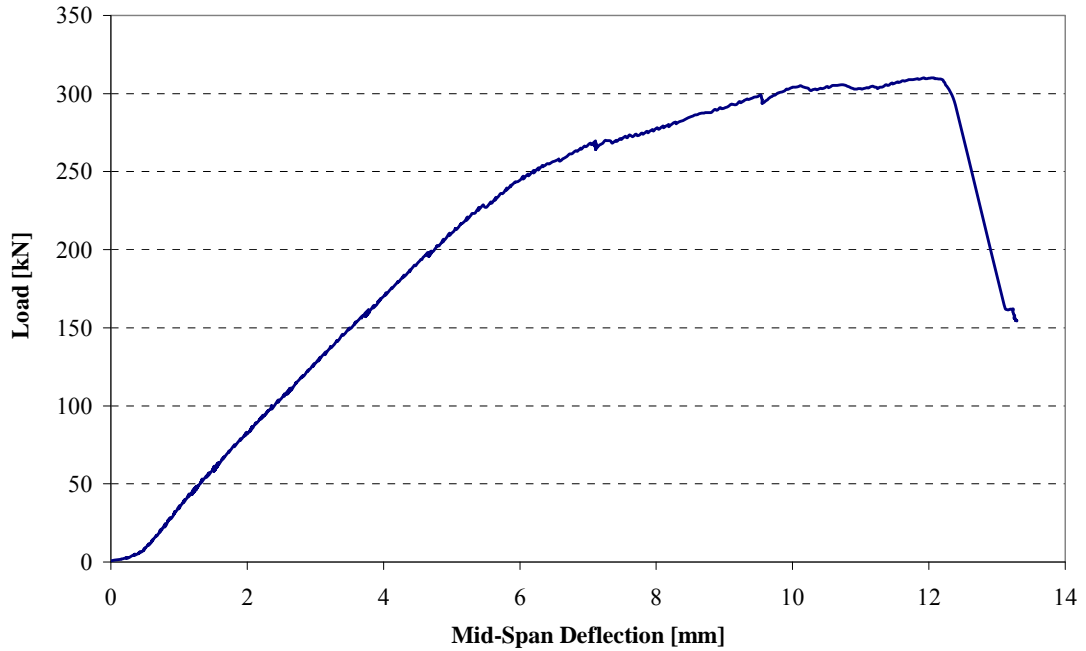
Figure 4.11. Load-deflection behaviour of EPT13

The last beam of Group 1, EPT14, was tested to determine the effect of external post-tensioning on the uncracked reinforced concrete beam. The beam was strengthened with same post-tensioning force of 152 kN and tested under similar loading conditions. The load-deflection behaviour of EPT14 is shown in Figure 4.12. The beam reached an ultimate load of 354 kN before it failed due to shear. The failure mode of EPT14 is similar to that of EPT13.
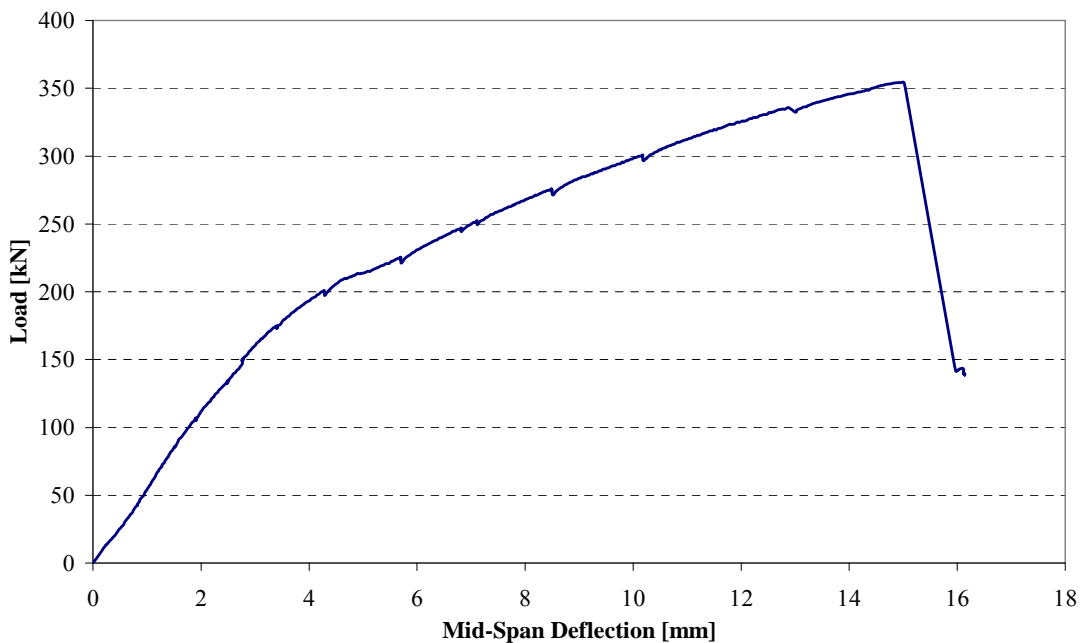
Figure 4.12. Load-deflection behaviour of EPT14

Force in the post-tensioning bars (tendons) will increase as the deflection of the beam increases, due to the expansion of the bars length. This variation of the external post-tensioning force for beams EPT12, EPT13 and EPT14 is shown in Figure 4.13.
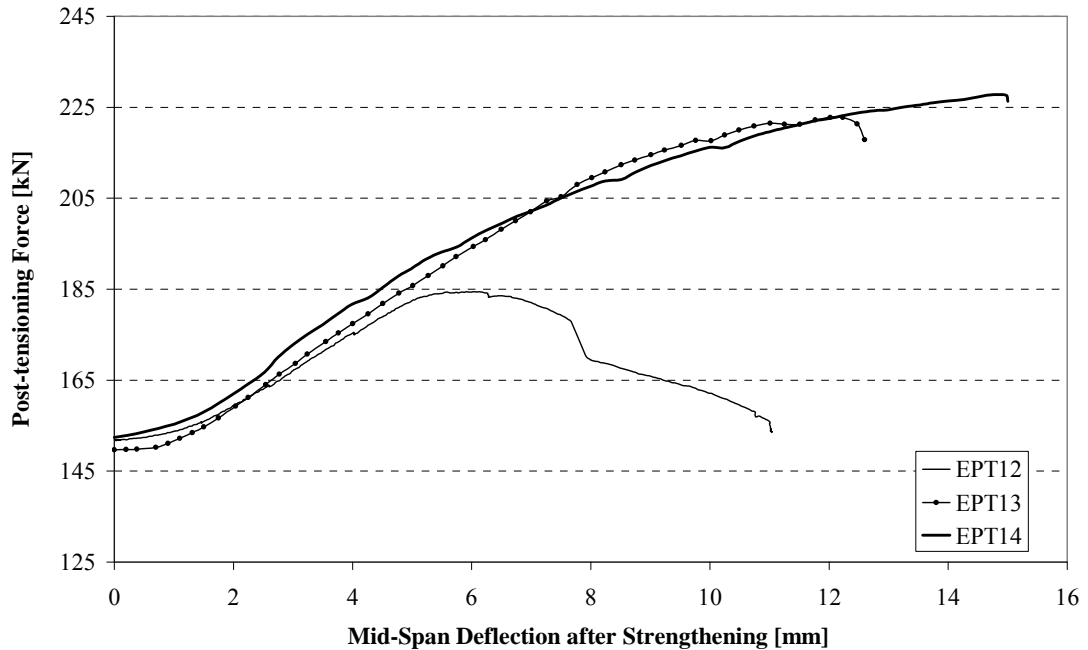
Figure 4.13. Increase in external post-tensioning force with deflection of the beams

It can be noted that the post-tensioning force in specimens EPT13 and EPT14 has increased dramatically more than that of specimen EPT12. This means that beam EPT12 did not expand in length as much as EPT13 and EPT14. The increased values of prestress are summarised in Table 4.2.

Table 4.2: Increase in the post-tensioning force

Specimen	Total Post-Tensioning Force [kN]	
	Initial	**Peak**
EPT11	-	-
EPT12	152	184
EPT13	150	223
EPT14	152	228

The reason for this is that the total deflection that occurred in EPT12 was mainly due to the increasing crack width and not to the beam bending. This further proves that existing shear cracks have a substantial effect on the behaviour of reinforced concrete beams strengthened by external post-tensioning. When a beam was repaired properly by epoxy injection (EPT13), its behaviour was similar to that of the uncracked beam (EPT14). Once again, it shows that the behaviour of a beam can be improved by proper repair of existing cracks prior to strengthening using external post-tensioning. Moreover, epoxy injection could be an effective repair technique for structures that exhibit shear cracks.

4.3.1.2 Group 2 (EPT21, EPT22, EPT23 and EPT24)

The behaviour of specimens in Group 2 was similar to that of Group 1 except for the propagation of shear crack. In the Group 2 specimens, unlike Group 1, two parallel cracks developed during the loading stage and led to failure. As expected, the shear capacities of the Group 2 specimens were also slightly higher than that of Group 1 specimens. The load-deflection behaviour of the control specimen, EPT21, is shown in Figure 4.14. The specimen reached 197 kN before failure.
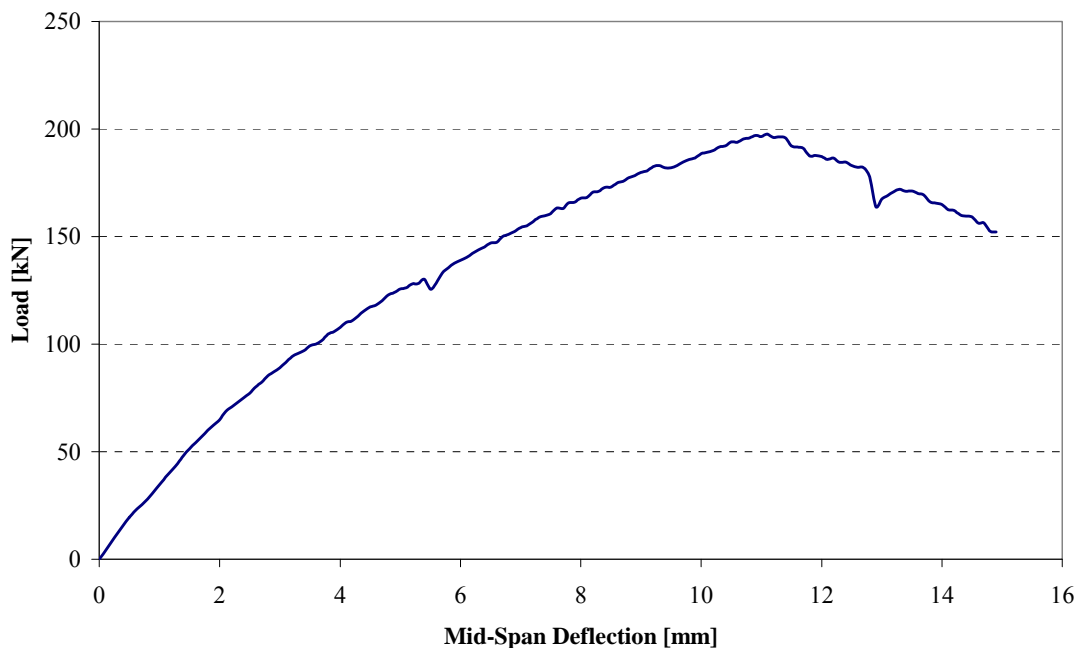
Figure 4.14. Load-deflection behaviour of control specimen EPT21

The load-deflection behaviour of specimen EPT22 after strengthening is shown in Figure 4.15 along with its preloading behaviour. Similarly the load-deflection behaviour of specimens EPT23 and EPT24 are shown in Figure 4.16. It was noted that the behaviour of these specimens was similar to that of the corresponding specimens in Group 1. However, the amount of increase or decrease in capacity after cracking and after repair is different from that of Group 1.
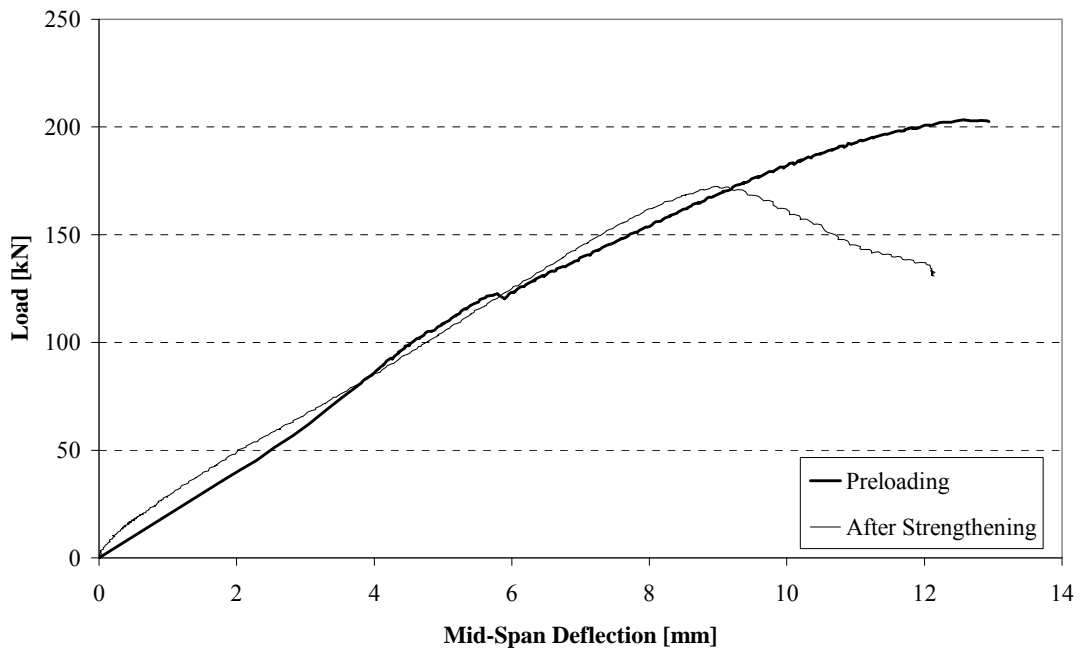
Figure 4.15. Load-deflection behaviour of EPT22
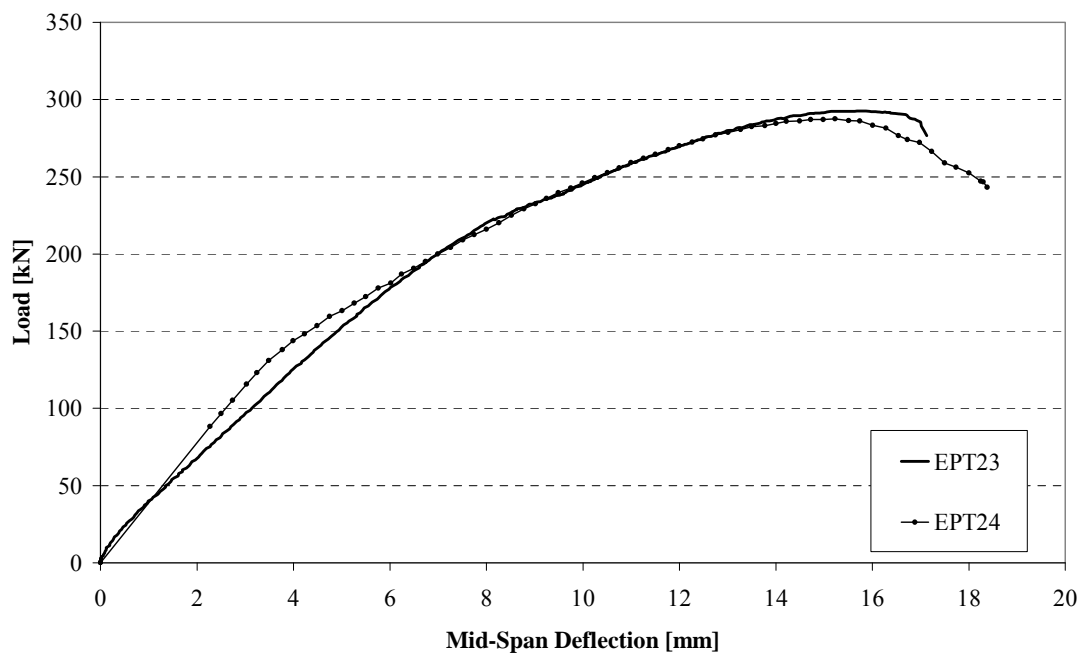
Figure 4.16. Load-deflection behaviour of EPT23 and EPT24

It should also be noted that, due to the low strength of the concrete (32.3 MPa) compared to other specimens, some cracks developed on the top of specimen EPT22 during the post-tensioning process. However, specimens EPT23 and EPT24 that were tested a week later reached a strength of more than 35 MPa and no cracks were observed on the top of these specimens during the strengthening process. The variation in the force of external post-tension for this particular group was similar to Group 1 specimens, which is given in Appendix B.

A summary of the experimental results for specimens in Group 1 and 2 are listed in Table 4.3 below.

Table 4.3: Summary of the experimental results of external post-tensioned beams

Specimen	Average Compressive Strength [MPa]	Preloading [kN]	Ultimate Load [kN]	Maximum Deflection at Centre Point[*] [mm]
EPT11	39.9	-	196	9.4
EPT12	40.3	181	194	5.2
EPT13	40.4	188	310	13.1
EPT14	40.4	-	354	15.3
EPT21	29.3	-	197	11.1
EPT22	32.3	202	173	9.2
EPT23	40.5	177	293	17
EPT24	36.5	-	288	14.2

[*] Measured (after post-tensioned, if applicable) at the time of the maximum load

4.3.2 Effect of Shear Cracks

It is evident from the above observations and Table 4.3 that, existing shear cracks have a substantial impact on the capacity of a reinforced concrete member strengthened by external post-tensioning. This section will look at the main parameters that may have influenced the effect of shear cracks on the behaviour of such members. The following parameters are discussed in this section:

- amount of shear reinforcement;

- repair by epoxy resin;

- strength of concrete.

4.3.2.1 Effect of Shear Reinforcement Ratio

Two different amounts of shear reinforcements were used to investigate the effect of shear reinforcement on the behaviour of shear cracks in a reinforced concrete member that was strengthened by external post-tensioning. Specimens of Group 1 had two stirrups within the shear span while Group 2 specimens had three within the same area. Since the concrete strength varies between the specimens, the capacities need to be normalised by concrete strength.

As the concrete strength differs between the specimens in Group 1 and 2, the ultimate capacities need to be normalised to understand the effect of the shear reinforcement ratio on the behaviour of the cracked and repaired beams. According to the Australian Standard AS3600 (Standards Australia 2001), the influence of shear reinforcement on the shear capacity is given by the term V_{us} and the influence of concrete is given by V_{uc} (Equation 2.6). For the convenience of the reader, Equation 2.6 is reproduced below:

$$V_u = V_{uc} + V_{us} \qquad (4.1)$$

As given in Equations 2.8 and 2.9 (Chapter 2), the ultimate shear strength of concrete, V_{uc}, can be expressed as a function of $\left[f_c'\right]^{1/3}$, where f'_c is the characteristic strength of concrete. Therefore the ultimate load, P_u obtained from the experiment was normalised by dividing by $\left[f_c'\right]^{1/3}$ in order to eliminate the influence of the concrete strength.

Figure 4.17 compares the contribution of the normalised ultimate load of each specimen from Groups 1 and 2. It can be noted from the results that, the effect of shear reinforcement in cracked beams is very minimal compared with that of repaired or new beams. This implies that the existing shear cracks have a substantial

effect on the capacity of a reinforced concrete beam when beams have minimum or near minimum shear reinforcement within the shear span area.
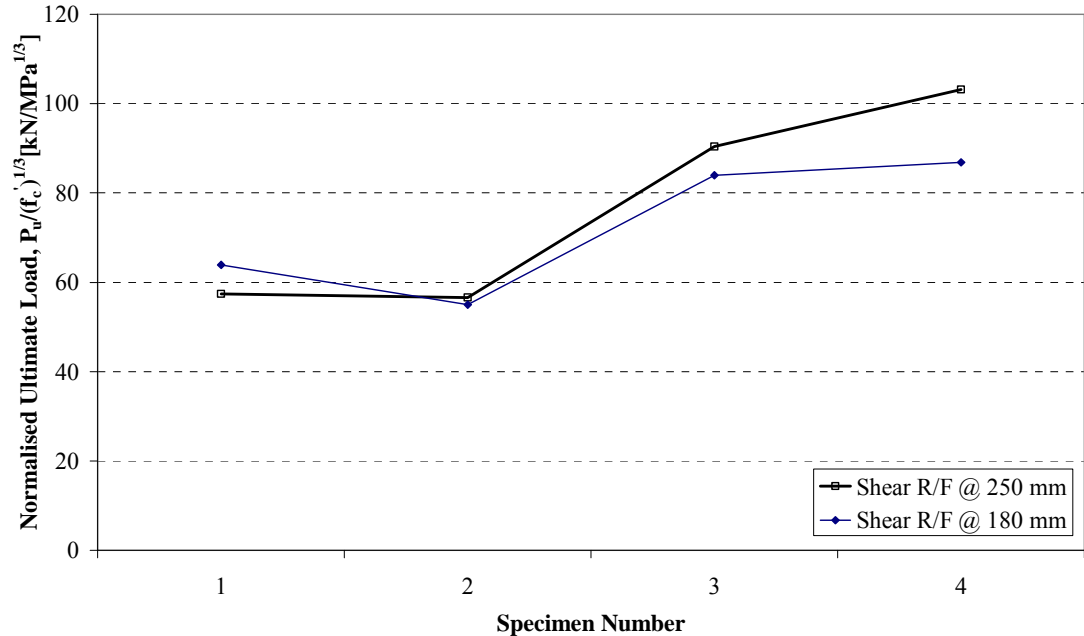
Figure 4.17. Effect of shear reinforcement ratio on the shear capacity

4.3.2.2 Effect of Repair of Cracks by Epoxy Resin

As part of this research study, the efficiency of repairing existing shear cracks using epoxy injection was investigated. As discussed in Chapter 2, experiments reported by Pantelides et al. (2001) are the only other investigations reported in this area. From these current research results it can be seen that epoxy resin repair could significantly increase the capacity of a shear damaged reinforced concrete beam. Due to limited resources only one type of epoxy resin was used in this experimental work. A parametric study simulating different resin types is presented in Chapter 6.

4.3.2.3 Effect of Concrete Strength

It was noted that the concrete strength of the specimens differed significantly between the two groups and this could affect the shear capacity of the specimens. However, with only two specimens of each type in the experimental program, it is not possible to explain in detail the effect of the concrete strength. A parametric

study simulating different concrete strengths and discussion on the effect of concrete strength are presented in Chapter 6.

4.3.2.4 Effect of External Post-Tensioning

It can be seen that the increase in external post-tension was substantial in beams with no shear crack or when the cracks were fully repaired using epoxy injections. In both groups, it was evident that when the crack was not repaired, the post-tensioning was not effective. This is shown by a drop in the external post-tensioning force, where it is believed that the aggregate interlocking was not effective, thus making the beam to slide along the crack.

4.3.2.5 Variation in Strain in Steel Reinforcement

The measured strain variation with applied loading is discussed in detail in Appendix B.5.2. It was noted that the shear reinforcements reached the yield strain in all the specimens, while the main steel reinforcement did not yield at mid span.

4.4   Specimens Strengthened by External Clamping

In Group 3, eight test beams were strengthened by external clamping. Loading and support conditions were the same as for Groups 1 and 2. Each specimen was clamped in both of their shear spans using high strength mild steel rods. Three pairs of rods were used in each shear span and each rod was given a same 15 Nm torque. Four beams were clamped vertically (ECL32, ECL33, ECL34 and ECL35); two were clamped with rods inclined about 45^0 to the vertical (ECL36 and ECL37); one beam (ECL38) was clamped with a combined (vertical and inclined) technique; and one was tested as control beam without any clamping (ECL31). Details of the external clamping and instrumentations can be found in Chapter 3.

The behaviour of the control beam, ECL31, was similar to that of the control beams of Group 1 and 2; EPT11 and EPT21. Control beam, ECL31, exhibited flexural

cracks at the bottom of mid span section at a load of about 100 kN. However, they did not appear to develop further with an increasing load until 110 kN. The first shear crack appeared at 110 kN and progressed with further loading. The control beam reached a load of 176 kN before failure. The load-deflection behaviour of this control beam is shown in Figure 4.18. Except for the initial seating error, the behaviour of the control beam was linear until about 120 kN. The formation of shear cracks reduced its stiffness, which is indicated in the Figure at a load of about 120 kN. The maximum crack width at failure was about 6 mm. The failure mode of the control beam is shown in Figure 4.19.
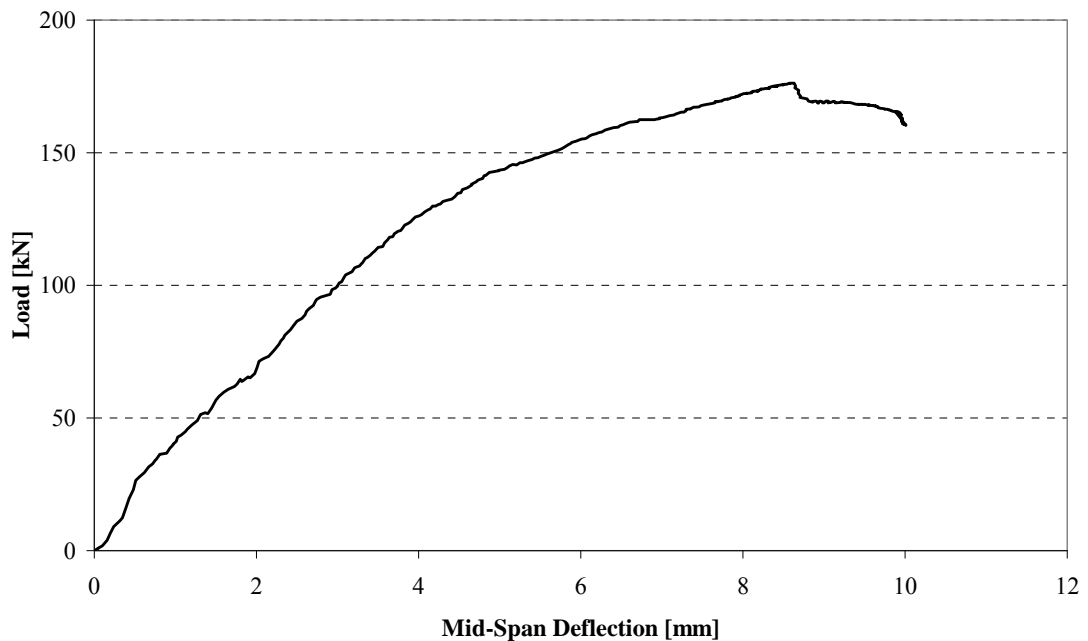
Figure 4.18. Load-deflection behaviour of control beam ECL31

Figure 4.19. Failure of control beam ECL31

4.4.1 Specimens with Vertical Clamping

Specimen ECL32 was loaded up to 145 kN to generate the initial shear cracks in the specimen. The formation of cracks and the beam's behaviour were similar to those of control beam ECL31. The load was released and the beam was strengthened by vertical clamping. Then the specimen was reloaded until failure. It was noted that the original crack reopened during the reloading process and some local shear cracks also developed between the vertical clamping as shown in Figure 4.20. The specimen later failed at a load of 262 kN. The load-deflection relationship for ECL32 is shown in Figure 4.21. A maximum crack width of 11 mm was observed at failure.
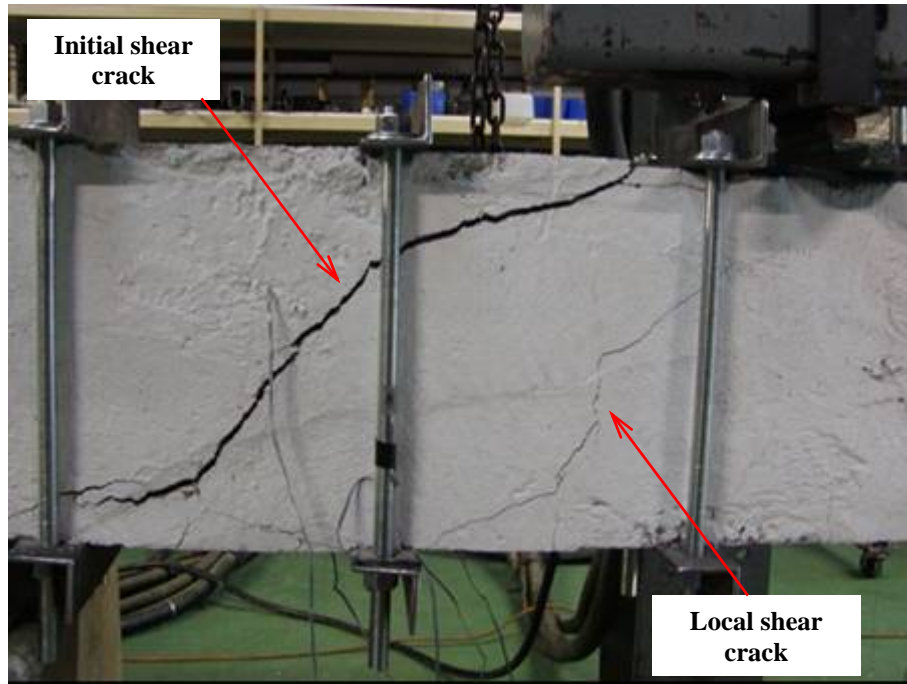
Figure 4.20. Failure of ECL32

Figure 4.21. Load-deflection behaviour of ECL32 plotted with ECL31

Specimen ECL33 was loaded in the same way as ECL32 and the initial crack generated. The behaviour of ECL33 during this preloading was observed to be similar to that of specimen ECL32. The cracks were repaired with epoxy injection and a week was allowed for the resin to cure and to develop a good bond. Then the specimen was externally clamped, similar to ECL32, and reloaded. A completely

new shear crack developed and lead to failure of this beam as shown in Figure 4.22. The beam reached a load of 279 kN before failure. The repaired crack did not open up during the whole reloading process. This suggested that epoxy resin injection is an efficient repair technique which significantly reduces the effect of existing shear cracks. Furthermore, it also increased the capacity of the member to 279 kN which is 18 kN higher than specimen ECL32. Load-deflection relationship including preloading for the ECL33 is shown in Figure 4.23.
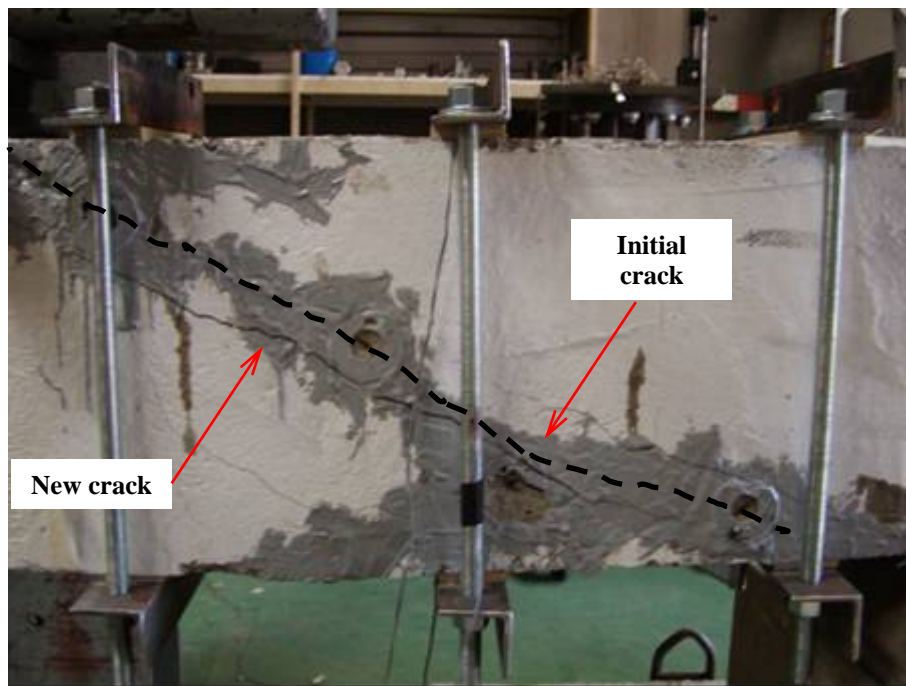
Figure 4.22. Failure of ECL33
(Initial crack is highlighted)
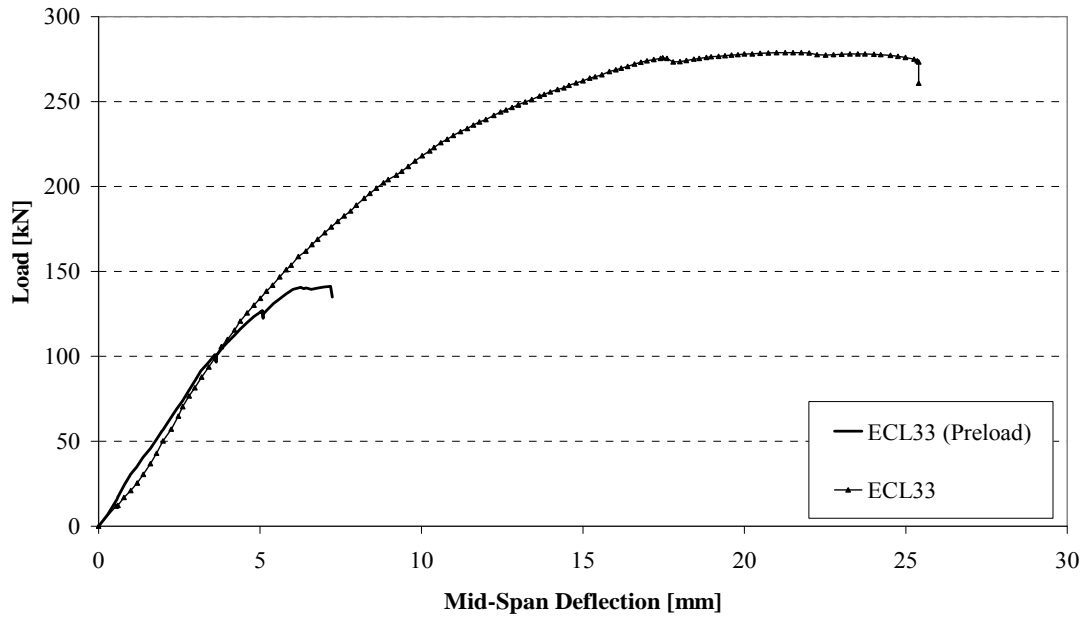
Figure 4.23. Load-deflection behaviour of ECL33

Specimen ECL34 was initially strengthened by vertical clamping and then loaded until failure. Clamping force was applied using 15 Nm torque as with the other specimens in Group 3. This uncracked RC beam with vertical clamping failed at a load of 287 kN. The major shear crack and local shear cracks were observed to be similar to those of ECL33 (Figure 4.24).
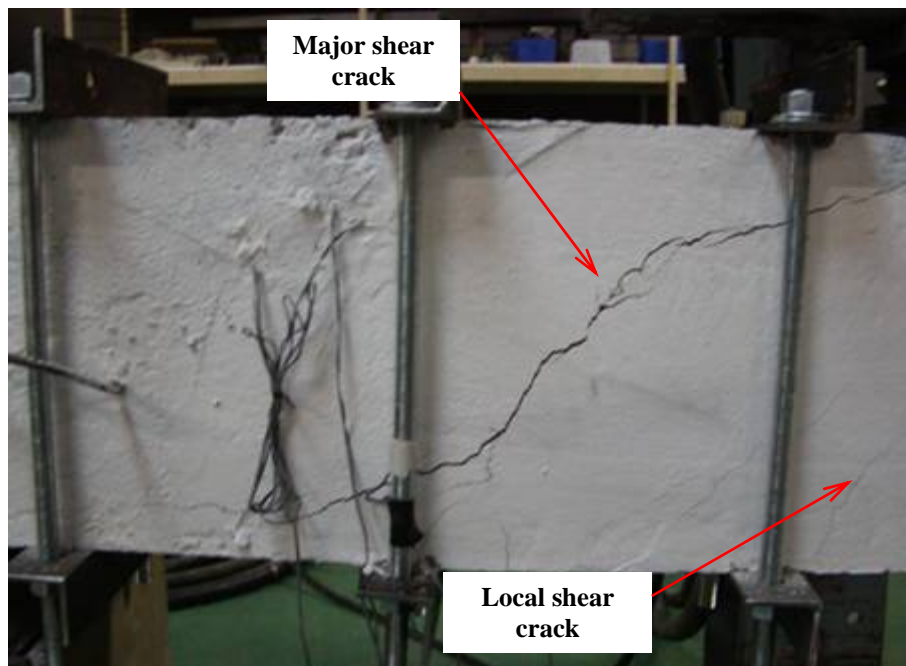
Figure 4.24. Failure of ECL34

Specimen ECL35 was repaired with epoxy resin after it failed during the preloading. The repaired specimen was strengthened by vertical clamping and retested. It was noted during repair that the repaired crack width was considerably large (6 mm). However, the specimen reached a load of 260 kN before failure. This shows that, even with a crack width of 6 mm which is significantly large for a reinforced concrete beam, the epoxy resin could significantly increase the capacity of the member.

The load-deflection behaviour of specimens ECL34 and ECL35 are shown in Figure 4.25. With reference to the load-deflection behaviour of all specimens it can be noted that, after strengthening, specimen ECL33 showed more ductile behaviour than ECL32 and that the behaviours of ECL33 and ECL34 were very similar. This implies that the epoxy repair technique can improve the behaviour of a cracked specimen to match the behaviour of an uncracked specimen. Since specimen ECL35 was repaired after failure, it showed the most ductility among the Group 3 specimens. However, the capacity of ECL35 did not increase as much as the other repaired specimen, ECL33.
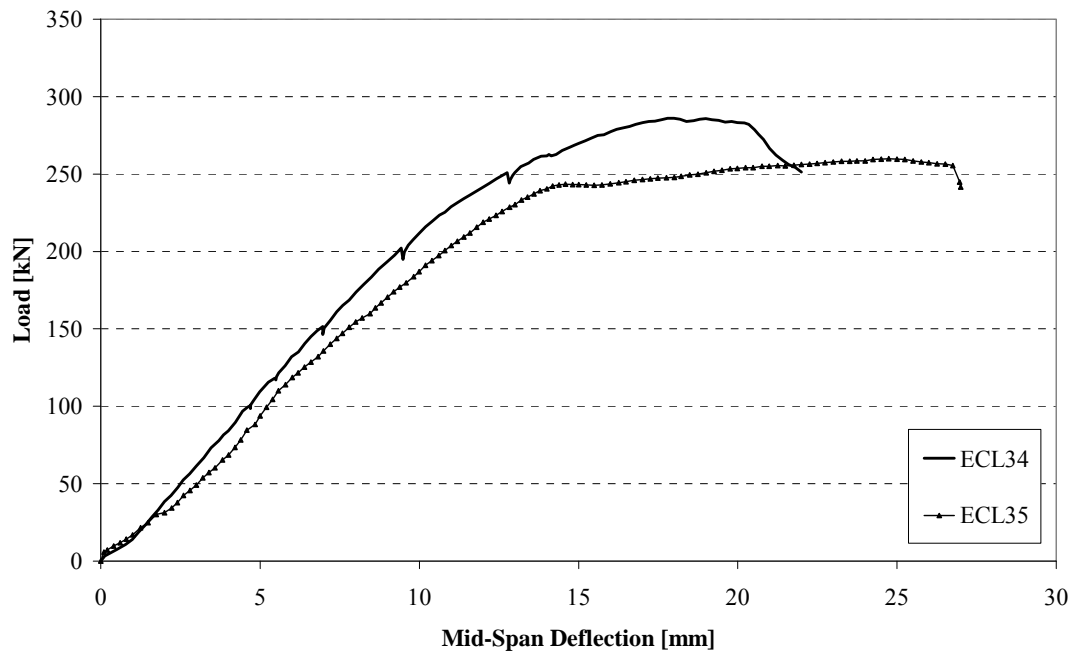
Figure 4.25. Load – deflection behaviour of specimens with vertical clamping

The effect of the external clamping and the epoxy injection can also be seen from the strain variation in the external clamping rods as shown in Figure 4.26. The strain measurement was recorded using the strain gauges attached to the clamping rods.
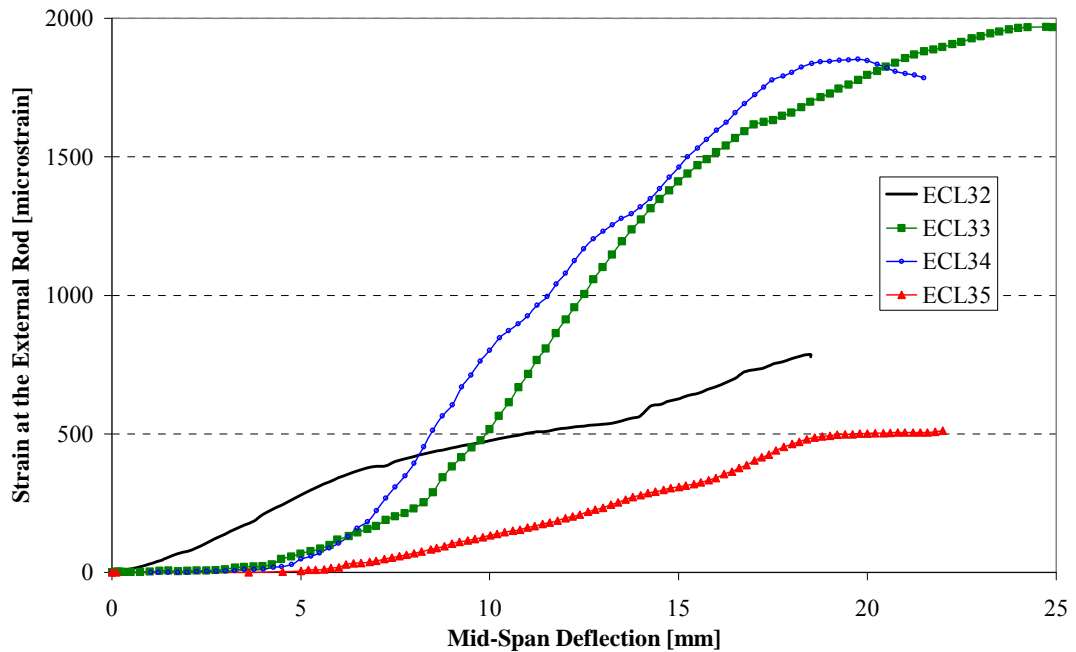
Figure 4.26. Variation of strain in the external clamping rods

It can be noted from Figure 4.25 and Figure 4.26 that, in the beam ECL34, there is no significant strain increase at the external clamping rods until the load reaches about 110 kN, which corresponds to the load at which a major shear crack developed in that specimen. This means that, until the formation of a major shear crack, the contribution of the external clamping in carrying the shear force was insignificant. Beyond the load of 110 kN, the strain in the external clamping increased gradually with the load increase indicating that the external clamping contributed to carrying additional load. As the crack width increased with the loading, the stress transferred through the concrete, which is mostly by aggregate interlocking, decreased. A gradual increment in the force on the external clamping due to this process was observed in the strain gauge readings.

The variation of strain in the external clamping rods of beams ECL33 and ECL35 (repaired with epoxy injection) were similar to that of ECL34. However, the

behaviour observed in specimen ECL32, which was not repaired with epoxy injection, was quite different from the other three specimens. From the strain measurements, it was noted that the force in the external rods increased right from the beginning of the reloading state in specimen ECL32. This implies that the concrete did not contribute much towards carrying the shear loads. In other words, the cracks immediately reopened during the reloading stage leaving the external clamps to take most of the additional loads. From this observation, it can be deduced that the epoxy repair significantly changed the behaviour of the cracked beams.

4.4.2 Specimens with Inclined Clamping

Specimen ECL36 was initially loaded up to 164 kN to create initial cracks. The formation of cracks and the performance of the beam were similar to that of the control beam ECL31. The load was then released and strengthening was carried out by inclined clamping. The same clamping force was applied using 15 Nm torque as vertical clamping. A crack approximately 3.5 mm wide was observed after the release of the loading. This crack width was reduced to less than 3 mm by the clamping. It was also noted that the same crack was reopened during the reloading process. However, the width of the crack was much less than ECL32 (with vertical clamping) for the same load. The inclined clamping restricted the crack opening compared to vertical clamping. Even though the inclined clamping effectively restricted the crack from opening, the specimen failed at a load of 214 kN due to premature crushing of concrete near the loading point (Figure 4.27 and Figure 4.28). A maximum crack width of 8 mm was observed at failure. This premature crushing near the loading zone occurred due to the 'wedge' shape formed by action of tensile forces (force along the existing crack plane and in line with the inclined clamping force) in the failure zone.
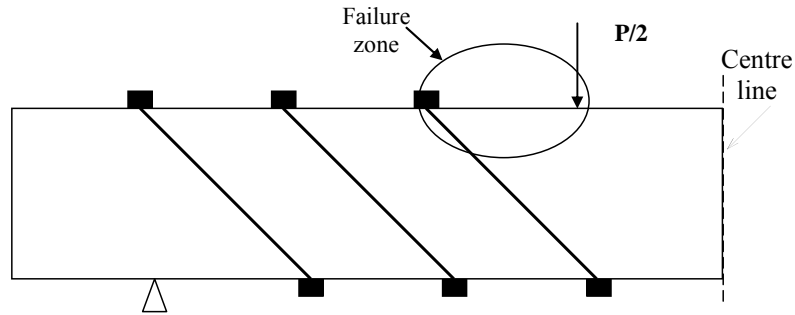
Figure 4.27. Failure zone of ECL36 and ECL37

Figure 4.28. Localised concrete failure near loading point of ECL36 and ECL37

Specimen ECL37 was loaded the same way as ECL36 and a similar progress applied for initial crack generation. After epoxy repair and curing, the specimen was externally clamped (similar to ECL36 – inclined clamping), and reloaded. A completely new shear crack was observed and that lead to failure of the beam. The repaired crack did not open up during the reloading process. This again proves that the epoxy resin injection is an efficient repair technique and significantly reduces the effect of existing shear cracks. Furthermore, it increased the capacity of the member to 233 kN from 214 kN when the crack was unrepaired. However, the beam also failed due to the concrete crushing near to the loading point, similar to ECL36. At the maximum load, the crack width was 4 mm and it increased to 7 mm at failure.

Load-deflection curves for specimens ECL36 and ECL37 are shown in Figure 4.29 along with the preloading curves for those specimens.
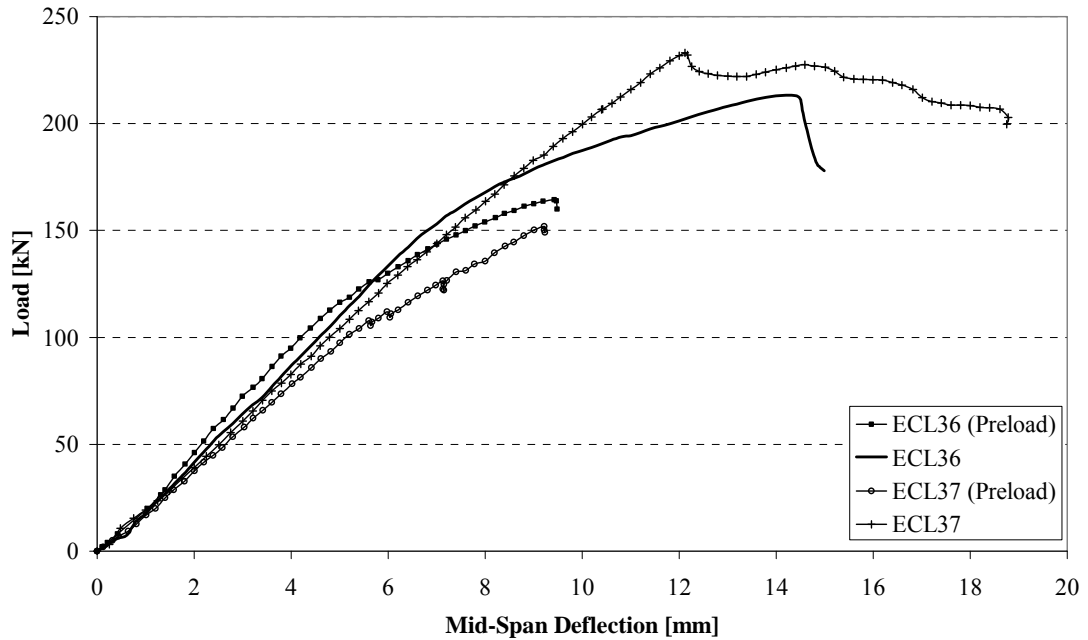
Figure 4.29. Load – deflection curves for specimens with inclined clamping

From the failure of ECL36 and ECL37 it could be concluded that, even though the inclined clamping effectively controlled further opening of the crack in the beam, failure occurred near to the loading point due to high stress concentration, which was further aggravated by the horizontal force component of the inclined clamping. Consequently, the last beam, ECL38, was strengthened with combined vertical and inclined clamping. The vertical clamping rods were placed near the support and the loading point, and the inclined clamping rod was placed in the middle region. With this arrangement the stress concentration was reduced at the loading point and the support region. This specimen was loaded up to 175 kN to generate initial cracks and then strengthened by clamping as described previously and as shown in Figure 4.30. When it was reloaded specimen ECL38 reached a load of 240 kN before failure. The load-deflection curve for specimen ECL38 is shown in Figure 4.31.
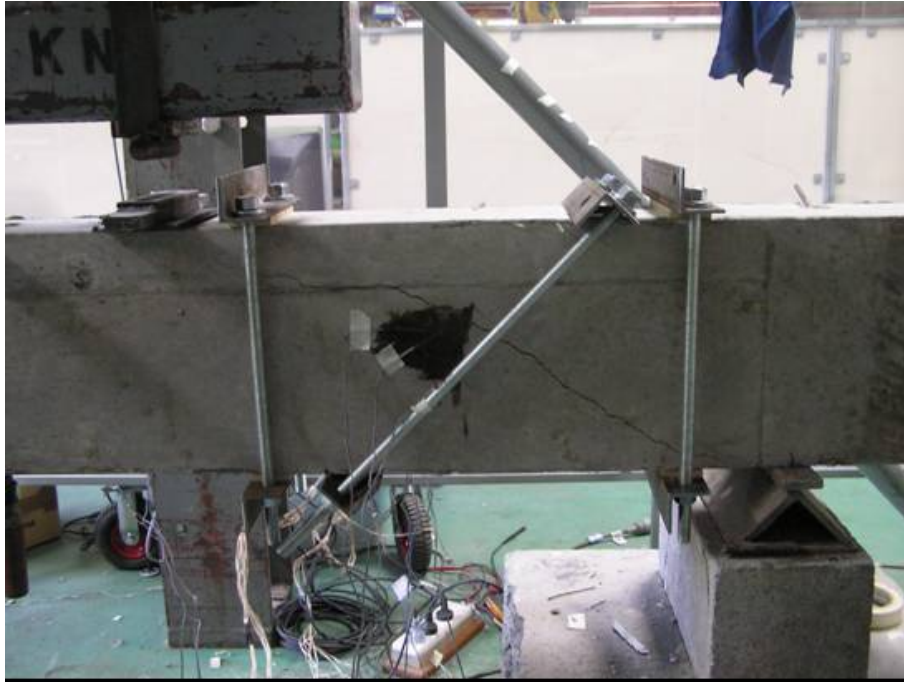
Figure 4.30. Specimen with combined vertical and inclined clamping
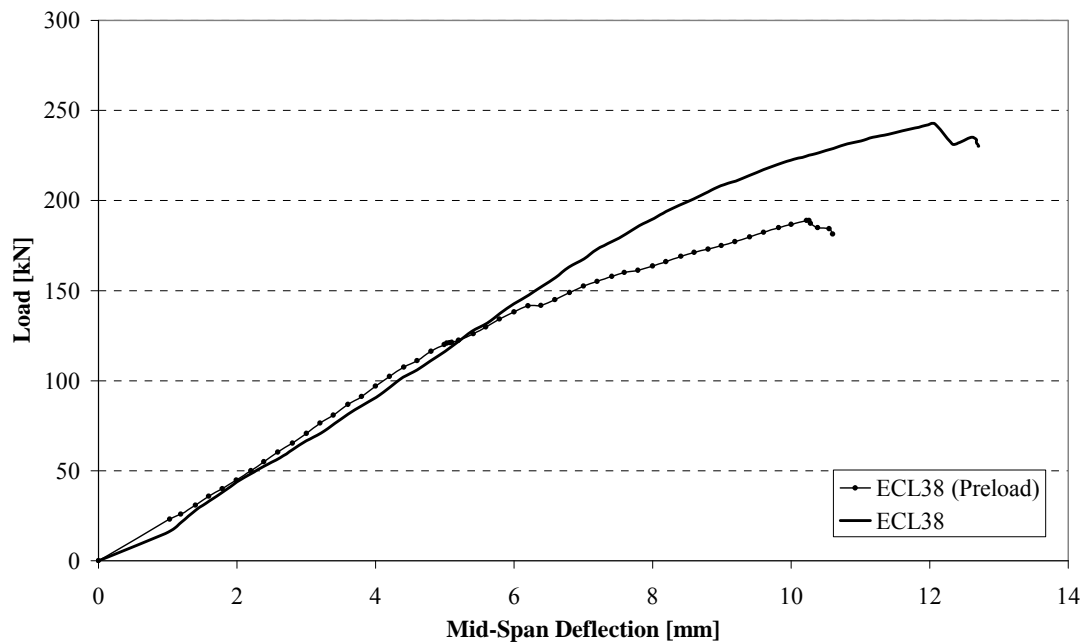
Figure 4.31. Load–deflection curve for ECL38

Although the effect of inclined clamping could not be observed very clearly due to the localised concrete failure near the loading point, the load-deflection behaviours of ECL36, ECL37 and ECL38 show that the epoxy repaired specimen exhibited better behaviour and carried significantly higher load than the un-repaired specimen.

As discussed earlier, the inclined clamping successfully controlled the crack width during the loading. However, due to the premature failure, the effectiveness of the inclined clamping could not be investigated in detail. Furthermore, specimens ECL36 and ECL37 failed even before the yielding of external clamping rods due to this premature failure (see Appendix B for detail discussion regarding the variation of stain in external clamping rod of specimens ECL36 and ECL37). Therefore, further investigation is necessary to explain the effectiveness of the inclined clamping technique. The test results are summarised in the Table 4.4.

Table 4.4: Summary of the experimental program of external clamping

Specimen	External Clamping Technique	Average Compressive Strength [MPa]	Initial Loading [kN]	Ultimate Load, P_u [kN]	Maximum Mid-Span Deflection[*] [mm]	Gain[^] in Ultimate Load [%]
ECL31	Control beam	39.4	-	176.2	8.6	-
ECL32	Vertical	37.7	144.8	262.3	14.0	48.9
ECL33	Vertical	41.6	141.3	278.9	21.2	58.3
ECL34	Vertical	37.7	-	286.6	17.6	62.7
ECL35	Vertical	41.6	176.0	260.0	24.8	47.6
ECL36	Inclined	41.5	164.6	213.7	14.3	21.3
ECL37	Inclined	40.0	151.8	233.0	12.1	32.2
ECL38	Combined (Vertical + Inclined)	39.0	189.0	242.6	12.1	37.7

[*] Measured (after clamping, if applicable) at the time of the maximum load

[^] 'Percentage gain' is with respect to the control beam's ultimate load

4.5   Summary

Based on the experimental results and discussion presented in this chapter, the following conclusions have been reached:

General Behaviour of Shear Damaged Reinforced Concrete Beams

- Existing shear cracks have a substantial effect on the shear capacity of reinforced concrete members.

- The width of existing cracks influences the behavior of these beam members.

- A suitable crack repair technique must be determined for concrete members with existing shear damage before attempting to strengthen them by external post-tensioning. An epoxy resin injection technique was found to be effective for crack repairs in this study.

- The failure of all the epoxy repaired beams, regardless of the type of strengthening method, was similar to that of new beams strengthened with the corresponding technique. In particular, the crack development was very similar to a new beam. This suggests that the injection of epoxy resin into shear cracks is an effective repair technique in shear strengthening.

External Post-Tensioned Specimens

- Unrepaired existing shear cracks have a significant effect on the capacity of a reinforced concrete beam strengthened by external post-tensioning. It was observed that, even with a higher post-tensioning force, the member capacity did not increase.

- The proper repair of existing shear cracks can increase the capacity of a member be as much as 70% when externally post-tensioned.

- The external post-tensioning force increased up to 50% of its initial value during the loading process.

Specimen with External Clamping

- Strengthening by external clamping can be used to reduce the effect of existing shear cracks.

- Vertical clamping is a more effective method to increase the member capacity than inclined clamping. However, both external clamping methods effectively reduced the reopening of existing shear cracks.

- Inclined clamping might be an effective technique to reduce the effect of shear cracks provided that localised concrete failure due to high stress concentration can be avoided. The appropriate positioning of inclined clamping could prevent

the localised crushing near the loading point, which needs to be further investigated.

Further research is needed to determine a more effective strengthening technique for shear damaged reinforced concrete members. As a small number of specimens were tested in each case, the above experimental results regarding the effect of existing shear cracks in a reinforced concrete beam are not generally conclusive. Therefore, numerical analysis was used to investigate the effect of shear damage in a reinforced concrete member. This numerical investigation is presented in the following chapters.

Chapter 5

NUMERICAL ANALYSIS
METHODOLOGY

In order to understand the effect of existing shear cracks in a reinforced concrete beam, a comprehensive numerical analysis was conducted. This was completed in two phases as follows:

1.　Simple mathematical method – to develop a simple mathematical model to explain the behaviour of the shear damaged reinforced concrete beam.

2.　Finite element method (FEM) – to model the shear damaged reinforced concrete member and analyse using a finite element package.

This chapter presents a brief summary of the numerical analysis and verifications of the models based on the results obtained from the experimental program (Chapter 4).

5.1　Objectives of the Numerical Study

Overall goal of the numerical study related to this study was to develop a reasonably accurate method to determine the behaviour of shear damaged reinforced concrete members strengthened by external post-tensioning. To understand the influence of various parameters on the behaviour of such members, first a simplified

mathematical model was developed to estimate the capacity of such members based on the modified compression field theory (Vecchio and Collins 1986) and the strut-and-tie model (Tan and Naaman 1993). Later a finite element analysis was completed using a commercial finite element package, Abaqus (Version 6.6).

The objectives of this numerical study were as follows:

- development of a simplified mathematical model to estimate the capacity of cracked reinforced concrete members strengthened by external post-tensioning or external clamping;

- verification of the simplified mathematical model using the experimental results;

- development of a finite element model to describe the behaviour of a shear damaged reinforced concrete beam;

- verification of the finite element model using the results of the experimental program described in Chapter 4.

5.2   Simplified Model to Estimate the Shear Capacity

As explained in Chapter 2 current design codes including AS3600 (2001), and various empirical equations proposed by researchers to estimate the shear strength of a reinforced concrete beam are defined by functions of a number of primary design parameters such as the compressive strength of concrete, the amount of tensile reinforcement and the size of the beam. However, most of the proposed equations were developed for an uncracked beam and, therefore, do not explain the influence of any existing shear cracks on the capacity of a beam. In this section, a theoretical approach to predict the shear capacity of shear damaged reinforced concrete beams strengthened by external post-tensioning is presented. For this purpose, the following two basic theories were considered:

- strut-and-tie model;

- modified compression field theory.

5.2.1 Strut-and-Tie Model

The strut-and-tie model was developed on the basis that concrete is strong in compression (compression struts) and steel is strong in tension (tension ties). The basic concept of the model is to visualize a truss-like system (see Figure 5.1) to transfer load to the supports where:

- compressive forces are resisted by concrete "struts";

- tensile forces are resisted by steel "ties"; and

- struts and ties meet at "nodes".
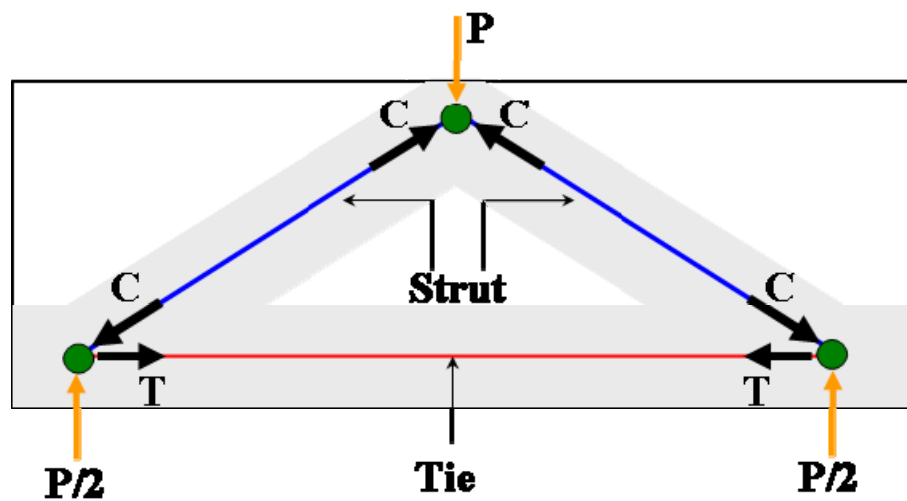
Figure 5.1. Basic concept of the strut-and-tie model

When a structure is subjected to external loads, the stresses and internal forces of that structure can be plotted and visualized in the form of trajectories. The trajectory patterns and the motion of forces flowing from the loaded edges throughout the structure and into the supports give very helpful information to enable the correct understanding of the load-bearing performance of a given structure. However, trajectory patterns are fairly complicated and are, at best, available only for linear elastic material behaviour. Accordingly, in the case of an RC structure in which concrete exhibits cracking and plastic deformation and in which the paths of the tensile forces must follow the reinforcement, the stress trajectories need to be simplified and adopted to suit the specific characteristics and properties of structural concrete. Based on these factors, a more generalized truss model named the "strut-and-tie model" was developed and is broadly applied to all kinds of RC members

and entire structures (Dux 2007; Tan and Naaman 1993; Wight and Parra-Montesinos 2003; Zwicky and Vogel 2006).

The strut-and-tie model approach evolves as one of the most useful design methods for shear critical members. Basically this model provides a rational approach by representing a complex structural member with an appropriate simplified truss model. Due to this reason, there is no single, unique strut-and-tie model for most design situations encountered. In this study, strut-and-tie model is used to predict the crack pattern of externally post-tensioned reinforced concrete beams. Comparison of strut-and-tie model predicted crack pattern with experimental results can be found in Appendix D.

5.2.2 Modified Compression Field Theory

Modified compression field theory (MCFT) was introduced in 1986 by Vecchio and Collins (1986) and was developed from the original compression field theory developed by Mitchell and Collins (1974). In these theories, the relationship between average stresses and strains was postulated based on experimental observations. Cracks, in these theories, are treated in a distributed sense.

The following assumptions apply to the modified compression field theory:

- There is a one-to-one correspondence between stresses and strains. That is, the model is non-linear elastic.

- Average stresses and strains are used for all calculations.

- There is perfect bonding between reinforcing bars and concrete (i.e. no slip).

- The longitudinal and transverse reinforcing bars are uniformly distributed.

- The principal strain directions are coincident with the principal stress directions.

Three main components of the modified compression field theory are: equilibrium equations, constitutive relationships and load transmission conditions at cracks. These components are extensively described elsewhere (Vecchio and Collins 1986) and are briefly outlined below for completeness.

5.2.2.1 Constitutive Relationships in Modified Compression Field Theory

The constitutive relationships involved in modified compression field theory are presented in principal stress-strain space. Vecchio and Collins (1986) reported that the principal compressive stress at a point in concrete depends on both the principal tensile and compressive strains, while the principal tensile stress was only dependent on the principal tensile strain (i.e. decoupled from the compressive strain).

The compressive stress is calculated in modified compression field theory as

$$f_{c2} = f_{c2,\max}\left(2\frac{\varepsilon_2}{\varepsilon_o} - \left(\frac{\varepsilon_2}{\varepsilon_o}\right)^2\right),$$ (5.1)

where,

f_{c2} = Average principal compressive stress in concrete,

ε_o = Strain at the peak stress in a uniaxial compression test, and

ε_2 = Average principal compressive strain in concrete.

The factor $f_{c2,\max}$ accounts for the state of biaxial tension-compression state and is calculated as,

$$f_{c2,\max} = \frac{f_c'}{0.8 - 0.34\dfrac{\varepsilon_1}{\varepsilon_o}},$$ (5.2)

where,

f_c' = Compressive strength of the concrete, and

ε_1 = Average principal tensile strain in concrete.

The stress-strain curve of concrete under tension is defined as linear elastic up to cracking as

$$f_{c1} = E_c \varepsilon_1.$$

(5.3)

After cracking, the tensile stress in the concrete is taken as

$$f_{c1} = \frac{f_{cr}}{1 + \sqrt{200\varepsilon_1}}.$$

(5.4)

where,

f_{c1} =   Average principal tensile stress in concrete,

E_c =   Modulus of elasticity of concrete, and

f_{cr} =   Cracking strength of the concrete.

The above stress-strain relationship of the cracked reinforced concrete member is illustrated in Figure 5.2.

(a) Stress-strain relationship for cracked concrete in compression

(b) Proposed relationship for maximum compressive stress

(c) Correlation of test data for cracked concrete in compression

(d) Three-dimensional representation of compressive stress-strain relationship
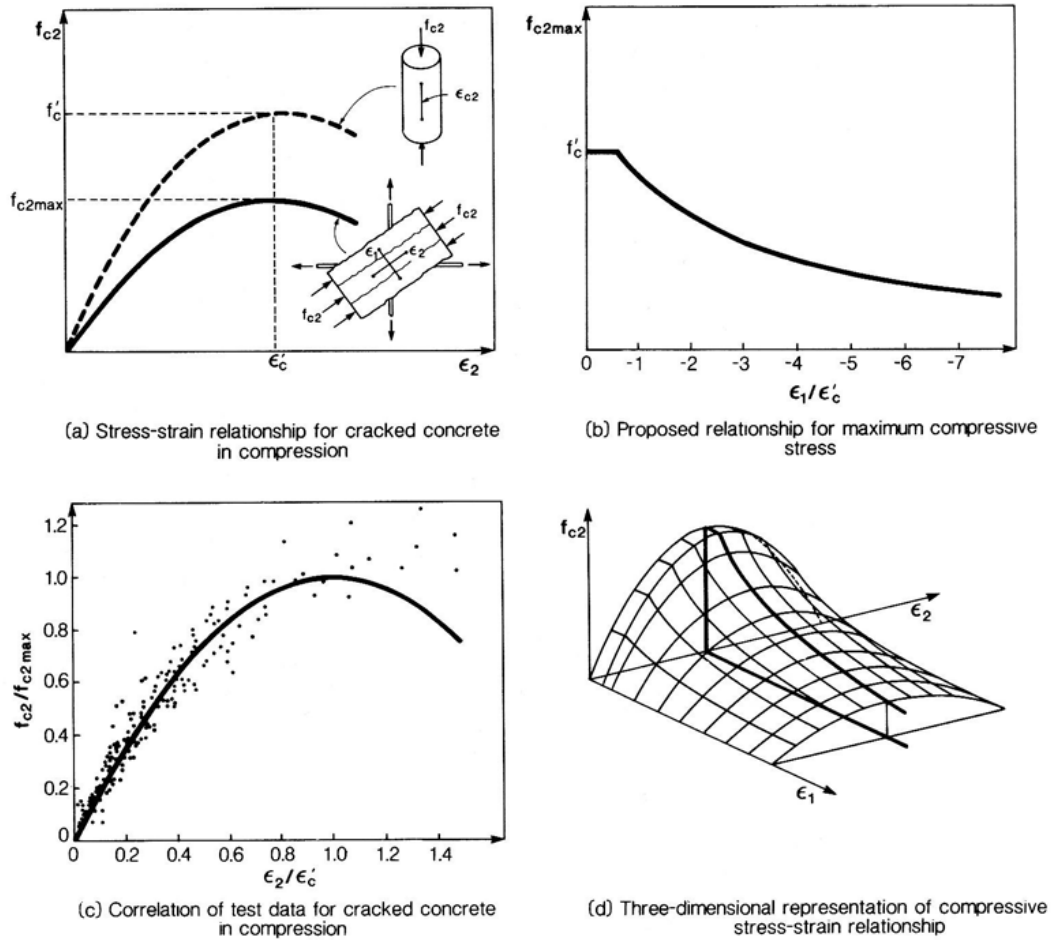
Figure 5.2. Compressive stress–strain relationship for cracked concrete defined in MCFT
Source: Prestressed Concrete Structures (Collins and Mitchell 1991)

5.2.2.2 Equilibrium Equations

Equilibrium equations are used to calculate the average stresses at a point from the concrete and steel contributions. The average shear stress contribution by the steel is neglected in the derivation of the following equilibrium equations.

$$\sigma_x = \sigma_{cx} + \rho_{sx}\sigma_{sx}$$
$$\sigma_y = \sigma_{cy} + \rho_{sx}\sigma_{sy} \qquad (5.5)$$
$$\sigma_{xy} = \sigma_{cxy}$$

where,

σ_x	=	Average stresses in the X direction calculated at a material point in reinforced concrete,
σ_y	=	Average stresses in the Y direction calculated at a material

point in reinforced concrete,

σ_{xy} = Average shear stress calculated at a material point in reinforced concrete,

σ_{cx} = Axial stresses in the concrete in the X direction,

σ_{cy} = Axial stresses in the concrete in the Y direction,

σ_{sx} = Axial stresses in the steel in the X direction,

σ_{sy} = Axial stresses in the steel in the Y direction,

ρ_{sx} = Reinforcement ratios in the X direction, and

ρ_{sy} = Reinforcement ratios in the Y direction,

The X and Y directions are the global coordinate axis system defined along the longitudinal direction and along the depth direction of the beam. Reinforcement ratio in any direction is defined as the total area of reinforcement provided along that direction divided by the effective area normal to that direction (see Equation 2.5 in Chapter 2).

5.2.2.3 Load Transmission Conditions at Cracks

The stress-strain relationships described above are valid in an average sense. However, stresses in the steel at cracks will be higher than their average values. Therefore, it is necessary to ensure that the steel reinforcement is capable of transmitting the demanded average tensile stresses across cracks.

Vecchio and Collins (1986) derived the following conditions which are used to ensure that enough capacity exists in the concrete and steel to properly transmit tension across cracks:

$$\begin{aligned}
\sigma_{sxcr} &= \sigma_{sx} + \frac{1}{\rho_{sx}}\left(f_{c1} + \sigma_{ci} + \frac{v_{ci}}{\tan\theta}\right) \le \sigma_{yx}^{yield} \\
\sigma_{sycr} &= \sigma_{sy} + \frac{1}{\rho_{sy}}\left(f_{c1} + \sigma_{ci} - \frac{v_{ci}}{\tan\theta}\right) \le \sigma_{yy}^{yield}
\end{aligned} \qquad (5.6)$$

where,

σ_{sxcr}	=	Axial stresses in the steel in the X direction at the crack face,
σ_{sycr}	=	Axial stresses in the steel in the Y direction at the crack face,
σ_{ci}	=	Compressive stress acting on the crack,
v_{ci}	=	Shear stress along the shear crack plane, which can be estimated using the Equation 2.10 given in Chapter 2,
θ	=	Angle between the concrete compression strut and the longitudinal axis of the member,,
σ_{yx}^{yield}	=	Yield stress in the X direction, and
σ_{yy}^{yield}	=	Yield stress in the Y direction.

5.2.3 Shear Strength Equation for the Shear Damaged Beams

In this section an attempt has been made to estimate theoretically the shear strength of a shear damaged reinforced concrete beam strengthened by one of the following techniques:

- external post-tensioning – with horizontal tendon profile only;

- external clamping.

Detail of these strengthening techniques can be found in Chapter 3 under Section 3.5. Basically the two existing theories outlined in the Sections 5.2.1 and 5.2.2 are used and extended as appropriate to develop a theoretical model.

5.2.3.1 Reinforced Concrete Beam Strengthened By External Post-Tensioning

Based on the modified compression field theory, the equilibrium of the stress acting on a cracked beam can be shown by the Mohr's circle as shown in Figure 5.3.
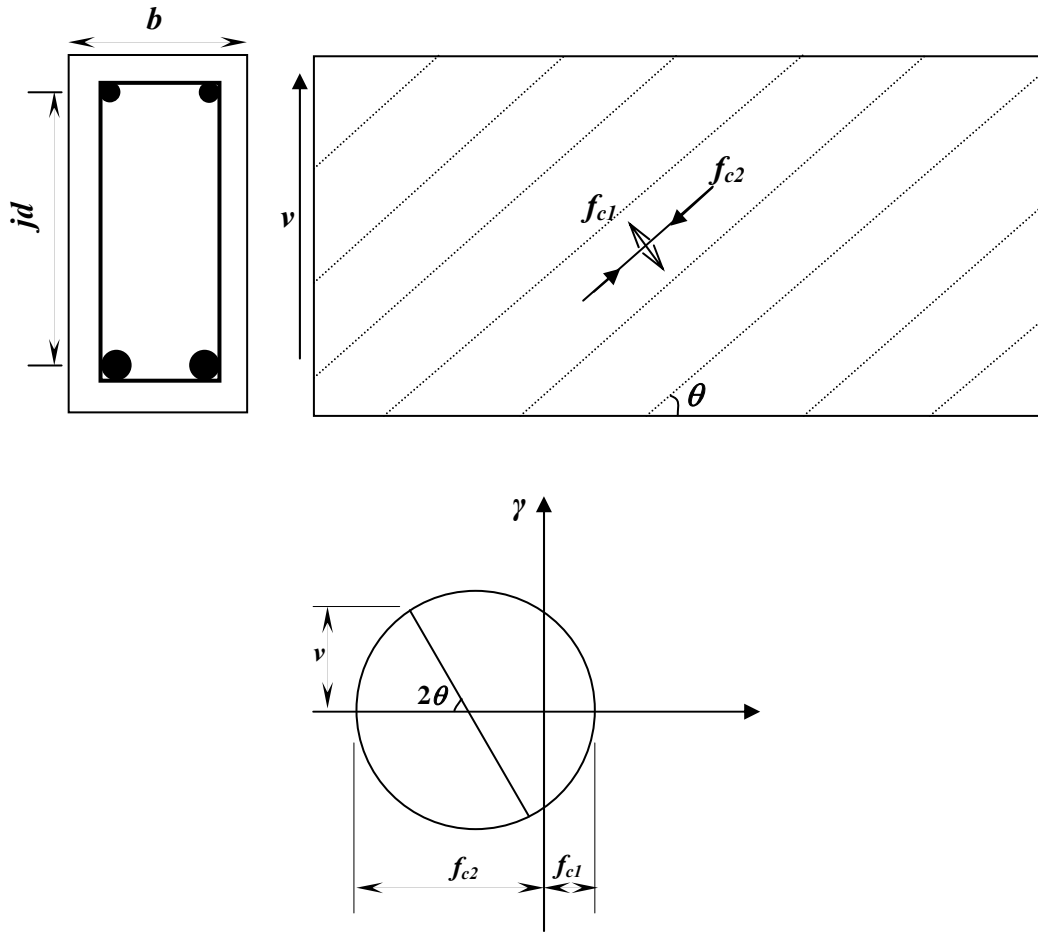
Figure 5.3. Mohr's circle for the equilibrium of the element

From the Mohr's stress circle following relationship can be derived:

$$f_{c2} = (\tan\theta + \cot\theta)v - f_{c1} \tag{5.7}$$

where, the shear stress acting along the section, v, is given by

$$v = \frac{V}{b_v jd} \tag{5.8}$$

where,

V = Shear capacity of the section, and

b_v = Effective width of web for shear (equal to width, b, for rectangular cross section),

jd = Flexural lever arm (the distance between the compressive reinforcement and tensile reinforcement).

To satisfy the equilibrium of the horizontal forces, the following requirement should be satisfied:

$$A_v f_v = \left(f_{c2} \sin^2 \theta - f_{c2} \cos^2 \theta \right) b_v s \qquad (5.9)$$

where,

A_v = Cross section area of shear reinforcement,

f_v = Average stress in the stirrups (shear reinforcement), and

s = Centre-to-centre spacing of shear reinforcement.

Substituting for f_{c2} from Equation 5.7 gives

$$V = f_{c1} b_v jd \cot \theta + \frac{A_v f_v}{s} jd \cot \theta \qquad (5.10)$$

In the above explanation local variation of stresses were not considered. Figure 5.4 shows the local stresses acting along the crack plane.
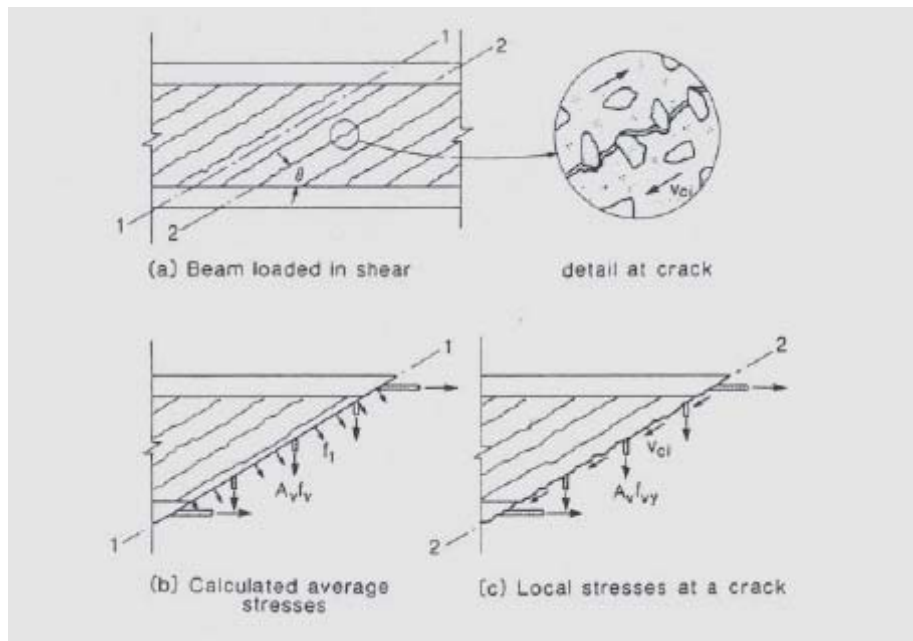
Figure 5.4. Transmitting forces across cracks
Source: Prestressed Concrete Structures (Collins and Mitchell 1991)

To maintain the equilibrium (Figure 5.4) the following condition should be satisfied:

$$f_{c1} = v_{ci} \tan\theta + \frac{A_v}{s\,b_v}\left(f_{sy} - f_v\right)$$

(5.11)

where,

f_{sy} =   Yield strength of shear reinforcement.

By substituting Equation (5.11) into the Equation (5.10), the shear capacity of the cracked beam is given by

$$V = v_{ci} b_v\,jd + \frac{A_v f_{sy}}{s}\,jd\cot\theta$$

(5.12)

With the prestressing tendons the following relationship can be obtained for the equilibrium:

$$A_{sx} f_l + A_p f_p = V\cot\theta - f_{c1} b_v\,jd$$

(5.13)

where,

A_{sx} =   Cross sectional area of longitudinal reinforcement steel,
A_p =   Cross sectional area of prestressing steel,
f_l =   Average stress in the longitudinal reinforcing steel, and
f_p =   Average stress in the prestressing steel.

Now V could be expressed as

$$V = \frac{A_v\,jd}{s}\left(f_{sy} - f_v\right)\tan\theta + \left(A_{sx} f_l + A_p f_p\right)\tan\theta + v_{ci} b_v\,jd\tan^2\theta$$

(5.14)

It should be noted that the expression of the shear capacity of a RC member, V, as the sum of the concrete contribution and the steel contribution (Equations 5.12 and 5.14). That is, it has a similar form as in the AS3600 shear strength equation, where the concrete contribution is replaced by a function of the shear stress acting along the cracked plane, v_{ci}.

5.2.3.2 Reinforced Concrete Beams Strengthened By External Clamping

As explained above, the shear capacity of a cracked beam without external clamping can be given by Equation 5.10 or Equation 5.12. For the cracked beam with external clamping, the clamping is assumed as extra shear reinforcement attached externally. This assumption was made based on the following observations from the experimental program:

- crack was reopened immediately;

- force was transferred through the external clamping immediately after the loading.

Based on the above observations, it is reasonable to assume that the possibility of forming a new strut-and-tie arrangement by external clamping is minimal. By considering this fact coupled with modified compression field theory, the shear capacity of a cracked reinforced concrete beam with external clamping can be expressed as follows:

$$V = f_{c1}b_v jd \cot\theta + \frac{A_v f_v}{s} jd \cot\theta + P_{v,ext} \qquad (5.15)$$

where,

$P_{v,ext}$ =   Force in the external clamping rods within the crack zone.

To calculate the shear capacity using the above equation, it is important to estimate the clamping force as a function of crack width and/or some other known parameters. Detail of this discussion is in Chapter 6.

5.3   Finite Element Modelling of Reinforced Concrete Beams

Even for a simply supported rectangular reinforced concrete beam retrofitted with external post-tensioning, shear failure is a far more complex mechanism than flexural failure. One reason for this is that the behaviour of these beams is determined by a large number of parameters such as the beam dimensions, the

amount of steel reinforcement and the external post-tensioning force. As a consequence, even though there have been a large number of experimental studies, the failure mechanisms are still not fully understood and the influences of several parameters are not yet clear.

Nonlinear finite element method (FEM) provides a powerful tool to study the behaviour of concrete structures. The general-purpose finite element program Abaqus (Abaqus Inc. 2006) was used in this research project to investigate the behaviour of shear damaged reinforced concrete beams strengthened by external post-tensioning. Details of the finite element modelling of reinforced concrete members using Abaqus is outlined in the following sections.

5.3.1 Modelling of Concrete

5.3.1.1 Constitutive Model

Concrete in compression is modelled as an elastic–plastic material with strain softening. The stress-strain relation used in Abaqus to model this behaviour is shown in Figure 5.5.
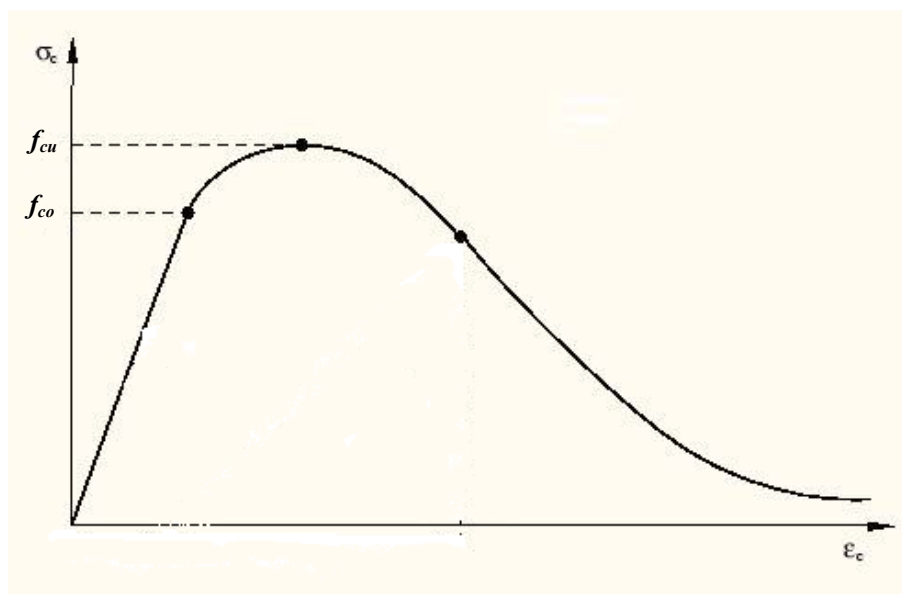
Figure 5.5. Stress-strain curve for concrete in compression
Source: Abaqus User Manual (Abaqus Inc. 2006)

To define the above relationship, a number of parameters such as ultimate stress (f_{cu}) and linear range (f_{co}) need to be given through input data. The following stress–strain relationship for concrete in uniaxial compression proposed by Carreira and Chu (1985) was used in this study to estimate the required parameters to define the stress-strain curve in Abaqus.

$$\sigma_c = \frac{f_c' \gamma \left(\varepsilon_c / \varepsilon_c' \right)}{\gamma - 1 + \gamma \left(\varepsilon_c / \varepsilon_c' \right)^2}$$
(5.16)

where,

σ_c = Compressive stress in concrete,

γ = Multiplying factor defined by Equation 5.17,

ε_c = Strain in concrete, and

ε_c' = Strain corresponding to f_c' (MPa).

$$\gamma = \left| \frac{f_c'}{32.4} \right|^3 + 1.55$$
(5.17)

The strain ε_c' is usually taken as 0.002 (Liang et al. 2004; Liang et al. 2005). In the present study, the stress–strain behaviour of concrete in compression was assumed to be linear elastic up to $0.4 f_c'$. Beyond this point, it is in the plastic region in which plastic strain should be given as input to define the stress–strain relationship in the finite element model. The failure ratio option was used to define the failure surface of concrete. The ratio of the ultimate biaxial compressive stress to the ultimate uniaxial compressive stress was taken as 1.16. The ratio of the uniaxial tensile stress to the uniaxial compressive stress at failure was taken as 0.0836 (Liang et al. 2005).

The behaviour of the concrete and the reinforcement in the concrete beam were modelled independently. The interaction between the concrete and reinforcing bars was simulated using the tension stiffening model. Tension stiffening was defined in the present study by using stress–strain data. Generally the tension stiffening of concrete was defined as shown in Figure 5.6. However, for the computational

purpose of this study, the model assumes that the direct stress across a crack gradually reduces to zero as the crack opens. This approximation was effectively used by many researchers for their computational calculation of the concrete element (Liang et al. 2005) and it significantly reduced the computational time of the finite element analysis.
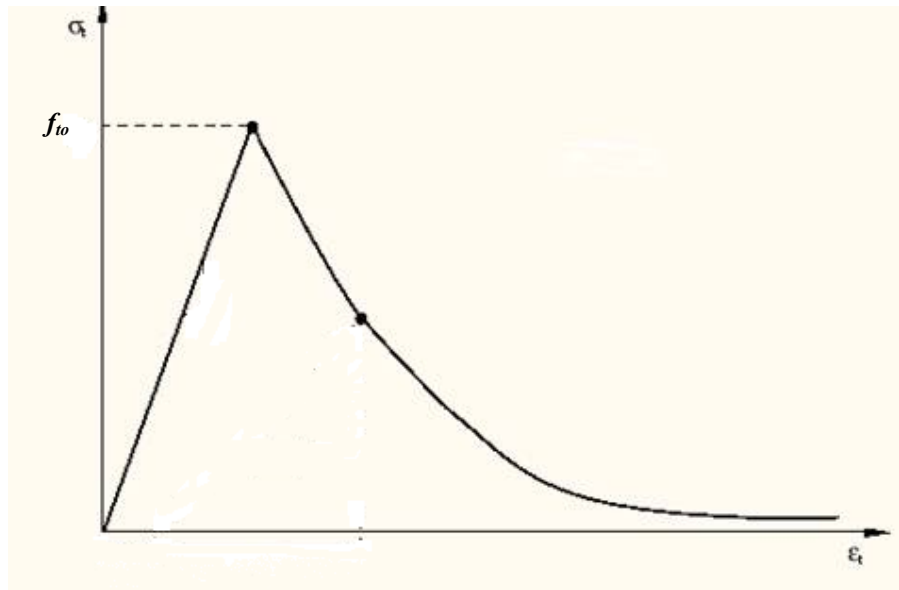
Figure 5.6. General form of tension stiffening model of concrete
Source: Abaqus User Manual (Abaqus Inc. 2006)

This study uses the stress–strain relationship as shown in Figure 5.7. It assumes that the tensile stress increases linearly with an increase in tensile strain up to concrete cracking. After concrete cracking, the tensile stress decreases linearly to zero as the concrete softens. The value of tension stiffening is an important parameter that affects the outcome of a nonlinear analysis of reinforced concrete. Tension stiffening is influenced by the density of reinforcing bars, the bond and the relative size of the aggregate compared to the rebar diameter. For heavily reinforced concrete members, the total strain at which the tensile stress is zero is usually taken as 10 times the strain at failure in the tension stiffening model.
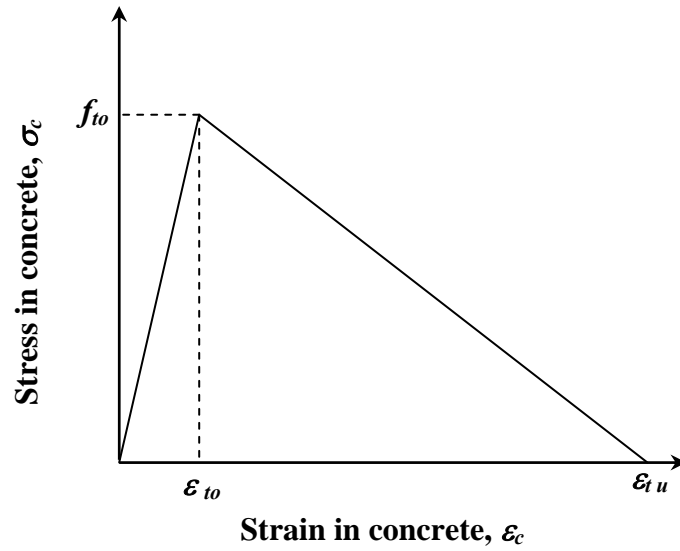
Figure 5.7. Stress-strain curve used for concrete in tension

The reduction in shear modulus due to concrete cracking was defined as a function of direct strain across the crack in the shear retention model. The shear modulus of cracked concrete is defined as

$$G = \varphi \, G_c \tag{5.18}$$

where,

    G_c =   Elastic shear modulus of uncracked concrete, and

    φ =   Reduction factor given by Equation 5.19.

$$\varphi = \begin{cases} 1 - \dfrac{\varepsilon_c}{\varepsilon_{max}} & for \ \varepsilon_c < \varepsilon_{max} \\ 0 & for \ \varepsilon_c \geq \varepsilon_{max} \end{cases} \tag{5.19}$$

where,

    ε_c =   Direct strain across the crack, and

    ε_{max} =   Maximum stain in concrete.

The shear retention model states that the shear stiffness of open cracks reduces linearly to zero as the crack opening increases. Parameters $\varepsilon_{max}=0.005$ and $\varphi=0.95$ were used in the present study to define the shear retention of concrete as suggested by Liang et al. (2004).

5.3.1.2 Concrete Element

There are number of element types available in Abaqus to model the beam using the thick shell element such as S4R, S8R, S10R and more. Many of these shell element types in Abaqus use reduced (lower-order) integration to form the element stiffness. The mass matrix and distributed loading are still integrated exactly. Reduced integration usually provides more accurate results and significantly reduces running time.

In this study, the concrete is modelled with four-node doubly curved thick shell element (S4R) with reduced integration (Figure 5.8). Unlike conventional shell elements, larger depths can be used for these shell elements. These elements allow transverse shear deformation. They use thick shell theory as the shell thickness increases and become discrete Kirchhoff thin shell element as the thickness decreases; the transverse shear deformation becomes very small as the shell thickness decrease (Abaqus Inc. 2006).
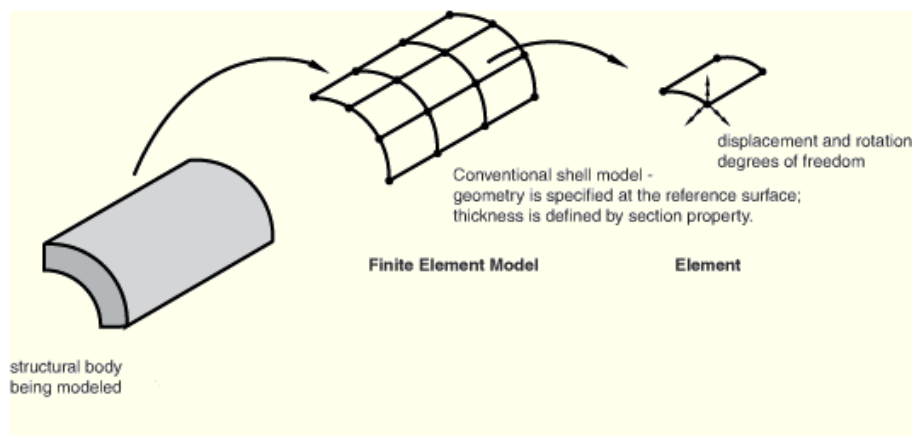
Figure 5.8. Four-node doubly curved thick shell element (S4R)
Source: Abaqus User Manual (Abaqus Inc. 2006)

The element type S4R accounts for finite element membrane strains and arbitrarily large rotations; therefore, they are suitable for large-strain analysis. In general, the use of such shell element for an intrinsically plane stress problem is incorrect. However, in the modelling made for this study, the applied loads and boundary constraints are in the plane of shell element (1-2 plane). Therefore, the stresses

developed due to loading are primarily in the 1-2 plane and stress normal to the 1-2 plane can be negligible. In addition to that, shell properties such as shell thickness were defined by considering the bending in the 1-2 plane (about the axis normal to the shell plane). Therefore, bending properties about other axes were not counted for the analysis. Due to these reasons, the shell element S4R could be effectively used to model the concrete beam in this study. That means, even though S4R element was classified under shell element in Abaqus, it can be used as plane stress element by defining its boundary conditions and loading accordingly.

5.3.2 Modelling of Reinforcement

5.3.2.1 Constitutive Model

The stress–strain curve of the reinforcing bar is assumed to be elastic perfectly plastic as shown in Figure 5.9. This is a reasonable assumption for the reinforcing steel bars and it is successfully used by other researchers in nonlinear finite element analysis using Abaqus (Hu et al. 2004). The same behaviour was assumed for both compression and tension. Material properties, such as the Young's modulus, Poisson's ratio, the yield stress were given as input to define the stress–strain curve.
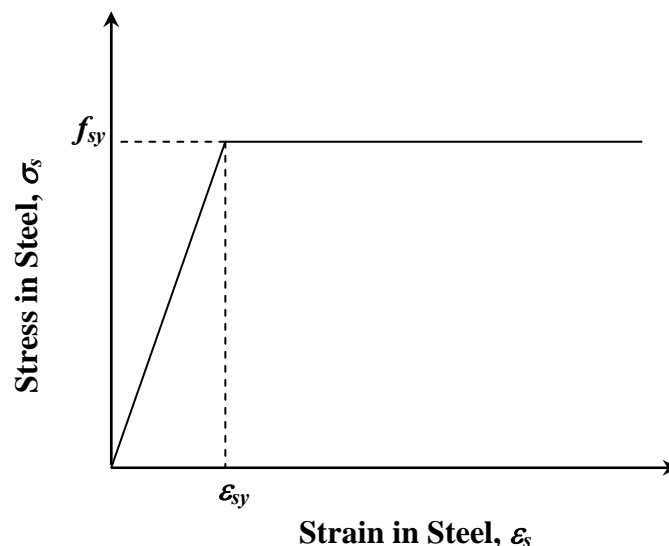
Figure 5.9. Stress-Strain Curve for Steel

As explained in Chapter 3, two types of steel bars, longitudinal reinforcement (N-type) and shear reinforcement (high strength mild steel), were used in the test specimens. To represent these two types of steels, two different material properties were defined in finite element analysis (FEA). Steel properties used in this FEA are shown in Table 5.1. Since the N-type bars were used as tensile and compressive reinforcements and they did not reach their ultimate strength during the experiment, the Elastic modulus (E) will be the governing factor in finite element model. Therefore, the standard values given by manufacturer were used to define its mechanical properties.

Table 5.1: Material properties of steel used in analytical approximation

Properties	Value
Young's modulus of steel rebar (GPa)	200
Poisson's ratio of steel, v	0.3
Yield stress of N-type bars, f_{sy} (MPa)	500[*]
Yield stress of shear reinforcement bars, f_{sy} (MPa)	365[**]

* From the material data sheet provided by manufacturer

** Experimental values (refer Table 3.3)

In Abaqus, steel reinforcement is treated as an equivalent uniaxial material smeared through out the element section. However, the bond–slip effect between concrete and steel is not considered. In order to model properly the constitutive behaviour of the reinforcement, the cross sectional area, the spacing, position and orientation of each layer of steel bar within each element needs to be specified. As the analysis was performed in 2-D model, an equivalent cross sectional area of reinforcing bar was used at the effective depth of the beam.

5.3.2.2 Steel Element

Steel reinforcement bars were modelled as a truss element using the 'rebar' option available in the shell element that is used for concrete. Bar diameter, depth and spacing need to be given as input for provide the reinforcement in a shell element. For an undamaged reinforced concrete beam or beam with a small crack width, the

same steel properties as explained above were assigned. However, the properties of the steel within a crack in a reinforced concrete beam with a significantly larger crack width were assumed to be slightly different from those explained in the previous section. In such cases, the steel within the crack (Figure 5.10) was assumed to be fully yielded and to behave as yielded steel during the loading process. This assumption will be justified in the following chapter (Chapter 6).

Yielded shear reinforcement

Yielded longitudinal steel
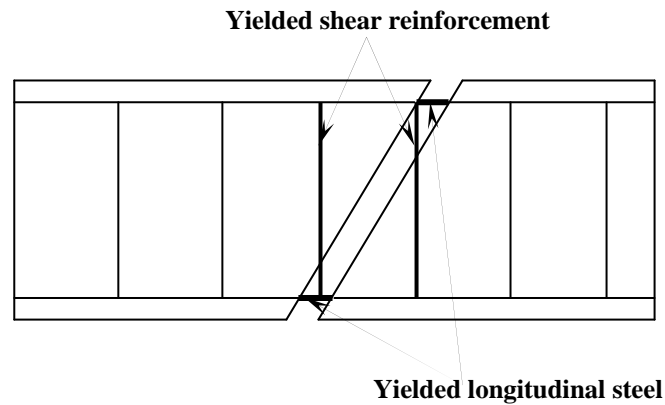
Figure 5.10. Detail of the cracked zone of shear damaged reinforced concrete beam

5.3.3 *Modelling of Connectors*

Several assumptions were made to simplify model development of shear crack without any loss in the accuracy of the representation. The cracked beam was modelled into two separate parts and connected with the 'connectors' (node-to-node connection) as shown in see Figure 5.11.
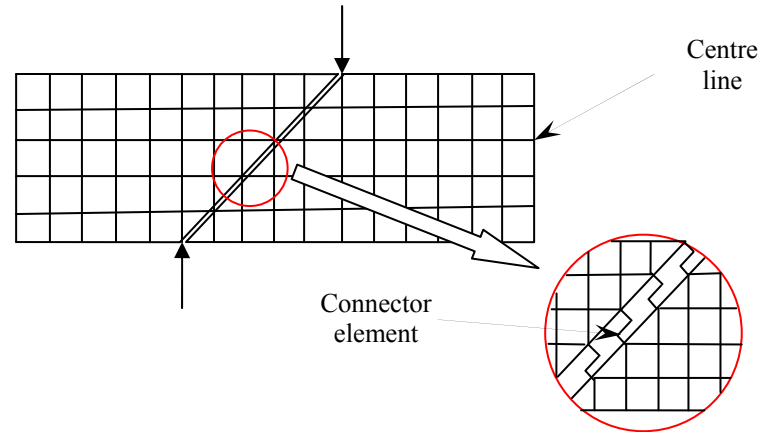
(a) Mesh arrangement near the shear crack
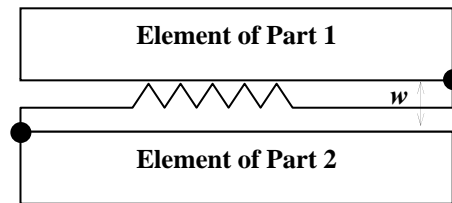
(b) Detail of a connector element

Figure 5.11. Detail of connectors

The properties of the connectors were defined using the relationship between the maximum stress that can be transferred across the crack and the crack width as defined in the modified compression field theory (Vecchio and Collins 1986). The equation (Equation 2.10) and associated parameters were defined in Chapter 2. For convenience, the equation is reproduced below:

$$v_{ci} = \frac{0.18\sqrt{f_c^{'}}}{0.3 + \dfrac{24w}{a+16}} \tag{5.20}$$

For modelling purposes, an average crack width was assumed to represent the properties of the connector. After some trial and error, it was found that using a crack width of about 70% of the maximum crack width measured at peak load enabled the prediction of the behaviour of the cracked beam with a reasonable degree of accuracy. This value was further verified by the theoretical calculation. Detailed discussion on this assumption can be found in Chapter 6. All the cracks were assumed as straight lines which were approximately similar in orientation to those obtained in the experimental program.

5.3.4 Modelling of Epoxy

To analyse the epoxy repaired reinforced concrete beam, it was assumed that the crack zone was completely filled with epoxy. Perfect bonding (no slip) property was also assumed between the epoxy and the concrete as well as the epoxy and the reinforcement steels. Detail of the modelling of the epoxy component is outlined below.

5.3.4.1 Constitutive Model

In the finite element modelling, the epoxy resin was assumed to be linear elastic material with significantly higher compressive and tensile strengths than concrete. This assumption is reasonable as the material testing of the epoxy (see Chapter 3 and Appendix A) showed a perfect elastic behaviour almost until its failure in tension. I also noted that, no cracks or failure were observed during experimental process along the repaired shear cracks using epoxy resin injection. A constant value of Young's modulus obtained from material testing was used with the minimum strength values provided by the manufacturer. These values are reported in Table 5.2. As discussed in Chapter 3, these minimum tensile and compressive strength values are significantly higher than tensile and compressive strength values of concrete respectively.

Table 5.2: Material properties of epoxy

Property	Value
Young's modulus (GPa)	3.03[*]
Compressive strength (MPa)	83[#]
Tensile strength (MPa)	25[#]

[*] Experimental values (refer to Table 3.6)

[#] From the material data sheet provided by manufacturer (refer Table 3.7)

5.3.4.2 Epoxy Element

The same element type used for the concrete (general purpose shell element S4R) was also used for the modelling of the epoxy. As explained under Section 5.3.2.2, the steel elements within the epoxy elements were considered as fully yielded and to behave as yielded steel during the loading process.

5.3.5 Beam Geometry and Boundary Conditions

The size of finite element models can be reduced significantly by the use of symmetry, resulting in substantial computational savings. In order to make use of symmetry, both loading and structural configuration must be symmetric. For the purpose of the parametric study of this study, a rectangular cross sectional beam with same the dimensions as in the experimental program (150×300×2500 mm) was used with four-point loading as shown in Figure 5.12(a). As the beam had one plane of symmetry about the centre line in the X-Y plane, only one half of each beam was analysed and symmetric boundary conditions were placed along the symmetric axis as shown in Figure 5.12(b).

With consideration of the symmetric behaviour of both the beam geometry and loading, the following restraint conditions were set for the finite element model:

- At the left support, no displacement was allowed in Y direction while displacement in X direction and rotation about Z-axis were allowed;

- At the centre line, only vertical (along Y-axis) displacement was allowed.
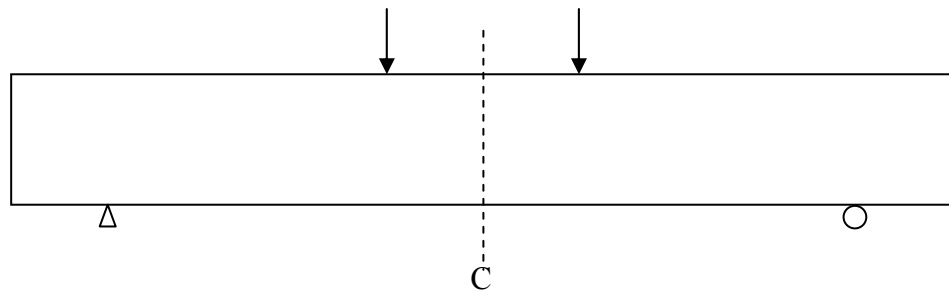
(a) Full beam
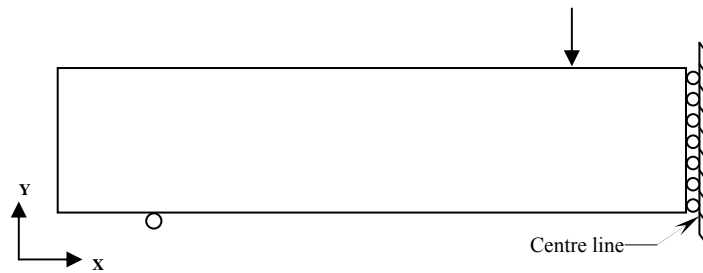
(b) Boundary condition at the centre line for the half beam (LHS)

Figure 5.12. Symmetric property of the beam and loading

Following methods were used to simulate the loading and external post-tensioning forces in the FEA:

- Loading: Vertical displacement was applied to the model at a constant rate of 2 mm/min;

- External post-tensioning force: Horizontal force was applied at both ends of the model at a depth of 200 mm (same as the experimental program). The external post-tensioning force was applied through the load input (load case) option available in the Abaqus for cater the increase in the post-tensioning force during the loading process.

5.4   Summary

In this chapter an explanation of the numerical analysis carried out in this study was presented in two sections:

- the development of a simplified mathematical model to estimate the shear capacity of a cracked beam with external post-tensioning as well as external clamping;

- the finite element modelling of reinforced concrete beam with and without shear crack using the commercial finite element package, Abaqus.

Validation of both the simplified mathematical model and the finite element model will be presented and discussed in the Chapter 6. A parametric study using the developed finite element model will also be presented.

<div align="right">

Chapter 6

NUMERICAL RESULTS,

VERIFICATION & DISCUSSION

</div>

The experimental program to investigate the behaviour of shear damaged reinforced concrete beams strengthened with external post-tensioning or external clamping has been explained in Chapters 3 and 4, followed by a brief discussion on the experimental results. The previous chapter (Chapter 5) explained the techniques and simplifications used in the numerical analysis of this research study in two stages:

- development of a simplified mathematical model to estimate the shear strength of cracked beams strengthened by external post-tensioning or external clamping;

- the finite element modelling of cracked and repaired beams using the commercial finite element package, Abaqus.

This chapter presents the results of the numerical analysis that includes a brief parametric study performed using the finite element model as well as the simplified mathematical model. At the end of this chapter the experimental and numerical results are discussed with a view to proposing for an effective strengthening system for shear damaged reinforced concrete beams. The influence of various parameters such as concrete strength, prestressing force and shear reinforcement ratio are considered.

These results are presented in the following sequence:

- verification of the developed mathematical equations to estimate the shear capacity of cracked reinforced concrete beams using the experimental results;

- discussion on the practical limitations and approximations related to the estimation of the shear capacity of cracked beam using the theoretical equations;

- verification of the developed finite element models using the experimental results;

- parametric studies to investigate the influence of a number of the primary parameters including concrete strength ($f_c^{'}$), post-tensioning, type of epoxy resin and force amount of shear reinforcement on the behaviour of shear damaged reinforced concrete beams strengthened by external post-tensioning;

- discussion on the effect of existing shear cracks on the behaviour of cracked reinforced concrete beams when strengthened by external post-tensioning and the influence of various parameters on the behaviour.

6.1 Shear Capacity of Cracked Reinforced Concrete Beams

The development of the shear strength equations is outlined in Chapter 5. Based on some of the existing theories such as modified compression field theory a number of assumptions were made to develop these equations. In this section, the application of the developed shear strength equations will be examined and the limitations or assumptions in the use of them in practical applications will be discussed.

First, the shear strength equation for cracked reinforced concrete beams strengthened by external post-tensioning is considered. As explained in Chapter 5, the shear strength of a cracked reinforced concrete beam is given by Equation 5.12. Similarly, for a cracked reinforced concrete beam with axial force, the shear capacity can be

expressed by Equation 5.14. For the reader's convenience both equations are reproduced below:

For a cracked beam without axial force,

$$V = v_{ci} b_v jd + \frac{A_v f_{sy}}{s} jd \cot\theta ; \qquad (6.1)$$

For a cracked beam with axial force,

$$V = \frac{A_v jd}{s}(f_{sy} - f_v)\tan\theta + (A_{sx} f_l + A_p f_p)\tan\theta + v_{ci} b_v jd \tan^2\theta . \qquad (6.2)$$

All parameters used in the above two equations were defined in Chapter 5.

In both of the above equations, it can be noted that the shear capacity of the cracked beam is given as a function of the average width of the shear crack. Practically it is difficult to determine the exact value of the average crack width as the crack width changes from point to point along the crack. Even though in ideal conditions it is possible to estimate the average crack width using some complex theoretical approaches, such methods may not be possible in practical situations. Therefore, this study used an approximate average shear crack width, which could be measured or estimated easily, to estimate shear capacity using the above equations. For this purpose, it was decided to use the average crack width as a linear function of maximum crack width measured in the specimen. That means the average crack width, w, can be expressed as,

$$w = k_w \times w_{max} , \qquad (6.3)$$

where,

k_w =   Multiplying factor for average crack width, and

w_{max} =   Maximum measured crack width (during experiment).

The value of the multiplying factor, k_w needs to be determined.

As explained in Chapter 5, the shear capacity of a cracked beam, V, with external clamping is given by Equation 5.15. For the reader's convenience that equation is reproduced below:

$$V = f_1 b_v \, jd \cot\theta + \frac{A_v f_v}{s} \, jd \cot\theta + P_{v,ext} \, , \tag{6.4}$$

All parameters used in the above equation are defined in Chapter 5. In this equation, f_{c1} is limited by a function of average crack width, w, and the same approach as explained above is used to estimate the value of w.

In order to estimate the multiplier, k_w the experimental shear capacities of the crack specimens EPT12, EPT22 and EPT32 were used. The experimental results were compared to the estimated capacities for different values of k_w and results are shown in Table 6.1.

Table 6.1: Comparison of shear capacities for different k_w for external post-tensioned specimens

Specimen	Experimental Capacity [kN]	Estimated Capacity [kN]			k_w value to get the Experimental Capacity
		$k_w = 0.65$	$k_w = 0.7$	$k_w = 0.75$	
EPT12	194	207	192	179	0.70
EPT22	173	181	162	154	0.73
ECL32	262	274	262	251	0.71

From the table above it can be noted that when $k_w = 0.7$, the equation predicts the shear capacity with significant accuracy. However, it was not possible to make a conclusion about the value of k_w from a sample size of three. To confirm this finding further analysis was conducted using finite element model developed as described in the previous chapter.

6.2   Comparison of Experimental Results with Theoretical Predictions

In this section, a comparison of experimental results with the theoretical estimation is discussed. As indicated in Chapter 2, a number of different methods and equations have been recommended and used worldwide to estimate the shear capacity of reinforced concrete beams with no cracks. In this section the equations given in the

Australian code AS3600 are used to estimate the shear capacity of the specimens wherever possible. The details of the equations are given in Chapter 2 under Section 2.3.2 or can be found in the relevant code. For the reader's convenience those equations are reproduced below as Equations 6.5–6.8:

Ultimate shear capacity of a reinforced concrete beam, V_u, is given by,

$$V_u = V_{uc} + V_{us},$$

(6.5)

Contribution by shear reinforcement, V_{us}, is given by,

$$V_{us} = \frac{A_{sv}}{s} f_{sy} d_o \cot\theta_v,$$

(6.6)

Contribution by concrete, V_{uc} is given by the following two equations:

For reinforced concrete beams without axial force;

$$V_{uc} = \beta_1\beta_2\beta_3 b_v d_0 \left[\frac{A_{st} f_c'}{b_v d_0}\right]^{\frac{1}{3}},$$

(6.7)

For reinforced concrete beams with axial force;

$$V_{uc} = \beta_1\beta_2\beta_3 b_v d_o \left[\frac{\left(A_{st} + A_{pt}\right)f_c'}{b_v d_o}\right]^{\frac{1}{3}} + V_{dec} + P_v.$$

(6.8)

All parameters used in these equations were defined in Chapter 2.

In this theoretical calculation the repaired beam was assumed to be free of cracks and, therefore, treated as an uncracked beam for the purpose of these capacity predictions.

It should be noted that, in the current code of practice AS3600 (2001), there are no provisions to estimate the shear capacity of reinforced concrete beams with cracks. Therefore, to estimate the theoretical shear capacity of the cracked beams, Equations

6.1, 6.2 and 6.4 were used. As discussed previously in this chapter, a multiplier, k_w, of 0.7 was used for these estimations.

Based on these equations and assumptions ultimate loads were calculated for all specimens used in the experiment. For the loading arrangement used in the experimental program (four-point loading), the ultimate load P_u is given as

$$P_u = 2 V_u \qquad (6.9)$$

The results are tabulated together with the experimental data in Table 6.2.

Table 6.2: Comparison of experimental results with theoretical estimations

Specimen	Average Compressive Strength [MPa]	Pre-loading [kN]	Ultimate Load, P_u [kN]		Remarks
			Experimental	Theoretical	
EPT11	39.9	-	196	162	Control beam
EPT12	40.3	180	194	192[*]	Pre-cracked + Post-tensioned
EPT13	40.4	188	310	341	Pre-cracked & Repaired + Post-tensioned
EPT14	40.4	-	354	344	Post-tensioned
EPT21	29.3	-	197	163	Control beam
EPT22	32.3	202	173	162[*]	Pre-cracked + Post-tensioned
EPT23	40.5	177	293	349	Pre-cracked & Repaired + Post-tensioned
EPT24	36.5	-	288	279	Post-tensioned
ECL31	39.4	-	176	176	Control beam
ECL32	37.7	145	262	262[*]	Pre-cracked + Clamped
ECL33	41.6	145	279	286	Pre-crack & Repaired + Clamped
ECL34	37.7	-	287	268	Clamped
ECL35	41.6	176	260	286	Loaded & Repaired + Clamped
ECL36	41.5	165	214	N/A	Failed due to concrete crushing
ECL37	40.0	152	233	N/A	
ECL38	39.0	189	243	N/A	

* Calculated using a crack width of 70% of the maximum crack width as measured in the experiment.

Since specimens ECL36, ECL37 and ECL38 failed due to concrete crushing near to the loading points, the failure mode was different from the other specimens reported

above. As it was expected that, in this research study, the failure of all specimens would be due to shear failure and, therefore, all the theoretical equations used in this dissertation are based on that assumption. The theoretical capacities of specimens ECL36, ECL37 and ECL38 were not calculated, as the assumption did not apply.

The theoretical equations discussed above predicted the capacity of the specimens reasonably well. For estimation of the capacity of cracked beams, a crack width of 70% of maximum crack width as measured in the experiment was used.

In Group 1 specimens, the experimental capacity was slightly less than the theoretical estimation for EPT13, while EPT11 and E PT14 had higher experimental values than theoretical estimations. This can be attributed to the presence of smaller cracks that may not have been filled during the epoxy injection process. For specimen EPT12, the average crack width was taken as 70% of the maximum crack width measured in the experiment and the theoretical capacity was almost the same. A similar pattern was evident in Group 2 and in Group 3.

From this it can be noted that the developed shear strength equations and the use of a multiplier as 0.7 to estimate the average crack width predicted the shear capacity of the cracked beams to a significant accuracy. This is comparable to the accuracy of the predicted shear capacity of uncracked beams using the code (Australian Standard, AS3600). Furthermore, it can be noted that the assumptions applied to the repaired beams also predicted the shear capacity with reasonable accuracy.

Further investigations using finite element modelling were undertaken to determine the behaviour of post-tensioned reinforced concrete beams with existing shear cracks and to test further the assumption made to estimate the theoretical shear capacities. This is explained in the following sections.

6.3   Finite Element Analysis of Shear Damaged RC Beams

6.3.1 Convergence of the Finite Element Modelling

In general, it is necessary to conduct a convergence test on a finite element model to confirm that a sufficiently fine element discretization has been used. Therefore, convergence of this model was checked to decide the suitability of the mesh and optimum mesh (element) size by considering the accuracy and required time to run each case. The running time of a model depends on various factors including the complexity of the finite element mesh arrangement, the material constitutive models and the specification of the computer used for the analysis.

6.3.1.1 Material Constitutive Model

The material constitutive models for steel, concrete and epoxy used in this analysis were explained in Chapter 5.

6.3.1.2 Computer Specifications

For this analysis a Pentium$^{®}$ 4 (DELL$^{™}$) desktop computer with the following specifications was used:

- Operation System: Microsoft Window$^{®}$ XP Professional (Service Pack 2)

- CPU: 2.40 GHz & 512 MB RAM, 40 GB Hard drive

6.3.1.3 Mesh Arrangement

Initially a simple model without any pre-crack or strengthening (Figure 6.1) was modelled in Abaqus according to the specifications given in Chapter 5. Different mesh sizes as shown in Table 6.3 and Table 6.4 were selected to check the convergence of the model.

$^{®}$ Registered trade mark of Microsoft
$^{™}$ Trade mark of Dell Corporation

Figure 6.1. FEM mesh of the uncracked beam used to check the convergence

The model was analysed using displacement-control until it reached the peak loads. The time to run each case and the maximum load are shown in Table 6.3. Convergence of the model analysis is shown in Figure 6.3.

Table 6.3: Convergence and analysis time for the uncracked beam model

Number of Element X-direction × Y-direction	Element size [mm] X-direction × Y-direction	Approximate Time Taken to Run One Model	Ultimate Load [kN]
100×30	25×10	5 hrs 15 min	193.5
125×30	20×10	6 hrs 45 min	193.8
250×30	10×10	10 hrs 30 min	194.0
333×30	7.5×10	12 hrs 45 min	194.0

To ensure the convergence of the cracked model, the same analysis was carried out for the cracked reinforced concrete beam (Figure 6.2) with external post-tensioning under a monotonically increasing load (with displacement control). The results are shown in Table 6.4 and Figure 6.3.
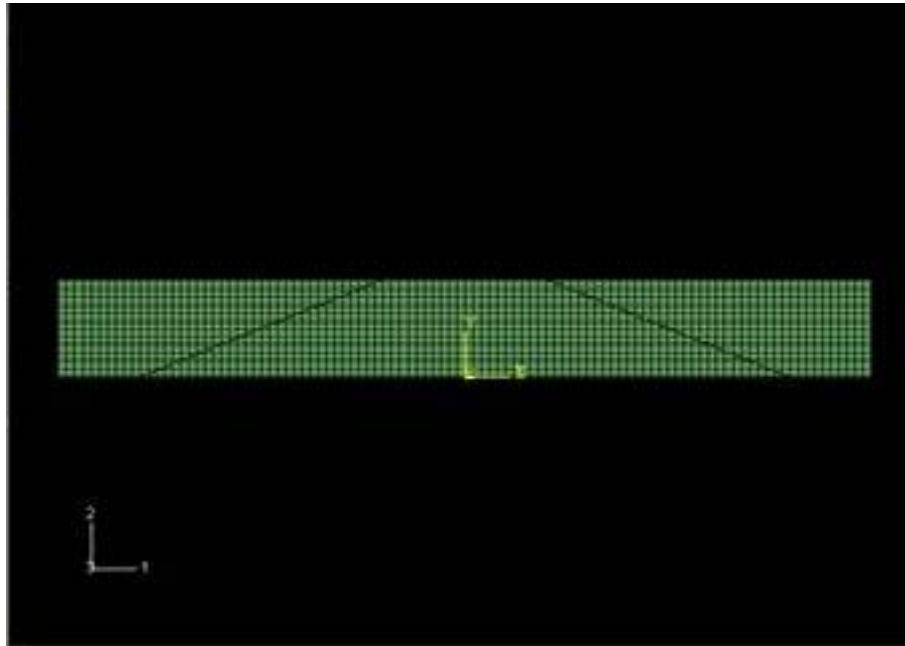
Figure 6.2. FEM mesh of the cracked beam used to check the convergence

Table 6.4: Convergence and analysis time for the cracked beam model

Number of Element X-direction × Y-direction	Element size [mm] X-direction × Y-direction	Approximate Time Taken to Run One Model	Ultimate Load [kN]
100×30	25×10	6 hrs 00 min	192.6
125×30	20×10	8 hrs 15 min	193.1
250×30	10×10	14 hrs 15 min	193.2
333×30	7.5×10	17 hrs 00 min	193.2
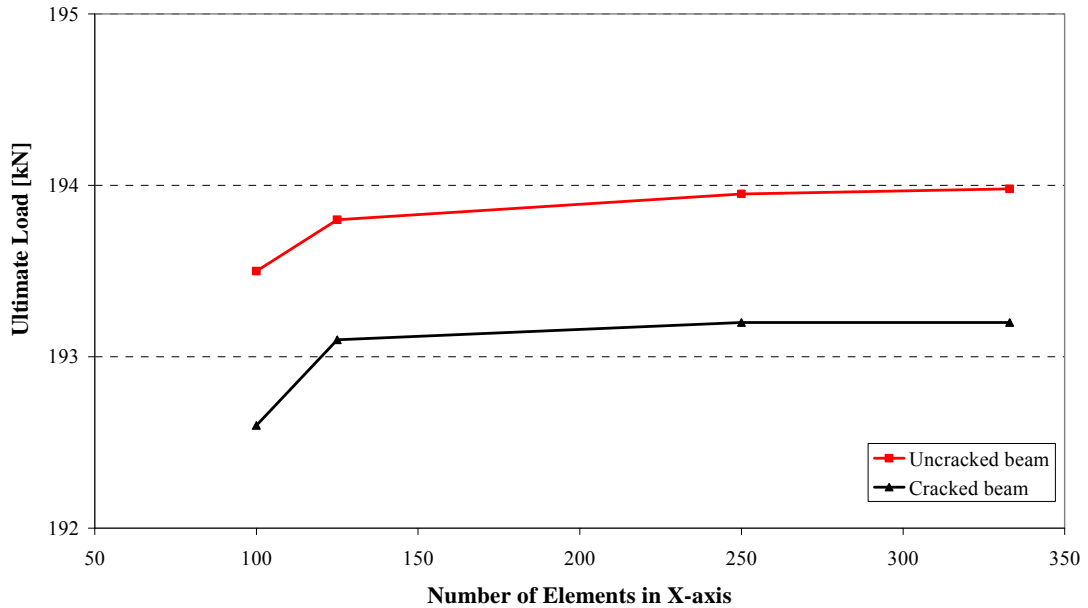
Figure 6.3. Convergence of the finite element model

Based on the above results, it was decided that an element size of 20×10 would be suitable for subsequent analysis to obtain reasonable accuracy with significantly reduced time.

6.3.2 *Verification of the Finite Element Model*

In this section, the validity of the developed model including the material constitutive models for steel, concrete and epoxy is verified by comparing with the corresponding experimental data given in Chapter 4. For verification purposes, the specifications of Group 1 specimens were used. Details of the specimens and the loading arrangements, including loading rate, were given in Chapters 3 and 4 and are not duplicated in this section.

The load-displacement curve of the control beam, EPT11, (no initial cracks, no strengthening) predicted by the finite element model was plotted with experimental data as shown in Figure 6.4. Similarly the comparison of the load-displacement behaviour of cracked beam, EPT12, (pre-cracked, strengthened by external post-tensioning) is shown in Figure 6.5.
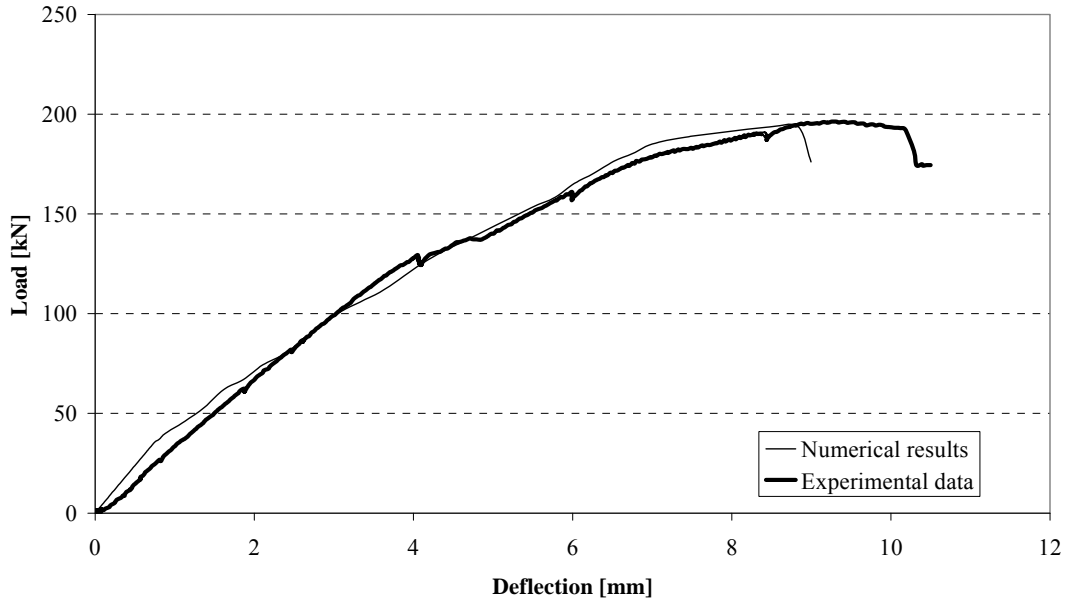
Figure 6.4. Comparison of the load-displacement behaviour of the control beam
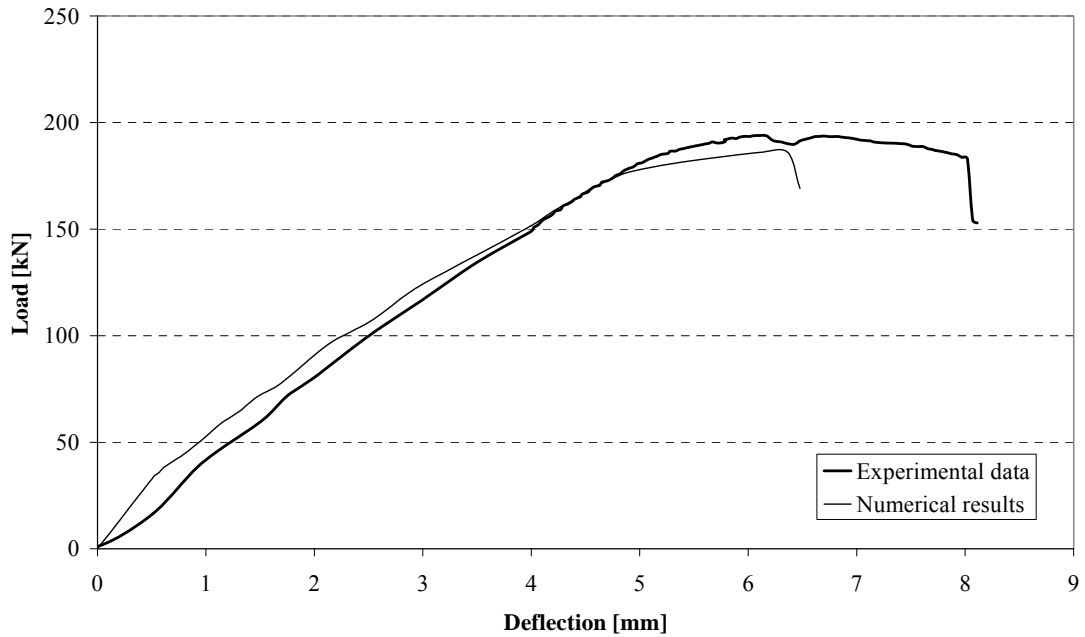
Figure 6.5. Comparison of the load-displacement behaviour of the cracked beam

From the above figures, it can be noted that the experimental data and the finite element results have quite good correlation. For the control beam, the predicted ultimate load capacity 193.8 kN (within 1.2% accuracy) did not vary significantly from the experimental ultimate load capacity 196 kN. Similarly for the cracked beam with external post-tensioning the predicted ultimate load capacity was approximately

96% of that of the experimental value. It also can be noted that the initial stiffness of both of the above beams predicted by finite element model is similar to that of the experimental one. However, the experimental behaviour of the above two beams shows more ductile behaviour than that predicted by the finite element analysis. This variation can be attributed to the simplifications made to develop constitutive models of the steel and the concrete for finite element modelling.

Based on the above comparison, the developed finite element model and material constitutive models were accepted as able to simulate to a significant accuracy of the behaviour of reinforced concrete beams with existing shear cracks strengthened by external post-tensioning. From this, it was concluded that the finite element model developed in this study is reliable in predicting the behaviour, up to the ultimate load capacity, of reinforced concrete beams with exiting shear cracks.

In order to validate the crack pattern used in the finite element model, a separate analysis was performed using a computer program called Response-2000 (Bentz 2001). This program was developed based on the modified compression field theory (MCFT) proposed by Collins et al. This is a useful tool to get an indication of crack pattern and crack width in reinforced concrete beams. The results are presented in Appendix E. It can be noted that even though the program predict a number of smaller crack in the shear span region, the sum of these predicted crack widths is nearly the same as the observed single crack width during the experiment.

6.4   Parametric Study

To investigate the influence of various parameters on the behaviour of shear damaged reinforced concrete beams, a parametric study was conducted using the developed finite element model as explained in Chapter 5.

Since a large amount of computation and time is involved in the analysis of each finite element model, using symmetry of loading and geometry a half model of

reinforced concrete beams was used for the parametric study. A boundary condition equivalent to a roller support was used along the centre line of the half beam model. More details can be found in Chapter 5. As expected the half beam model yielded almost the same results (193.72 kN) as the full beam model as explained in the previous section (193.78 kN).

Although there are a number of various parameters that could influence the behaviour of a shear damaged reinforced concrete beam, only the following major parameters were considered in this study:

- concrete strength;

- shear reinforcement ratio;

- post-tensioning force;

- crack width;

- type of epoxy resin.

Details of the parametric study concluded to investigate the influence of each of the above parameters on the behaviour of shear damaged reinforced concrete beams are explained in the following sub sections.

6.4.1 Concrete Strength

A range of concrete strength from 25 MPa to 50 MPa was considered in this parametric study to investigate the influence of concrete strength on the shear capacity of cracked and repaired reinforced concrete beams strengthened by external post-tensioning. In order to understand the effect of concrete strength, other parameters were fixed at experimental values as follows:

- initial post-tensioning force = 150 kN;

- Young's modulus of the epoxy = 3.0 GPa;

- maximum crack width is taken as 4 mm;

- shear reinforcement spacing = 250 mm & 180 mm.

The predicted ultimate loads from the finite element analysis of the cracked and repaired reinforced concrete beams strengthened by external post-tensioning for different concrete strengths are summarised in Table 6.5. Furthermore, this variation is shown in Figure 6.6 and Figure 6.7 for cracked and repaired beams respectively.

Table 6.5: Maximum load of reinforced concrete beams strengthened by external post-tensioning

Specimen	Spacing of Shear R/F [mm]	Ultimate Load [kN]			
		$f_c' = 25$ MPa	$f_c' = 32$ MPa	$f_c' = 40$ MPa	$f_c' = 50$ MPa
Cracked	250	146	161	188	207
	180	155	168	194	211
Repaired	250	N/A[*]	326	357	388
	180	N/A[*]	338	364	396

* Applied post-tensioning force is not suitable for 25 MPa concrete.
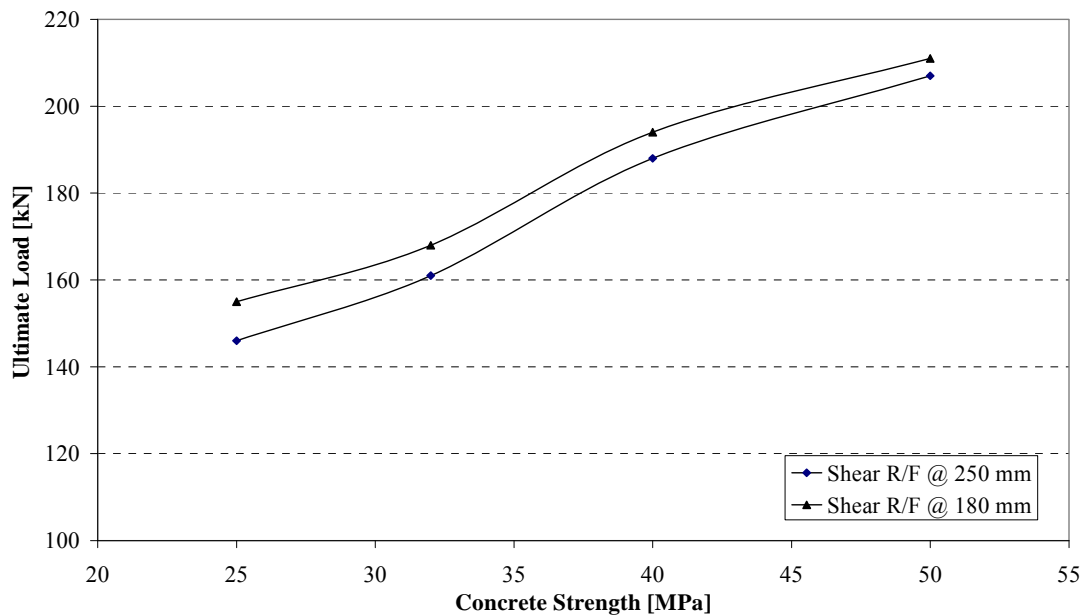
Figure 6.6. Shear capacities of cracked reinforced concrete beam for different concrete strengths
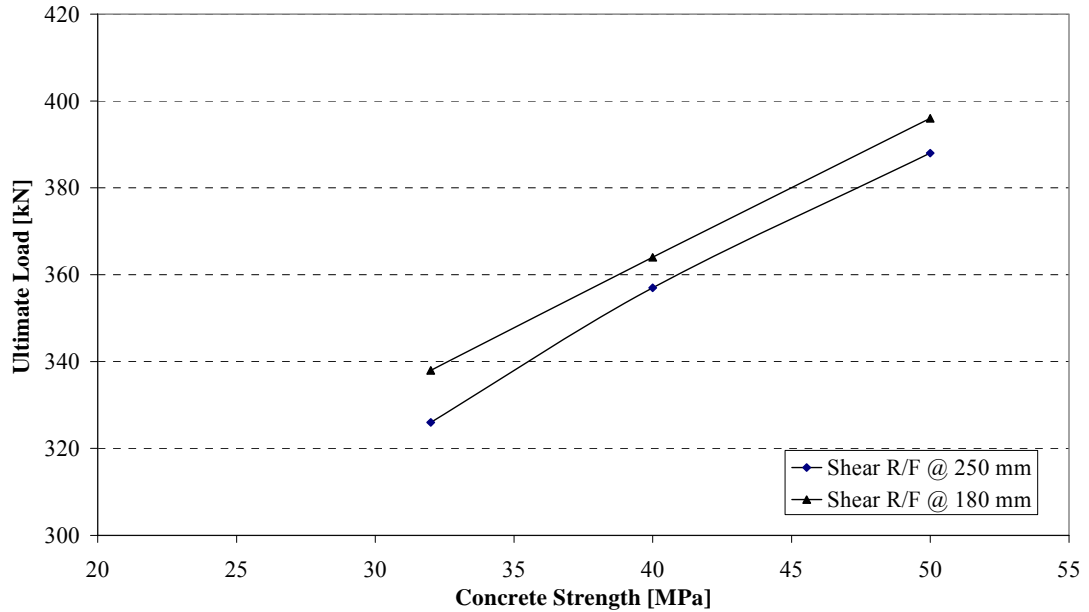
Figure 6.7. Shear capacities of repaired reinforced concrete beam for different concrete strengths

From the results presented above it can be noted that the capacity of both cracked and repaired beam increases with the strength of the concrete. However, the capacity of the cracked and repaired beams does not increase as much as the concrete strength does. This may be due to the constant area of longitudinal reinforcement placed in the beam, which could limit the force that could be carried by concrete section.

Since the 150 kN post-tensioning force is significantly higher for the 25 MPa concrete, the corresponding case was not analysed using finite element model. More detail on the limitation of the post-tensioning force that could be applied for a given section is explained in Section 6.4.3.

6.4.2 Amount of Shear Reinforcement

As indicated in Section 6.4.1 above, two different spacings (250 mm and 180 mm) were used to examine the influence of the shear reinforcement ratio on the behaviour of shear damaged reinforced concrete beams. These two different spacings were only applied within the effective span (distance between supports) of the specimen. The variation of the shear capacities of cracked and repaired beams for different shear reinforcement ratios can be seen in Figure 6.6 and Figure 6.7 respectively.

The effect of shear reinforcement is higher in low grade concrete in the case of cracked beams. This implies that the shear reinforcement plays a major part in the stress transferring mechanism when the concrete is weaker. In the case of repaired beams also, as concrete strength increases, the influence of the shear reinforcement ratio decreases.

6.4.3 Post-Tensioning Force

External post-tensioning force is another important parameter in the design of post-tensioned reinforced concrete members. The amount of applied post-tensioning force is limited by a number of conditions. For an uncracked reinforced concrete beam these limitations can be expressed by the following inequality (Burgoyne 2005):

$$f_{t,allowable} \leq \frac{P}{A} + \frac{Pe}{Z} - \frac{M}{Z} \leq f_{c,allowable} \qquad (6.10)$$

where

$$\begin{aligned}
f_{t,allowable} \quad &= \quad \text{Permissible tensile stress in concrete,}\\
f_{c,allowable} \quad &= \quad \text{Permissible compressive stress in concrete,}\\
P \quad &= \quad \text{Prestressing force,}\\
A \quad &= \quad \text{Cross section area of the section,}\\
e \quad &= \quad \text{Eccentricity,}\\
Z \quad &= \quad \text{Elastic section modulus, and}\\
M \quad &= \quad \text{Applied moment.}
\end{aligned}$$

It was necessary to check the tensile and compressive stresses, in both the top and bottom fibre of the section, for every load case. The critical sections are normally, but not always, the mid-span and the sections over supports (for continuous beams). The stresses at any position are made up of three components, one of which normally has a different sign from the other two (see Equation 6.10); consistency of sign convention is essential.

When these limitations are plotted in a diagram, which is also known as 'Magnel diagram', the desirable post-tensioning force should be within the 'feasible region' of the diagram as shown in Figure 6.8. However, for a reinforced concrete beam with an existing shear crack an additional limitation need to be considered to satisfy the amount of stress that can be transferred across the shear crack.
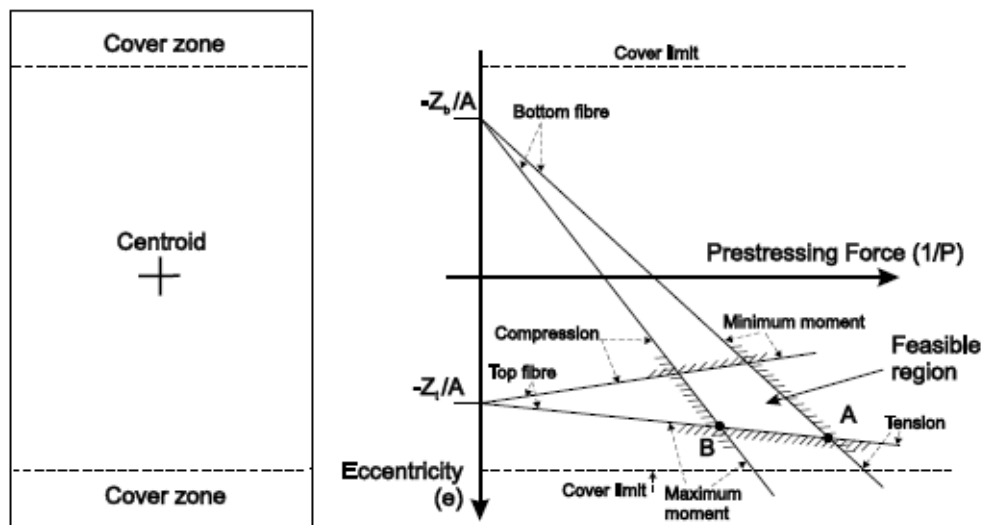
Figure 6.8. Magnel diagram for an uncracked section
Source: (Burgoyne 2005)
[Subscripts *b* and *t* denote bottom and top respectively]

In the case of a cracked section, the prestressing force applied to the section should satisfy the internal equilibrium of the forces. Modified compression field theory (MCFT) explains the basic stress transfer mechanism across the shear crack and the internal force equilibrium of a reinforced concrete section with existing shear cracks. Details of the MCFT can be found in Chapter 5.

By considering these facts together, a range of initial post-tensioned forces were selected to investigate the influence of initial external post-tensioning force on the behaviour of shear damaged reinforced concrete beams strengthened by external post-tensioning. Other parameters were fixed at experimental values as follows:

- concrete strength = 40 MPa;

- Young's modulus of the epoxy = 3.0 GPa;

- maximum crack width = 5 mm;

- shear reinforcement spacing = 250 mm.

Results obtained from the finite element analysis for different post-tensioning forces are summarised in Table 6.6.

Table 6.6: Variation of ultimate load for different initial post-tensioning force

Post-Tensioning Force [kN]	Ultimate Load [kN]	
	Cracked beam	**Repaired beam**
125	161	304
140	176	332
150	188	357
160	192	365

From Table 6.6, it can be noticed that existing shear crack has a significant influence on the capacity of the cracked beam with higher post-tensioning force. The increase in capacity is significantly lower in the cracked beam compared with that of the repaired beam as the post-tensioning force increases. In other words, a higher post-tensioning force does not increase the capacity of a cracked beam as much as it does in a repaired beam. A possible explanation is that the higher post-tensioning could lead to slip along the cracked plane. This is because the additional post-tensioning force increases the stress that needs to be transferred through the crack even before loading has commenced. That end up with early slip along the crack plane as the maximum stress that can transferred across the crack is the same regardless the amount of the post-tensioning force.

6.4.4 Crack Width

To investigate the influence of crack width in a shear damaged reinforced concrete beam strengthened by external post-tensioning, different multiplier values, k_w, were

considered to vary the average crack width according to Equation 6.3. Results obtained for different values of k_w are summarised in Table 6.7. Other parameters were set as follows:

- concrete strength = 40 MPa;

- initial post-tensioning force = 150 kN;

- maximum crack width = 5 mm;

- shear reinforcement spacing = 250 mm.

Table 6.7: Variation of ultimate load of a cracked beam with different value of k_w

k_w	Ultimate load [kN]
0.6	227
0.65	205
0.7	188
0.75	174
0.8	163

It can be noted from Table 6.7 that the ultimate load of a cracked section is quite sensitive to the average crack width (or k_w value). As can be seen from Figure 6.9 the stress that can be transferred across the shear crack, v_{ci} is very sensitive to the change of crack width for lower values of crack width. In general, the average crack width of an existing structure could be up to 2-3 mm, which is within the most sensitive range in terms of the maximum stress that could transfer across the crack. That means the crack width is one of the most important parameters in the determination of the capacity of cracked reinforced concrete members.
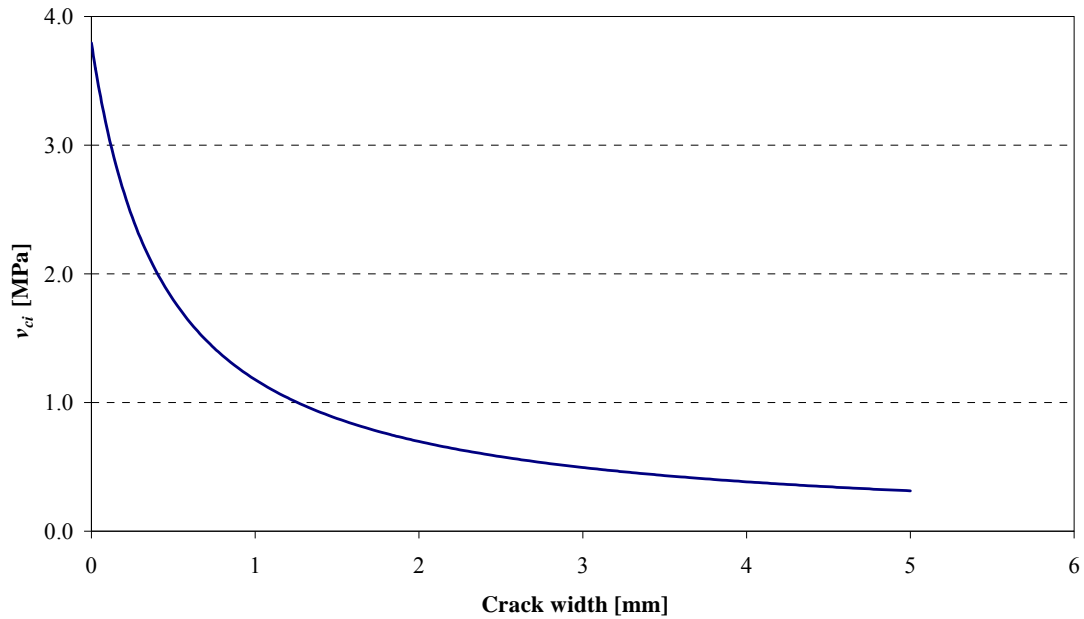
Figure 6.9. Variation of v_{ci} with crack width according to MCFT

6.4.5 Type of Epoxy Resin

To investigate the effect of the epoxy on the behaviour of a repaired beam, different values of Young's modulus for the epoxy resin were considered. For this parametric study a range from 2 GPa to 4 GPa was selected, which is the common range for most epoxies. Other parameters were fixed to the experimental values as follows:

- initial post-tensioning force = 150 kN;

- concrete Strength = 40 MPa;

- maximum crack width = 5 mm;

- shear reinforcement spacing = 250 mm.

The average crack width was taken as 0.7 of the maximum crack width.

The variation of the ultimate load of repaired reinforced concrete beams after strengthening by external post-tensioning is given in Table 6.8 for different values of Young's modulus for the epoxy resin while other parameters were set as above. It should be noted that normally the Young's modulus of commercially available epoxy resin will be close to 3 GPa.

Table 6.8: Variation of ultimate load for different values of Young's modulus of epoxy resin

Young's Modulus of Epoxy [GPa]	Predicted Ultimate Load [kN]	Increase in Ultimate Load[*] [%]
2.0	337	- 5.6
3.0	357	0
4.0	366	2.5

* Young's modulus of 3.0 GPa is considered as the reference value.

It can be seen from Table 6.8 that the increase in the Young's modulus of the epoxy from 2 GPa to 4 GPa (by 100%) could increase the capacity only by about 8.6%. This could be due to the following reasons:

- The epoxy filling region is insignificant compared to the volume of concrete.

- The epoxy has significantly higher compressive and tensile strengths than concrete.

- The epoxy was modelled as perfectly elastic material.

By considering these facts and the general range of Young's modulus in commercially available epoxy resin, it is suggested that the influence of different types of epoxy on the capacity of repaired beams will be minimal provided that the compressive and tensile strengths of the epoxy are significantly higher than those of concrete.

6.5   Discussion on Experimental and Numerical Results

In this section a comparison between the predicted shear capacities (or ultimate loads) using the finite element analysis (FEA) and experimental data is presented and discussed. Convergence and verification of the developed finite element model for cracked reinforced concrete beam are presented in Section 6.3 of this chapter.

As the FEA was performed only for cracked and repaired beams in this study, experimental data of the cracked and repaired beams strengthened by external post-

tensioning are compared with the predicted capacities of similar beams using FEA. Experimental data of the second (cracked) and the third (repaired) beams of both Group 1 and 2 (EPT12, EPT13, EPT22 and EPT23) are given with the predicted capacities of similar beams using FEA in Table 6.9. As explained previously, details of the experimental results were given in Chapter 4. The FEA predicted values are taken from the parametric study results presented in the previous section (Section 6.4).

Table 6.9: Comparison of finite element predicted ultimate loads with experimental data

Specimen	Experimental Data		Finite Element Analysis		Remarks
	Average Compressive Strength [MPa]	Ultimate load [kN]	Concrete Strength [MPa]	Predicted Ultimate Load [kN]	
EPT12	40.3	194	40	188	Pre-cracked + Post-tensioned
EPT22	32.3	173	32	168	
EPT13	40.4	310	40	357	Pre-cracked & Repaired + Post-tensioned
EPT23	40.5	293	40	364	

From Table 6.9 it can be noted that the finite element model predicts the capacities of externally post-tensioned cracked reinforced concrete beams to a reasonable level of accuracy. As noted earlier, the behaviour of the cracked beam strengthened by external post-tensioning is similar to that obtained from the FEA. Based on this it can be concluded that the finite element model developed in this study is reliable and conservative in predicting the ultimate strength of a shear damaged reinforced concrete beam strengthened by external post-tensioning.

Furthermore, it can also be noted from Table 6.9 that, the finite element predicted capacity is higher than that obtained from the experiment for the repaired beams strengthened by external post-tensioning. This is due to the assumption made in the FEA. As discussed in Chapter 5, to reduce the complexity associated with the repaired beam and simplify the modelling work for this study it was assumed that the beams were fully repaired with epoxy resin and free from any cracks. However, in

practice it is not possible to achieve this assumption as there will be some minor cracks which are not possible to repair due to following reasons:

- Some cracks may not be filled with the epoxy due to its viscosity. The epoxy (Nitofill LV) used in this research project can be used to fill cracks down to a width of 0.01 mm.

- Some cracks may be not visible from outside.

Due to these reasons the experimental beams reached a lower capacity than predicted using FEA and possibly with a lower Young's modulus. This can be seen in Figure 6.10 which compares the behaviour of an epoxy repaired beam as predicted by the FEA with the experimental data.
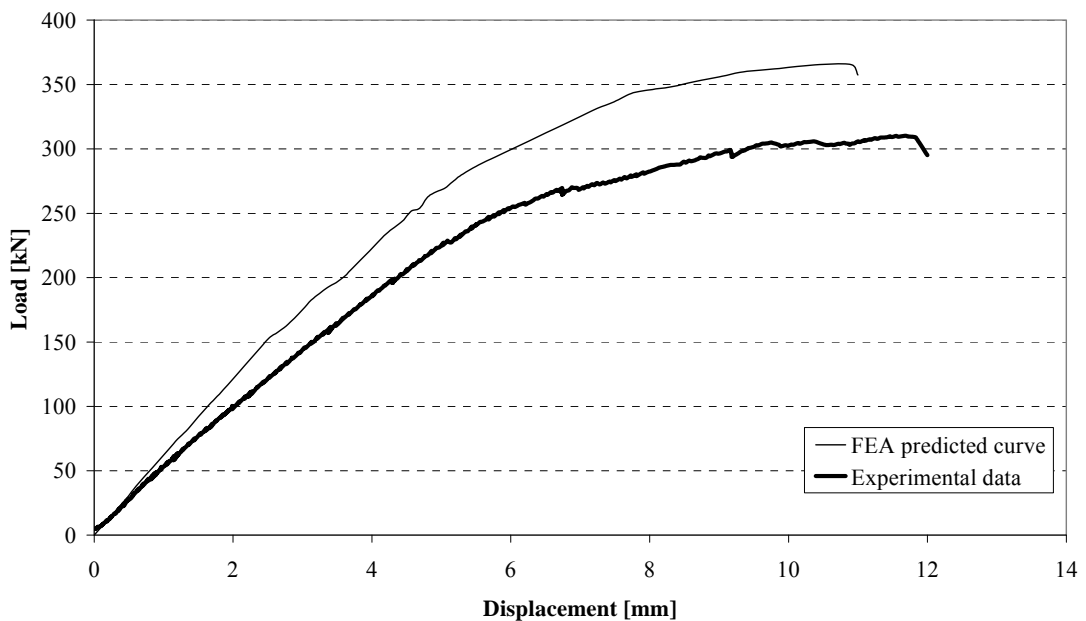
Figure 6.10. Comparison of FEA predicted behaviour of repaired beam with experimental data

The variation in the capacities of a repaired beam and the theoretical predictions can also be noted in Table 6.2, where the same assumption was made to predict the capacity of repaired beams strengthened by external post-tensioning. For comparison purposes the corresponding theoretical predictions of the repaired beams are reproduced in Table 6.10.

Table 6.10: Comparison of ultimate loads of repaired beams strengthened by external post-tensioning

Specimen	Average Compressive Strength [MPa]	Ultimate load [kN]			Remarks
		Experimental Data	Theoretical Prediction[*]	Finite Element Analysis[^]	
EPT13	40.4	310	341	357	Pre-cracked & Repaired + Post-tensioned
EPT23	40.5	293	349	364	

[*] No effect of epoxy resin was considered

[^] Concrete strength was taken as 40 MPa

From the comparison it can be concluded that the developed finite element model is reliable in predicting capacities of repaired reinforced concrete beams strengthened by external post-tensioning.

In general, it can be concluded that the developed finite element model could be used to estimate the capacities of both cracked and epoxy repaired reinforced concrete beams strengthened by external post-tensioning. In addition the developed finite element model is conservative in predicting the capacity of cracked reinforced concrete beams strengthened by external post-tensioning. Further improvements may be needed in the finite element modelling of repaired beams to make it a more conservative model for predicting capacities.

The experimental results reported in Chapter 4 indicate that compared to conventional external post-tensioning, external clamping significantly reduces the influence of shear cracks on the behaviour of cracked reinforced concrete beams and on the capacity of the member. In addition the increase in member capacity due to epoxy repair was insignificant with the external clamped specimens compared to the specimens with external post-tensioning. Since the experimental results suggested that external clamping could reduce the effect of existing shear cracks on member capacity, the influence of other parameters such as concrete strength, and crack width may be minimal. However due to time limitation of the PhD program, a

detailed parametric study related to external clamping was not carried out as part of this project.

6.6   Summary

The results of numerical analysis including theoretical predictions and finite element results were presented in this chapter. The numerical results were verified using the data obtained from the experimental program presented in Chapter 4. An attempt to determine an assigned value for average shear crack width using the maximum crack width appearing in a reinforced concrete beam was also presented. Using the experimental data, it was suggested that a value of 0.7 of the maximum crack width can be used as the average crack width to calculate the capacity of a cracked reinforced concrete beam to a reasonable level of accuracy. Available computer program for crack width prediction is also useful to get idea about the crack pattern and crack width in a reinforced concrete beam with a reasonable level of accuracy.

Results of a detailed parametric study were also presented in this chapter. The influence of a number of parameters such as concrete strength, amount of shear reinforcement, crack width, epoxy resin type and post-tensioning force on the behaviour of shear damaged reinforced concrete beams were investigated in the parametric study. It was concluded that crack width and post-tensioning force have a significant influence on the capacity of shear damaged concrete beams. In the case of repaired beams, the post-tensioning force is the most influential parameter while the type of epoxy has only a minimal effect on the capacity of repaired beams, provided that the epoxy resin has significantly higher compressive and tensile strengths than concrete.

In general, based on the outcomes of the parametric study, the following experimental results were confirmed:

- Shear cracks have a substantial effect on capacity of the reinforced concrete beams strengthened by external post-tensioning. The crack width and the

external post-tensioning force are the most important parameters when estimating the capacity of such members.

- Proper repair could significantly minimise the effect of shear cracks on the behaviour of cracked beams.

Detailed conclusions of this research study are given in the next chapter.

Chapter 7
CONCLUSIONS

The main objective and the background of this research project are outlined in the initial chapters of this thesis. The experimental program and the numerical study performed during the research project to achieve the objective are explained and discussed in Chapters 3 to 6. In general, both the main and specific objectives as indicated in Chapter 1 have been achieved.

This chapter will conclude the research study with the view to design an effective strengthening technique for shear damaged reinforced concrete beams. Due to time and resource constraints, it was not possible to address all of the issues associated with the current topic and, therefore, a number of possible scenarios are listed at the end of this chapter for researchers who are interested in this area.

7.1   General and Specific Conclusions

7.1.1 Conclusions Based on the Experimental Results

Based on the experimental data obtained from sixteen beams, the following conclusions were made:

- Existing shear cracks have a substantial effect on the shear capacity of reinforced concrete members. Unrepaired shear cracks significantly reduce

the efficiency of strengthening when the reinforced concrete members are strengthened by external post-tensioning.

- Compared to external post-tensioning, the application of external clamping to a shear damaged reinforced concrete member is more effective in reducing the effect of existing shear cracks on the behaviour of shear damaged concrete beams.

- Vertical clamping is a more effective method to increase member capacity than inclined clamping. However, both external clamping methods effectively reduced the reopening of existing shear cracks. Inclined clamping is an effective technique to reduce the effect of shear cracks provided that localised concrete failure due to high stress concentration is avoided. Further investigation is required in this regard.

- A suitable crack repair technique must be determined for concrete members with existing shear damage before attempting to strengthen them by external post-tensioning. An epoxy injection technique was found to be effective for crack repairs in this study. The proper repair of existing shear cracks using epoxy resin injection increases the capacity of a member as much as 70% when used with external post-tensioning.

- The failure of all the epoxy repaired beams, regardless of the type of strengthening methods, was similar to that of a new beam with the same strengthening technique. In particular, the crack development in repaired beams is very similar to a new beam.

7.1.2 Conclusions Based on the Simplified Mathematical Approach

A simplified approach to estimate the shear capacity of cracked beams strengthened by external post-tensioning and external clamping was developed in this research and presented in detail in Chapter 5. Results from the simplified approach developed in this study had a good correlation with the experimental results.

The attempt to relate the average crack width with the maximum crack width using a multiplier, k_w of 0.7 (linear relation) predicted the capacity to a reasonable level of accuracy.

It can be concluded that the simplified approach developed in this research is reliable and conservative in predicting the capacity of shear damaged concrete members strengthened by external applications.

7.1.3 Conclusions Based on the Numerical Results

A finite element model of shear damaged concrete beams was developed using the finite element package, Abaqus. Constitutive models of materials and element types were discussed in Chapter 5. Based on the parametric study performed using the developed finite element model, the following conclusions were drawn:

- Member capacity is very sensitive to the change of average crack width compared to the other parameters used in this study such as concrete strength, post-tensioning force and type of epoxy. This implies that the crack width need to be measured accurately and incorporated into the design of strengthening project for shear damaged reinforced concrete beams.

- The type of epoxy resin does not have much influence on the behaviour of repaired beams provided that the compressive and tensile strengths of the epoxy resin are significantly higher than those of concrete.

- Post-tensioning force also plays an important role in determining the capacity of cracked beams. A higher post-tensioning force did not increase the capacity as expected. In addition to the normal limitations considered during any prestressing reinforced concrete design, the limitation of the maximum stress transfer across the shear crack also needs to be considered when deciding the feasible post-tensioning force for a cracked reinforced concrete beam.

7.1.4 Overall Conclusions

Based on both the experimental and numerical results and discussions presented in previous chapters the following conclusions were made:

- Shear cracks in reinforced concrete beams have a substantial effect on the capacity and the behaviour of the beams when strengthened by conventional external post-tensioning. Although the effect of shear cracks is minimal when strengthened by external clamping, proper repair could increase the capacity by a significant amount (up to 20% of the unrepaired beam capacity).

- The simplified mathematical approach developed in this research project can be effectively used to estimate the shear capacity of the cracked reinforced concrete members strengthened by either external post-tensioning or external clamping.

- Any existing shear cracks need to be properly repaired prior to the strengthening of reinforced concrete beams. Epoxy resin can be used as an effective technique to repair the cracks.

7.2   Recommendations for Future Studies

Based on the findings and conclusions of this study, the following recommendations are provided for future research in the field of strengthening of shear damaged reinforced concrete members:

- A similar study is needed to investigate the effect of existing shear cracks in deep beams and to evaluate the influence of different parameters on the behaviour of such beams when strengthened with external post-tensioning.

- Further experimental studies are needed to understand the effect of external clamping, particularly inclined clamping, on the behaviour of shear damaged reinforced concrete beams. Special attention may be required to avoid localised failure near the clamping or loading positions as reported in this study. The use of high strength concrete may help to overcome this issue.

- It is also possible to eliminate the influence of shear cracks on the behaviour of cracked beams by using a combination of vertical clamping together with

external post-tensioning. By selecting correct values for external clamping and external post-tensioning, it is possible to get a similar effect as with inclined clamping. This will also prevent localised failure which happened with inclined clamping in this research. This could be an interesting topic for future research.

- There is a need to investigate a simplified standard method to measure the crack width as it is the most influential parameter in determining the member capacity of a cracked reinforced concrete member.

- In the numerical analysis associated with this research study, the epoxy repaired beams were assumed to be free of cracks after repair. The numerical methods predicted higher capacities than the experimental results as minor cracks were likely to have remained unrepaired. Therefore, further study is needed to develop a more reliable model to estimate the correct capacity of repaired beams. Although it is quite challenging to estimate internal cracks, they can significantly influence the capacity of repaired beams. A more effective strengthening method for shear damaged reinforced concrete structures could result from this model development.

- Further expansion of the strut-and-tie model to predict the crack pattern of a reinforced concrete beam with external clamping could be another potential area that needs to be investigated. This study could also combine the application of external post-tensioning together with the external clamping to investigate the optimum ratio of these external strengthening techniques.

REFERENCES

AASHTO. (2004). "AASHTO LRFD Bridge Design Specifications." American Association of State Highway and Transportation Officials.

Abaqus Inc. (2006). "Abaqus 6.6." SIMULIA, Providence, RI.

American Concrete Institute. (2002). "Building Code Requirements for Structural Concrete (ACI 318-02) and Commentary (ACI 318R-02)." ACI Standard, A. C. 318, ed., American Concrete Institute, Michigan, 443.

American Concrete Institute. (2003). "Structural Crack Repair by Epoxy Injection." *ACI RAP-1*, American Concrete Institute, Michigan.

American Concrete Institute. (2005). "Building Code Requirements for Structural Concrete (ACI 318-05) and Commentary (ACI 318R-05)." ACI Standard, A. C. 318, ed., American Concrete Institute, Michigan, 430.

Aravinthan, T. (1999). "Flexural Behaviour and Design Methodology of Externally Prestressed Concrete Beams" PhD thesis, Saitama University, Saitama Japan.

Aravinthan, T. (2006). "Is External Post-Tensioning an Effective Solution for Shear Strengthening of Bridge Elements?" 11th International Conference on Extending the Life of Bridges Concrete + Composites Buildings, Masonry + Civil Structures (Structural Faults + Repair 2006), M. C. Forde, ed., Engineering Technics Press, Edinburgh, U.K., on CD Rom.

Aravinthan, T., and Heldt, T. (2005). "Strengthening of Headstocks in Bridges with External Post-Tensioning." 22nd Biennial Conference Concrete 05, F. Andrews, B. Corcoran, and J. Sanjayan, eds., Melbourne, Australia.

Aravinthan, T., Sabonchy, E., and Heldt, T. (2004). "Application of External Post-tensioning for Strengthening of Headstocks in Bridges." 4th International Conference on Concrete under Severe Conditions: Environment and Loading, M. H. OH, ed., Seoul National University and Korea Concrete Institute, Seoul, South Korea, 1737-1744.

Aravinthan, T., and Suntharavadivel, T. G. (2007). "Effects of Existing Shear Damage on Externally Post Tensioned Repair of Bent Caps." *Journal of Structural Engineering*, 133(11), 1662-1669.

ASCE-ACI Committee 445 on Shear and Torsion. (1998). "Recent Approaches to Shear Design of Structural Concrete." *Journal of Structural Engineering*, 124(12), 1375-1417.

Bangash, M. Y. H. (2001). *Manual of Numerical Methods in Concrete: Modelling and applications validated by experimental and site-monitoring data*, Thomas Telford Publishing, Thomas Telford Ltd.

Bazant, Z. P., and Yu, Q. (2005a). "Designing Against Size Effect on Shear Strength of Reinforced Concrete Beams Without Stirrups: I. Formulation." *Journal of Structural Engineering*, 131(12), 1877-1885.

Bazant, Z. P., and Yu, Q. (2005b). "Designing Against Size Effect on Shear Strength of Reinforced Concrete Beams Without Stirrups: II. Verification and Calibration." *Journal of Structural Engineering*, 131(12), 1886-1897.

Bentz, E. (2001). "Response-2000." Toronto, Canada.

Bentz, E. C., Vecchio, F. J., and Collins, M. P. (2006). "Simplified Modified Compression Field Theory for Calculating Shear Strength of Reinforced Concrete Elements." *ACI Structural Journal*, 103(4), 614-624.

Burgoyne, C. J. (2005). "Analysis of Continuous Prestressed Concrete Beams." Essays in the History of the Theory of Structures, S. Huerta, ed., Instituto Juan de Herrera, Madrid, 61-77.

Carreira, D. J., and Chu, K.-H. (1985). "Stress-Strain Relationship for Plain Concrete in Compression." *Journal of Structural Engineering*, 82(6), 797-804.

Choi, K.-K., and Park, H.-G. (2007). "Unified Shear Strength Model for Reinforced Concrete Beams - Part II: Verification and Simplified Method." *ACI Structural Journal*, 104(2), 153-161.

Choi, K.-K., Park, H.-G., and Wight, J. K. (2007). "Unified Shear Strength Model for Reinforced Concrete Beams - Part I: Development." *ACI Structural Journal*, 104(2), 142-152.

Collins, F., and Roper, H. (1990). "Laboratory Investigation of Shear Repair of Reinforced Concrete Beams Loaded in Flexure." *ACI Material Journal*, 87(2), 149-159.

Collins, M. P., and Mitchell, D. (1991). *Prestressed Concrete Structures*, Prentice Hall, Englewood Cliffs, N.J.

Daly, A. F., and Witarnawan, I. W. (2000). "A Method for Increasing the Capacity of Short and Medium Span Bridges." 10th REAAA (Road Engineering Association of Asia and Australasia) Conference, Tokyo, Japan.

Dux, P. F. (2007). "Truss Models in Concrete Beam Design." Concrete Institute of Australia, Brisbane, Presentation made at Concrete Institute of Australia seminar – Designing for Shear.

Emmons, P. H., and Sordyl, D. J. (2006). "The State of the Concrete Repair Industry, and a Vision for its Future." Concrete Repair Bulletin, 7-14.

Filippou, F. C., Popov, E. P., and Bertero, V. V. (1983). "Effects of Bond Deterioration on Histeretic Behavior of Reinforced Concrete Joints." *UCB/EERC-83/19*, Earthquake Engineering Research Center, University of California, Berkeley, California.

Harajli, M. H. (1993). "Strengthening of Concrete Beams by External Prestressing." *PCI Journal*, 38(6), 76-88.

Harajli, M. H., Khairallah, N., and Nassif, H. (1999). "Externally Prestressed Members: Evaluation of Second- Order Effects." *Journal of Structural Engineering*, 125(10), 1151-1161.

Harajli, M. H., Mabsout, M. E., and Al-Hajj, J. A. (2002). "Response of Externally Post-Tensioned Continuous Members." *ACI Structural Journal*, 99(5), 671-680.

Hu, H.-T., Lin, F.-M., and Jan, Y.-Y. (2004). "Nonlinear Finite Element Analysis of Reinforced Concrete Beams Strengthened by Fiber-Reinforced Plastics." *Composite Structures*, 63, 271-281.

International Organization for Standardization. (1993). "Plastics - Determination of Tensile Properties - Part 2: Test Conditions for Moulding and Extrusion Plastics (ISO 527-2)." International Organization for Standardization, 5.

Karsan, I. D., and Jirsa, J. O. (1969). "Behavior of Concrete Under Compressive Loadings." *ASCE Journal of Structural Division*, 95(12), 2543-2563.

Khaloo, A. R. (2000). "Shear Repair of Reinforced Concrete Beams Using Post-Tensioning." Fourth International Conference on Repair, Rehabilitation, and Maintenance of Concrete Structures, and Innovations in Design and Construction, V. M. Malhotra, ed., American Concrete Institute, Seoul, Korea, 519-550.

Liang, Q. Q., Uy, B., Bradford, M. A., and Ronagh, H. R. (2004). "Ultimate Strength of Continuous Composite Beams in Combined Bending and Shear." *Journal of Constructional Steel Research*, 60, 1109-1128.

Liang, Q. Q., Uy, B., Bradford, M. A., and Ronagh, H. R. (2005). "Strength Analysis of Steel–Concrete Composite Beams in Combined Bending and Shear." *Journal of Structural Engineering*, 131(10), 1593-1600.

Maekawa, K., Pimanmas, A., and Okamura, H. (2003). *Nonlinear Mechanics of Reinforced Concrete*, Spon Press, London.

Mitchell, D., and Collins, M. P. (1974). "Diagonal Compression Field theory-A Rational Model For Structural Concrete in Pure Torsion." *ACI Journal*, 71(8), 396-408.

Miyamoto, A., Tei, K., Nakamura, H., and Bull, J. W. (2000). "Behavior of Prestressed Beam Strengthened with External Tendons." *Journal of Structural Engineering*, 126(9), 1033-1044.

Moon, J.-H., and Burns, N. H. (1997a). "Flexural Behaviors of Member with Unbonded Tendons I: Theory." *Journal of Structural Engineering*, 123(8), 1087-1094.

Moon, J.-H., and Burns, N. H. (1997b). "Flexural Behaviors of Member with Unbonded Tendons II: Applications." *Journal of Structural Engineering*, 123(8), 1095-1101.

Naaman, A. E., and Alkhairi, F. M. (1991). "Stress at Ultimate in Unbonded Post-Tensioning Tendons: Part 1 - Evaluation of the State of the Art." *ACI Structural Journal*, 88(5), 641-649.

Ngo, D., and Scordelis, A. C. (1967). "Finite Element Analysis of Reinforced Concrete Beams." *ACI Journal*, 64(3), 152-163.

Pantelides, C. P., Gergely, J., and Reaveley, L. D. (2001). "In-situ Verification of Rehabilitation and Repair of Reinforced Concrete Bridge Bents under Simulated Seismic Loads." *Earthquake Spectra*, 17(3), 507-530.

Pisani, M. A. (1999). "Strengthening by means of External Prestressing." *Journal of Bridge Engineering*, 4(2), 131-135.

Rabbat, B. G., and Sowlat, K. (1987). "Testing of Segmental Concrete Girders with External Tendons." *PCI Journal*, 32(2), 86-107.

Snelling, G. N. (2003). "The Shear Strengthening of Bridge Headstocks Using External Prestressing," Undergraduate Thesis, University of Southern Queensland, Toowoomba.

Standards Australia. (1981). "Australian Standard on Methods of Testing Concrete (AS 1012)." Standards Australia International Ltd,, Sydney.

Standards Australia. (1991). "Australian Standard on Methods of Testing Concrete (Method 14: Method for securing and testing cores from hardened concrete for compressive strength)." Standards Australia International Ltd,, Sydney.

Standards Australia. (1993). "Australian Standard on Methods of Testing Concrete (Method 1: Sampling of fresh concrete)." Standards Australia International Ltd,, Sydney.

Standards Australia. (2000). "Australian Standard on Methods of Testing Concrete (Method 10: Determination of indirect tensile strength of concrete cylinders)." Standards Australia International Ltd,, Sydney.

Standards Australia. (2001). "Australian Standard Concrete Structures (AS 3600)." Standards Australia International Ltd,, Sydney, 175.

Stevens, N. J. (2007). "Using Truss Models and Compression Field Theory to Maximise Predicted Shear Capacity." Concrete Institute of Australia, Brisbane, Presentation made at Concrete Institute of Australia seminar – Designing for Shear.

Suntharavadivel, T. G., and Aravinthan, T. (2005). "Overview of External Post-Tensioning in Bridges." Southern Engineering Conference, D. Thorpe, U. Yadav, C. Snook, and G. Liang, eds., Engineers Australia, Queensland Division, Toowoomba, Australia, 29-38.

Suntharavadivel, T. G., and Aravinthan, T. (2007). "Strengthening of Shear Damaged RC Beams with External Clamping." 4th International Structural Engineering & Construction Conference M. Xie and I. Patnaikuni, eds., Taylor & Francis, Melbourne, Australia, 375-380.

Tan, K. H., Farooq, M. A.-A., and Ng, C. K. (2001). "Behavior of Simple-Span Reinforced Concrete Beams Locally Strengthened with External Tendons." *ACI Structural Journal*, 98(2), 174-183.

Tan, K. H., and Naaman, A. E. (1993). "Strut-and-Tie Model for Externally Prestressed Concrete Beams." *ACI Structural Journal*, 90(6), 683-691.

Tan, K. H., and Ng, C. K. (1998). "Effect of Shear in Externally Prestressed Beams." *ACI Structural Journal*, 95(2), 116-128.

Tan, K. H., and Tjandra, R. A. (2003). "Shear Deficiency in Reinforced Concrete Continuous Beams Strengthened with External Tendons." *ACI Structural Journal*, 100(5), 565-572.

Teng, S., Kong, F. K., Poh, S. P., Guan, L. W., and Tan, K. H. (1996). "Performance of Strengthened Concrete Deep Beams Predamaged in Shear." *ACI Structural Journal*, 93(2), 159-171.

Vecchio, F. J., and Bucci, F. (1999). "Analysis of Repaired Reinforced Concrete Structures." *Journal of Structural Engineering*, 125(6), 644-652

Vecchio, F. J., and Collins, M. P. (1986). "The Modified Compression-Field Theory for Reinforced Concrete Elements Subjected to Shear." *ACI Journal Proceedings*, 83(2), 219-231.

Vecchio, F. J., and Collins, M. P. (1993). "Compression Response of Cracked Reinforced Concrete." *Journal of Structural Engineering*, 119(12), 3590-3610.

Vecchio, F. J., Gauvreau, P., and Liu, K. (2006). "Modeling of Unbonded Post-Tensioned Concrete Beams Critical in Shear." *ACI Structural Journal*, 103(1), 57-64.

Virlogeux, M. (1993). "External Prestressing Historical and Modern Applications." Workshop on Behaviour of External Prestressing in Structures, E. Conti and B. Foure, eds., France, 13-42.

Vishay Micro-Measurements. (2003). "System 5000 (Model 5100B Scanner) - Instruction Manual." Vishay Micro-Measurements, Raleigh, North Carolina.

Wagner, H. (1929). "Ebene Blechwandtrager mit sehr dunnem Stegblech (Metal Beams with Very Thin Webs)." *Zeitschrift fur Flugtechnik und Motorluftschiffahr*, 20(8 to 12).

Wight, J. K., and Parra-Montesinos, G. J. (2003). "Strut-and-Tie Model for Deep Beam Design: A practical exercise using Appendix A of the 2002 ACI Building Code." *Concrete International*, 63-70.

Woods, E. A. (2004). "Shear Strengthening and Model Testing of Concrete Bridge Headstocks," Undergraduate Thesis, University of Southern Queensland, Toowoomba.

Zwicky, D., and Vogel, T. (2006). "Critical Inclination of Compression Struts in Concrete Beams." *Journal of Structural Engineering*, 132(5), 686-693.

APPENDICES

<div align="right">

Appendix A
EXPERIMENTAL DATA
(Supplement to Chapter 3)

</div>

A.1 Material Properties

A.1.1 Concrete Strength

Details of the testing procedures to measure the concrete strength (both compressive and tensile strengths) were explained in Section 3.3.1.

Detailed results of the compressive and tensile strength tests are given in Table A. 1 and Table A.2 respectively. Average compressive strength was given in Table 3.2 (in Chapter 3). As specified in Chapter 3, the following ready-mix concrete was used to prepare the specimens:

- concrete mix - Ready mix;

- specification - 32 MPa, 20 mm nominal aggregate, 80 mm slump;

- supplier - Wagner, Toowoomba.

Table A. 1: Experimental results of concrete compressive strength

Specimen	Average Diameter [mm]	Peak Load [kN]	Compressive Strength [MPa]	
			Individual	Average
	99.95	317	40.4	
EPT11	99.99	318	40.5	39.9
	100.00	300	38.2	

	99.95	317	40.4	
	100.04	316	40.2	
EPT12	100.00	322	41	40.3
	100.03	312	39.7	
	100.02	308	39.2	
	99.95	317	40.4	
	100.00	322	41	
EPT13	100.02	319	40.6	40.4
	99.97	314	40	
	100.04	305	38.8	
	100.01	315	40.1	
	100.00	333	42.4	
EPT14	100.03	312	39.7	40.4
	100.02	308	39.2	
	99.95	317	40.4	
	100.02	319	40.6	
	100.05	331	42.1	
EPT21	100.20	243	30.8	29.3
	99.50	214	27.5	
	100.10	224	28.5	
	100.04	240	30.5	
	99.96	229	29.2	
EPT22	100.25	257	32.5	32.3
	100.05	248	31.6	
	99.98	248	31.6	
	99.97	257	32.8	
	100.00	258	32.8	
EPT23	100.00	319	40.6	40.5
	99.94	314	40	
	99.92	305	38.9	
	100.12	319	40.5	
	100.10	334	42.4	
EPT24	100.02	289	36.8	36.5
	99.97	276	35.2	
	100.04	292	37.2	
	100.01	290	36.9	
ECL31	100.00	309	39.3	39.4
	100.03	316	40.2	

	100.02	303	38.5	
	99.95	310	39.5	
	100.02	309	39.3	
ECL32	100.05	317	40.3	37.7
	99.95	301	38.3	
	99.99	280	35.6	
	100.00	295	37.6	
	99.95	288	36.7	
ECL33	100.04	334	42.5	41.6
	100.00	324	41.2	
	100.03	319	40.6	
	100.02	328	41.8	
	99.95	329	41.9	
ECL34	100.00	317	40.3	37.7
	99.89	300	38.3	
	100.00	280	35.6	
	99.94	295	37.6	
	99.92	288	36.7	
ECL35	100.12	335	42.5	41.6
	100.10	324	41.2	
	99.87	318	40.6	
	100.05	329	41.8	
	99.98	329	41.9	
ECL36	99.97	333	42.4	41.5
	100.00	324	41.2	
	100.00	324	41.2	
	99.94	320	40.8	
	99.92	329	41.9	
ECL37	100.12	320	40.6	40.0
	100.10	315	40	
	100.02	303	38.5	
	99.97	315	40.1	
	100.04	322	40.9	
ECL38	100.01	304	38.7	39.0
	100.03	300	38.2	
	100.02	310	39.4	
	99.95	308	39.2	
	100.00	310	39.5	

Table A.2: Experimental results of concrete indirect tensile strength

Specimen	Average Diameter [mm]	Height [mm]	Peak Load [kN	Tensile Strength [MPa]	
				Individual	Average
EPT11	150.35	299.6	210	2.97	3.04
	150.2	299.8	220	3.11	
EPT12	150.15	300	225	3.18	3.21
	150.3	299.9	230	3.25	
EPT13	150.1	300	230	3.25	3.29
	150.05	300	235	3.32	
EPT14	150.15	299.9	240	3.39	3.36
	150.1	299.9	235	3.32	
EPT21	150.1	299.9	185	2.62	2.58
	150.15	300	180	2.54	
EPT22	150.1	300.2	195	2.76	2.86
	149.95	300	210	2.97	
EPT23	149.95	300.1	255	3.61	3.54
	149.9	299.9	245	3.47	
EPT24	149.9	299.8	210	2.97	3.08
	150	300	225	3.18	
ECL31	149.65	299.7	190	2.70	2.91
	149.9	299.9	220	3.12	
ECL32	150	300.1	220	3.11	3.04
	150.1	300	210	2.97	
ECL33	150.1	299.6	285	4.03	3.96
	150	299.9	275	3.89	
ECL34	150	300.1	220	3.11	3.04
	150.1	300	210	2.97	
ECL35	149.85	300.1	285	4.03	3.97
	149.75	300	275	3.90	
ECL36	149.65	299.6	270	3.83	3.86
	149.9	299.9	275	3.89	
ECL37	150.25	300	270	3.81	3.78
	150.2	300.1	265	3.74	
ECL38	150	300	255	3.61	3.54
	150.1	300	245	3.46	

A.2   Data Sheets

A.2.1 Epoxy Resin

In the experimental program, cracked reinforced concrete beams were repaired using epoxy resin. Two types of epoxy components, namely Lokset E (structural epoxy adhesive paste and filler) and Nitofill LV (a low viscosity epoxy) were used for these repair purposes. Initially, the cracks were sealed with Lokset E. After allowing two days to cure the external seal, Nitofill LV was injected through holes at various points along the cracks. Details of the both Lokset E and Nitofill LV are given below (Figure A.1 and Figure A.2):

FOSROC

Lokset E

Structural epoxy adhesive paste and filler

Uses

For speedy and permanent patching repairs to concrete structures; bonding of precast concrete components and all repair work to concrete cementitious substrates where strength, impermeability to water, and resistance to aggressive chemicals is essential; emergency repairs to concrete structures, sea walls, and industrial floors in chemical handling and process areas.

The thixotropic nature of Lokset E makes the product ideal for setting starter bars, dowels, holding down bolts and anchoring in general.

Advantages

- Early development of initial hardness, minimises maintenance disruption

- Pre-weighed quality controlled materials ensure consistency and reduce risk of site errors

- Two pack colour coding gives visual check on correct mixing

- Unaffected by a wide range of acids, alkalis and industrial chemicals

- 3 to 4 times stronger than typical concrete. Excellent resistance to abrasion and impact

- Natural grey colour sympathetic to aesthetic requirements

Description

Lokset E is a two-component, epoxy paste consistency, structural adhesive/filler. It cures, with minimal shrinkage, at temperatures above 5°C to a very strong, dense solid.

The mixed material is applied to a suitably prepared surface and quickly cures to form a complete impermeable repair unaffected by many forms of chemical attack.

It is supplied as a two pack colour coded material in pre-weighed quantities ready for on-site mixing and use.

Technical support

Parbury Technologies offers a comprehensive range of high quality, high performance construction products. In addition, Parbury Technologies offers technical support and on-site service to specifiers, end-users and contractors.

Lokset E: 1/1999

Properties

Data quoted is typical for this product but does not constitute a specification.

Pot life:	1.5 litre mix at 25°C – 25-35 minutes. Note: To obtain maximum pot life, spread Lokset E into a thin (less than 10 mm) layer immediately after mixing.
Initial hardness:	24 hours.
Full cure:	7 days. Below 20°C the curing time will be increased.
Minimum application temperature:	5°C.
Maximum service temperature:	50°C.
Specific gravity (mixed):	1.7 (approx.)

Chemical resistance:

Citric Acid 10%	Excellent
Tartaric Acid 10%	Excellent
Sodium Hydroxide 50%	Excellent
Diesel Fuel/Petrol	Excellent
Sugar Solutions	Very Good
Lactic Acid 10%	Very Good
Hydrocarbons	Very Good
Phosphoric Acid 50%	Very Good

Colour:	Grey, when mixed (may yellow and/or darken when exposed to sunlight or certain chemicals.

Instructions for use

Preparation

All grease, oil, chemical contamination, dust, laitance and loose concrete must be removed by scabbling or light bush hammering to provide a sound substrate.

All concrete must be at least 14 days old prior to treatment.

Steel surfaces should be grit blasted to white metal. Surfaces which show any traces of oil must be degreased with a chemical degreaser prior to grit blasting.

FOSROC

Mixing

Thoroughly mix resin (white) and curing agent (black) until an even grey colour is obtained. Mix for minimum 3 - 5 minutes.

Application

Apply the mixed Lokset E with a notched trowel, putty knife, caulking gun, twin cartridge gun etc., depending upon the application. Bonded surfaces should be held rigidly together until the Lokset E has set.

Cleaning

All tools and equipment should be cleaned immediately after use with Fosroc Solvent 20. Hardened material can only be removed mechanically.

Estimating

Supply

Lokset E is supplied in 1.5 litre and 6 litre two component packs and a convenient 450 ml twin cartridge pack.

Quantity estimating guide

Table indicates volume of Lokset E in ml/100 mm bond.

Hole Diameter (mm)	Volume of grout for bolt diameter (mm)					
	12	16	20	25	32	40
20	25					
25	50	40	25			
32	80	70	60	40		
38		100	100	75	45	
45			150	130	100	45
50				180	150	90
62					280	225

These figures allow for a 25% wastage factor.

Storage

Lokset E has a shelf life of 12 months when stored in a dry place below 35°C in unopened containers.

Precautions

Health and safety

Prolonged and repeated skin contact with epoxy resins and curing agents may cause dermatitis in persons sensitive to these products. Gloves, barrier creams, protective clothing and eye protection should be worn when handling these products. If poisoning occurs, contact a doctor or Poisons Information Centre. If swallowed, do NOT induce vomiting - give a glass of water. If in eyes, hold eyes open, flood with water for at least 15 minutes. If skin contact occurs, remove contaminated clothing and wash skin thoroughly.

Material Safety Data Sheets (MSDS) are available to users of Parbury Technologies products on request to their nearest Parbury Technologies branch. Read MSDS, data sheet and label carefully before first use of any product.

Fire

Lokset E is non-flammable.

Additional information

Lokset E is only one product in the Parbury Technologies range of construction products. Ancillary products include concrete repair products, grouts, joint sealants, protective coatings, anchoring and flooring products, all ideally suited for industrial maintenance and construction requirements.

Manufactured and sold under license from Fosroc International Limited, England. Fosroc, the Fosroc logo and Lokset are trade marks of Fosroc International Limited, used under license.

PARBURY
TECHNOLOGIES

PARBURY TECHNOLOGIES PTY LTD	Sales Offices:	
A.C.N. 069 961 968	St Peters, Sydney	(02) 9519 4722
	Wetherill Park, Sydney	(02) 9604 9399
33 Lucca Road	Archerfield, Brisbane	(07) 3255 5666
NORTH WYONG, N.S.W. 2259	Gold Coast	(07) 5539 3822
Tel (02) 4350 5000	Townsville	(07) 4725 4394
Fax (02) 4351 2024	Gladstone	(07) 4972 6499
	Adelaide	(08) 8293 2222
	Perth	(08) 9356 2533
	Melbourne	(03) 9326 3100
Email: pttech@partech.com.au	7 days a week, 24 hour	1800 817 779
Internet: www.partech.com.au	Technical Support Hotlines:	1800 812 864

Important note

Parbury Technologies products are guaranteed against defective materials and manufacture and are sold subject to its standard terms and conditions of sale, copies of which may be obtained on request. Whilst the company endeavours to ensure that any advice, recommendation, specification or information it may give is accurate and correct, it cannot, because it has no direct or continuous control over where or how its products are applied, accept any liability either directly or indirectly arising from the use of its products, whether or not in accordance with any advice, specification, recommendation or information given by it.

AUS/0040/99/A

Figure A.1. Data sheet of Lokset E

FOSROC

Nitofill LV

6/1997

Nitofill LV

Pre-packaged low viscosity epoxy crack injection system

Uses

Nitofill LV is designed for injecting cracks in concrete and masonry wherever there is a need to consolidate a structure or exclude water and air from contact with the reinforcement.

Nitofill LV is a low viscosity system and is suitable for cracks down to 0.2 mm at the surface and cracks tapering internally down to 0.01 mm.

The Nitofill LV system is ideal for small scale repairs on site and is also suitable for insitu or precast concrete elements

Advantages

System includes everything necessary to complete the crack injection.

Convenient to use, disposable cartridge pack contains both base and hardener.

Safe and clean to use.

High strength, excellent bond to concrete and masonry.

Low viscosity allows cost effective and efficient repair.

Description

Nitofill LV crack injection system incorporates a two part epoxy base and hardener contained in a dual cartridge pack.

The Nitofill LV accessory items which are packed individually and complimentary to the cartridge pack are - a cartridge gun, injection flanges, static mixers and hoses, flange adaptors and a removing tool.

Technical support

Parbury Technologies offers a comprehensive range of high performance, high quality construction products. In addition, Parbury Technologies offers a technical support service to specifiers, end-users and and contractors, as well as on site technical support.

Design criteria

Nitofill LV is suitable for injecting cracks in concrete and masonry down to 0.2 mm at the surface and internal cracks tapering down to 0.01 mm.

The system should not be used for cracks where movement is expected to continue.

Properties

The following results are typical for the hardened Nitofill LV epoxy resin.

Usable life at	10°C:	40 minutes
	20°C:	20 minutes
	30°C:	10 minutes
Viscosity at	10°C:	250-450 cps
	20°C:	150-200 cps
	30°C:	50-100 cps
Compressive strength	1 day	57MPa
(BS 6319)	3 day	66MPa
	7 day	83MPa
Tensile strength (BS 6319):	>25 MPa	
Flexural strength (BS 6319):	>50 MPa	

Chemical resistance

The cured Nitofill LV epoxy is resistant to oil, grease, fats, most chemicals, mild acids and alkalis, fresh and sea water. Consult Parbury Technologies Technical Department when exposure to solvents or concentrated chemicals is anticipated.

Specification clauses

Low viscosity crack injection system

The crack injection system shall be Nitofill LV. It shall be applied strictly in acordance with the application instructions given in the product data sheet.

Instructions for use

Surface preparation

All contact surfaces must be free from oil, grease, free standing water or any loosely adherent material. All dust must be removed.

Mixing the surface sealant

Lokset E is used to bond the injection flanges to the substrate and to seal the face of the crack. Pour all the contents of the Lokset E hardener pack into the base container. Mix using a slow speed mixer until homogeneous.

Nitofill LV: 6/1997

FOSROC

Application of the surface sealant

Immediately after mixing apply a small amount of product to the underside of each flange, making sure that the valve will not be blocked and place the flange centrally over the crack. Flanges should be placed between 200 mm and 500 mm apart dependent on crack size, along the length of the crack. Additional surface sealant should be applied around each flange edge and to the remainder of the crack between the flanges to ensure a resin tight seal to the substrate.

Where cracks can be sealed on one side only, flanges should be placed at centres which are 80% of the depth to which the resin is required to penetrate.

Application of the Nitofill LV injection resin can commence as soon as the Lokset E has fully hardened, (at least 12 hours at 20°C)

Injection of the Nitofill LV epoxy resin

The Nitofill LV static mixer/hose should be screwed onto the cartridge. The cartridge is then placed into the gun and the outlet end of the hose pushed onto the lowest flange using the adaptor.

The contents of the cartridge are then injected until the resin flows from an adjacent flange, or until firm and sustained hand pressure on the gun trigger signifies that no further resin will be accepted. Then pull the barb on the flange away from the base. Remove the liner strip out of the barb on the flange. Hold the base of the flange while removing the liner slip from the barb. This will ensure the flange is not accidentally removed from the substrate. The flange should be in the closed position when the liner slip is pulled totally away from the base. This will prevent material flowing out from the crack. The pressure should be released and the hose disconnected from the flange using the adaptor and tool.

The injection hose can then be refixed to an adjacent flange, and more Nitofill LV resin injected. Repeat the process until the entire length of crack has been injected.

In the case of cracks which go all the way through a wall or slab, the resin should be injected through alternate flanges on both sides where access is possible. In the case of slabs, injection from the underside takes precedence to top injection.

Making good

After the Nitofill LV injection resin has set, remove the flanges. These can be knocked off with a hammer. Make good any holes or voids with Lokset E.

The existing surface sealant can then be removed using a sharp broad-chisel or by grinding until the original substrate profile is restored.

Cleaning

All tools and equipment should be cleaned immediately after use with Fosroc Solvent 10.

Limitations

The Nitofill LV resin injection system should not be used for cracks where movement is expected to continue. Other measures should be taken to accommodate such movement, ie cutting and forming a movement joint.

Contact your local Parbury Technologies branch for further information.

Estimating

Nitofill LV resin:	450 ml pack (12 per carton)
Lokset E:	1.5 and 6 litre packs
Fosroc Solvent 10:	20 litre pails

Nitofill LV system accessory items

Nitofill LV Gun:	single item
Nitofill LV Flange:	50 per bag
Nitofill LV Adaptor:	10 per bag
Nitofill LV Static mixer/hose:	10 per bag
Nitofill LV Flange tool:	10 per bag

Storage

Nitofill LV resin, Lokset E and Fosroc Solvent 10 have a shelf life of 12 months if kept in dry conditions at 20°C.

Precautions

Fire

Fosroc Solvent 10 is flammable. In the event of fire extinguish with CO_2 or foam.

Health and safety

Nitofill LV resin and Lokset E contain resins which may cause sensitisation by skin contact. Avoid contact with skin and eyes and inhalation of vapour. Wear suitable protective clothing, gloves and eye/face protection. Barrier creams provide additional skin protection. Should accidental skin contact occur, remove immediately with a resin removing cream, followed by soap and water. Do not use solvent. In case of contact with eyes, rinse immediately with plenty of clean water and seek medical advice. If swallowed seek medical attention immediately - **do not** induce vomiting.

Nitofill LV

6/1997

Fosroc Solvent 10: Flammable liquid.
Flash point: 27°C.

Keep away from sources of ignition - no smoking. Wear
suitable protective clothing, gloves and eye/face protection.
Use only in well ventilated areas.

A product Material Safety Data Sheet is available to users on
request to their nearest Parbury Technologies branch. Read
MSDS and product data sheet carefully before first use. In
emergency, contact any Poisons Information Centre.

Manufactured and sold under license from Fosroc International Limited,
England. Fosroc, the Fosroc logo, Nitofill and Lokset are trade marks of
Fosroc International Limited, used under license.

PARBURY
T E C H N O L O G I E S

PARBURY TECHNOLOGIES PTY LTD
A.C.N. 069 961 968

33 Lucca Road
NORTH WYONG, N.S.W. 2259
Tel (02) 4350 5000
Fax (02) 4351 2024

Sales Offices:

St Peters, Sydney	(02) 9519 4722
Wetherill Park, Sydney	(02) 9604 9399
Archerfield, Brisbane	(07) 3255 5666
Gold Coast	(07) 5539 3822
Townsville	(077) 254 394
Gladstone	(079) 726 499
Adelaide	(08) 8293 2222
Perth	(08) 9356 2533
Melbourne	(03) 9326 3100

7 days a week, 24 hour   1800 817 779
Technical Support Hotlines :   1800 812 864

Important note

Parbury Technologies products are guaranteed against defective materials and manufacture and are sold subject to its standard terms and conditions of sale,
copies of which may be obtained on request. Whilst the company endeavours to ensure that any advice, recommendation, specification or information it may
give is accurate and correct, it cannot, because it has no direct or continuous control over where or how its products are applied, accept any liability either
directly or indirectly arising from the use of its products, whether or not in accordance with any advice, specification, recommendation or information given
by it.

AUS/121/97/B

Figure A.2. Data sheet of Nitofill LV

A.2.2 Strain Gauges

In the experimental program, the strain in the reinforcement bar was measured by 2
mm (FLA-2-11 type) strain gauges while 30 mm (PFL-30-11 type) gauges were used
to measure the strain in the concrete. Both types were 120.4 Ω ($\pm$ 0.5%) linear strain
gauges with a gauge factor of 2.11 ($\pm$ 1%). Data sheets for both the 2 mm and the 30
mm strain gauges are shown in Figure A.3 and Figure A.4.

TML STRAIN GAUGE TEST DATA

GAUGE TYPE	: FLA-2-11		TESTED ON	: SS 400

COEFFICIENT OF
THERMAL EXPANSION : 11.8 $\times 10^{-6}/°C$

LOT NO.	: A513411

GAUGE FACTOR	: 2.11	±1%

TEMPERATURE
COEFFICIENT OF G.F. : $+0.1\pm0.05$ %/10°C

ADHESIVE	: P-2		DATA NO.	: A0480

THERMAL OUTPUT (ε app : APPARENT STRAIN)

ε app $= -2.33\times10^{1}+1.57\times T^{1}-1.21\times10^{-2}\times T^{2}-4.97\times10^{-4}\times T^{3}+4.55\times10^{-6}\times T^{4}$ (μm/m)

TOLERANCE : ±0.85 [(μm/m)/°C] , T : TEMPERATURE

ひずみゲージ取扱いの注意事項

● 上記の特性データは、リード線の取付けによる影響を含んでおりません。裏面記載のリード線の測定値への影響に従って補正してください。
● ゲージの使用温度は、接着剤の耐熱温度などにより変わります。
● 絶縁抵抗などの点検は、印加電圧を５０V以下にしてください。
● ゲージリード線に無理な力を加えないでください。
● ゲージ裏面に接着剤を塗布して接着してください。
● ひずみゲージの裏面は脱脂洗浄してありますので、汚さないように取扱いしてください。
● ゲージの包装を開封後は、乾燥した場所で保管してください。
● ご使用に際してご不明な点などがございましたら、当社までお問い合わせください。

CAUTIONS ON HANDLING STRAIN GAUGES

● The above characteristic data do not include influence due to lead wires. Correct the data in accordance with the influence of lead wires on measured values described overleaf.
● The service temperature of strain gauge depends on the operating temperature of adhesive, etc.
● Check of insulation resistance, etc. should be made at a voltage of less than 50V.
● Do not apply an excessive force to the gauge leads.
● Apply an adhesive to the back of a strain gauge and stick the gauge to a specimen.
● As the back of strain gauge has been degreased and washed, do not contaminate it.
● After unpacking, store strain gauges in a dry place.
● If you have any questions on strain gauges or installation, contact TML or your local agent.

Made in Japan

TML 株式會社 東京測器研究所

〒 140-8560 東京都品川区南大井 6 - 8 - 2
TEL 03 - 3763 - 5611
FAX 03 - 3763 - 6128

Tokyo Sokki Kenkyujo Co., Ltd.

8 - 2, Minami - Ohi 6 - Chome
Shinagawa - ku, Tokyo 140-8560

Figure A.3. Data sheet of 2 mm strain gauge

TML STRAIN GAUGE TEST DATA

GAUGE TYPE	: PFL-30-11	TESTED ON	: SS 400
LOT NO.	: A701615	COEFFICIENT OF THERMAL EXPANSION	: 11.8 $\times 10^{-6}/°C$
GAUGE FACTOR	: 2.13 ±1%	TEMPERATURE COEFFICIENT OF G.F.	: +0.15±0.05 %/10°C
ADHESIVE	: P-2	DATA NO.	: D0030

THERMAL OUTPUT (ε app : APPARENT STRAIN)

$\varepsilon\,app = -1.62\times10^{1}+1.63\times T^{1}-4.55\times10^{-2}\times T^{2}+2.27\times10^{-4}\times T^{3}+3.52\times10^{-8}\times T^{4}$ (μm/m)

TOLERANCE : ±0.85 [(μm/m)/°C] , T : TEMPERATURE

ひずみゲージ取扱いの注意事項

● 上記の特性データは、リード線の取付けによる影響を含んでおりません。裏面記載のリード線の測定値への影響に従って補正してください。
● ゲージの使用温度は、接着剤の耐熱温度などにより変わります。
● 絶縁抵抗などの点検は、印加電圧を50V以下にしてください。
● ゲージリード線に無理な力を加えないでください。
● ゲージ裏面に接着剤を塗布して接着してください。
● ひずみゲージの裏面は脱脂洗浄してありますので、汚さないように取扱いしてください。
● ゲージの包装を開封後は、乾燥した場所で保管してください。
● ご使用に際してご不明な点などがございましたら、当社までお問い合わせください。

CAUTIONS ON HANDLING STRAIN GAUGES

● The above characteristic data do not include influence due to lead wires. Correct the data in accordance with the influence of lead wires on measured values described overleaf.
● The service temperature of strain gauge depends on the operating temperature of adhesive, etc.
● Check of insulation resistance, etc. should be made at a voltage of less than 50V.
● Do not apply an excessive force to the gauge leads.
● Apply an adhesive to the back of a strain gauge and stick the gauge to a specimen.
● As the back of strain gauge has been degreased and washed, do not contaminate it.
● After unpacking, store strain gauges in a dry place.
● If you have any questions on strain gauges or installation, contact TML or your local agent.

Made in Japan

TML 株式会社 東京測器研究所
〒140-8560 東京都品川区南大井 6-8-2
TEL 03-3763-5611
FAX 03-3763-6128

Tokyo Sokki Kenkyujo Co., Ltd.
8-2, Minami-Ohi 6-Chome
Shinagawa-ku, Tokyo 140-8560

Figure A.4. Data sheet of 30 mm strain gauge

A.2.3 Post-tensioning Bar

In the experimental program, Two 26.5 mm high tensile Macalloy bars were used to apply the external post-tensioning force to the specimen. The mechanical properties of these Macalloy post-tensioning bars are given in Figure A.5.

BAR POST-TENSIONING

Macalloy
BAR & CABLE SYSTEMS

RANGE OF MACALLOY 1030 BAR

NOMINAL DIAMETER	NOMINAL CROSS SECTION AREA	MASS OF BAR		MAJOR DIAMETER OF THREADS	MIN. HOLE DIAMETER IN STEELWORK
		MACALLOY 1030	*MACALLOY S1030		
mm	mm²	kg/m	kg/m	mm	mm
20	315	-	2.53	22.0	24
25	491	4.09	4.09	28.9	31
26.5	552	4.58	-	30.4	33
32	804	6.63	6.63	36.2	40
36	1018	8.35	-	40.2	44
40	1257	10.30	10.30	45.3	49
50	1963	15.72	-	54.8	59
75	4185	33.00	-	77.2	82

MECHANICAL PROPERTIES OF MACALLOY 1030 BAR

GRADE	CHARACTERISTIC ULTIMATE TENSILE STRENGTH MPa	MINIMUM 0.1% PROOF STRESS MPa	MINIMUM ELONGATION %	APPROXIMATE MODULUS OF ELASTICITY GPa
Macalloy 1030 25-50mm	1030	835	6	170
Macalloy 1030 75mm	1030	835	6	205
*Macalloy S1030	1030	835	10	185

Figure A.5. Mechanical properties of Macalloy post-tensioning bars
Source: http://www.structuralsystems.com.au/

A.3   Risk Assessment

All test set-up and loading arrangements were checked and a detailed risk assessment was prepared by the University safety officer. The risk assessment sheet prepared for this research is shown in Table A.3.

Table A.3: Risk assessment sheet prepared during the experimental program

Hazard	People at Risk	Injury Type	Risk Level	Risk Management
Cuts when assembling cages	Only the People involved in the process (1-2 people)	Cuts to hands and arms	Low	Hold reinforcement in vice when cutting, take care when assembling cages
Slipping on wet floor when casting	All in the area (up to 6 people)	Could injure any part of body	Low	Avoid too much spillage of concrete, Wear boots with slip resistant or good grip sole
Eye contact with concrete	All in the area (up to 6 people)	Eye irritation	Low	Personal care
Test beams falling over when loading, post tensioning, moving, or curing	People within 1m of beams (up to 6 people)	Crushing of legs or feet	High	Wear steel capped boots, check support conditions, secure chains when moving, and avoid high stacks when curing
Lifting heavy objects (i.e. moving or positioning beams)	Up to 6 people	Muscular injuries to back, legs, or arms	Moderate	Use lifting trolley or forklift to move beams, manual lifting only for final positioning (use correct lifting position)
Breaking or slipping of post tensioning rods	All in area (up to 6 people)	Severe impact to any part of body	Very high	Check equipment thoroughly, no standing allowed behind either end of the rods when loaded, erect warning signs when post-tensioning in progress
Contact with epoxy resin or crack sealant	People when applying adhesives (1-2 people	Skin irritation, respiratory problems	Low	Wear gloves and long sleeve shirt, Follow MSDS handling instructions
Removal of Lokfix E sealant	People grinding sealant off (1-2 people)	Respiratory problems	Low	Wear dust mask when grinding sealant

<div align="right">

Appendix B
EXPERIMENTAL RESULTS
(Supplement to Chapter 4)

</div>

B.1   General

In this appendix the experimental data obtained during the testing of sixteen beams are given in detail. As the sampling rate of 1 Hz was used in System 5000, large amounts of data were recorded. Therefore, the data were filtered and given in the simplest form. These data were used to plot the graphs presented in Chapter 4. Full data are available in the CD Rom attached to this dissertation. Full data attached to the CD Rom are in text format which can be open in Excel. In order to identify the required data, guidance is given below.

A number of gauges were used to obtain measurements during the experiment. For the convenience of readers, a brief summary of instrumentation is given below.

Displacement: Measured at the mid point of the beam using String pot and/or LVDT.

Applied load: Measured using a load cell attached to the loading machine.

Post-tensioning force: Measured using load cells attached to the post-tensioning rods.

Strains in reinforcement bars & concrete: Measured using strain gauges attached to the reinforcements and concrete as shown in Figure B.1.

Strains in external clamping rods: Measured using strain gauges attached to the external clamping rods.

Details of instrumentation and gauge details were explained in Chapter 3.
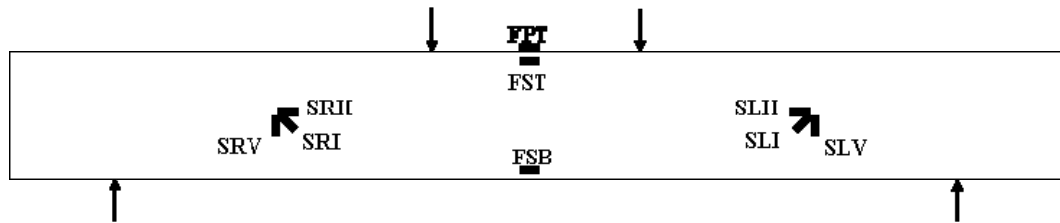
(a) Strain gauge locations in concrete (attached outer surface of the beam)

[**FS** – flexure side; **FP** – flexure plan; **S** – shear; **T** – top; **B** – bottom; **R** – right; **L** – left; **V** – vertical; **H** – horizontal; **I** – inclined]
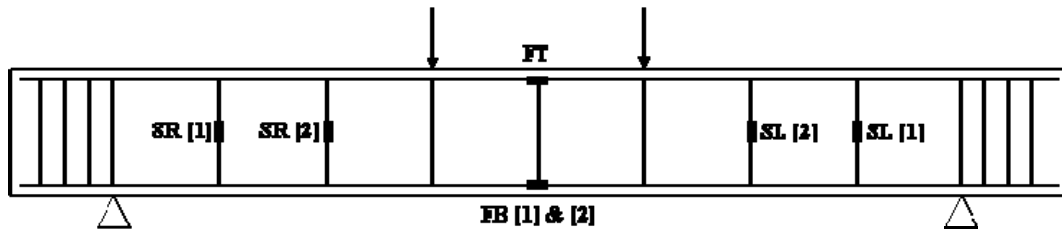
(b) Strain gauge locations in steel bars

[**F** – flexure; **S** – shear; **T** – top; **B** – bottom; **R** – right; **L** – left]

Figure B.1. Strain gauge locations in the testing specimen

The gauges indicated above were attached to the System 5000 through a channel using either a high level card or a strain gauge card. Again full details of System 5000 can be found in Chapter 3 under Section 3.4.5 (Data Acquisition System). Table B.1 summarises the details of the channel allocations for each of these gauges during the experiments.

Table B.1: Channels allocation in System 5000 for each measurement

Gauge Detail	Channel Number			Remarks
	Group 1	**Group 2**	**Group 3**	
LVDT	1	1	1	Displacement
String Pot	2	2	2	
SRV	20	11	11	Strain gauges attached to the reinforcement bars
SRI	19	12	12	
SRH	18	13	13	
FPT	14	14	14	
FST	16	16	16	
FSB	17	17	17	
SLH	13	18	18	
SLI	12	19	19	
SLV	11	20	20	
SR[1]	21 or 22	29 or 30	21	Strain gauges attached to the concrete
SR[2]	23 or 24	27 or 28	22	
FT	31	31	23	
FB[1]	25	25	24	
FB[2]	26	26	25	
SL[2]	27 or 28	23 or 24	26	
SL[1]	29 or 30	21 or 22	27	
Load cell 1	40	40	40	Applied load
Load cell 2	39	39	-	Post-tensioning force
Load cell 3	38	38	-	
Strain gauge 1	-	-	35	Strain gauges attached to the external clamping roads
Strain gauge 2	-	-	36	
Strain gauge 3	-	-	37	
Strain gauge 4	-	-	38	

Filtered data in its simplest format, for each group, is given in the following sections.

B.2 Group 1

Group 1 consisted of four reinforced concrete beams. All beams were designed with a rectangular cross section of 150×300 mm and a length of 2500 mm. 2-N24 bars were used as tensile reinforcement and 2-N16 bars were used as compressive reinforcement. R6 bars were placed at a spacing of 250 mm as shear reinforcements. Beams were named EPT11, EPT12, EPT13 and EPT14. All beams except the first beam EPT11 were strengthened by external post-tensioning.

Filtered data obtained for the specimens EPT11, EPT12, EPT13 and EPT14 are summarised in Table B.2, Table B.3, Table B.4 and Table B.5 respectively.

Table B.2: Experimental results for specimen EPT11

Deflection [mm]	Load [kN]
0	0
0.25	5.3
0.51	14.94
0.71	23.43
1.01	33.84
1.24	41.34
1.5	50.21
2	66.81
2.24	75.05
2.51	82.71
2.75	91.17
3.01	99.31
3.25	107.38
3.51	114.99
3.77	122.41
4	127.68
4.05	129.41
4.1	124.52
4.18	128.89
4.21	129.77
4.26	130.4
4.49	134.41
4.74	137.38
5.01	140.13
5.26	146.03
5.5	150.81

5.73	155.57
6	159.69
6.24	165.51
6.5	170.43
6.75	175.54
6.99	178.26
7.27	181.89
7.51	182.65
7.76	184.96
7.99	186.8
8.23	189.3
8.45	189
8.44	187.02
8.49	189.6
8.73	193.64
8.99	195.18
9.26	196.28
9.51	195.92
9.74	194.85
10.01	193.45
10.18	192.35
10.29	181.64
10.32	174.41
10.62	174.08
10.66	173.45

Table B.3: Experimental results for specimen EPT12

Pre-Loading		Loading after post-tensioning		
Deflection [mm]	Load [kN]	Deflection [mm]	Load [kN]	Additional deflection after PT [mm]
0	0.02	4.05	0.0	0.0
0.25	8.35	4.29	5.19	0.24
0.49	16.75	4.54	13.18	0.49
0.99	33.04	4.8	22.33	0.75
1.26	40.27	5.06	33.65	1.01
1.49	46.78	5.3	44	1.25
1.76	55.05	5.54	54.36	1.49
1.98	62.05	5.8	66.56	1.75
2.25	69.2	6.06	78.21	2.01
2.48	74.47	6.3	88.7	2.25
2.53	76.48	6.55	97.66	2.5
2.55	77.99	6.8	106.17	2.75
2.58	78.84	7.05	115.18	3

2.76	84.28	7.31	124.33	3.26
3	91.75	7.54	132.38	3.49
3.26	99.77	7.79	141.34	3.74
3.5	107.41	8.05	150.43	4
3.77	115.87	8.3	158.45	4.25
4	122.96	8.55	166.42	4.5
4.25	128.73	9.07	182.54	5.02
4.51	138.51	9.3	186.67	5.25
4.75	145.16	9.57	190.18	5.52
5	150.57	9.81	191.42	5.76
5.25	155.35	10.05	193.18	6
5.5	157.82	10.32	193.42	6.27
5.76	162.82	10.56	193.48	6.51
6	168.4	10.78	192.96	6.73
6.26	172.22	11.03	191.39	6.98
6.51	175.35	11.3	188.75	7.25
6.76	177.82	11.54	185.95	7.49
6.97	179.52	11.97	154.14	7.92
2.15	0.00	12.06	152.44	8.01
		12.28	151.97	8.23
		12.57	149.83	8.52
		12.76	148.01	8.71
		13.04	147.02	8.99
		13.36	145.81	9.31
		13.54	145.54	9.49
		13.81	145.16	9.76
		14.04	143.81	9.99
		14.26	142.63	10.21
		14.54	140.98	10.49
		14.81	139.55	10.76
		15.05	134.99	11

Table B.4: Experimental results for specimen EPT13

Pre-Loading		Loading after post-tensioning		
Deflection [mm]	Load [kN]	Deflection [mm]	Load [kN]	Additional deflection after PT [mm]
0	0	-0.58	0	0
0.25	5.98	-0.38	0.63	0.2
0.49	10.38	-0.1	2.58	0.48
0.74	15.21	0.16	9.2	0.74
1.01	24.69	0.43	23.21	1.01
1.27	32.52	0.66	36.15	1.24
1.49	39.47	0.91	48.45	1.49

1.77	47.58	1.19	61.34	1.77
2.01	54.25	1.46	75.02	2.04
2.27	62.49	1.67	83.12	2.25
2.51	70.1	1.9	93.62	2.48
2.77	77.49	2.19	107.35	2.77
3	84.99	2.46	119.28	3.04
3.25	93.73	2.66	127.74	3.24
3.51	101.39	2.88	137.11	3.46
3.76	109.83	3.18	150.02	3.76
4.01	116.91	3.42	160.05	4
4.03	114.61	3.69	172.41	4.27
4.05	115.87	3.93	181.91	4.51
4.08	117.24	4.2	193.84	4.78
4.14	120.27	4.43	202.38	5.01
4.24	123.67	4.69	212.54	5.27
4.51	128.67	4.94	222.43	5.52
4.77	135.49	5.16	227.19	5.74
5.01	141.36	5.4	236.09	5.98
5.27	146.91	5.65	244.58	6.23
5.5	151.23	5.92	252.46	6.5
5.75	155.62	6.16	256.77	6.74
5.99	160.51	6.41	261.42	6.99
6.25	164.69	6.68	268.15	7.26
6.5	168.26	6.92	269.74	7.5
6.75	171.8	7.19	272.51	7.77
7.02	175.21	7.44	274.58	8.02
7.26	178.53	7.66	278.06	8.24
7.5	180.65	7.93	281.77	8.51
7.63	182.9	8.16	285.34	8.74
7.65	182.08	8.43	287.87	9.01
7.38	162.68	8.66	290.98	9.24
5.6	87.68	8.94	295.62	9.52
2.02	-0.03	9.18	299.19	9.76
		9.44	300.45	10.02
		9.67	304.05	10.25
		9.91	301.91	10.49
		10.16	304.6	10.74
		10.43	305.12	11.01
		10.67	302.95	11.25
		10.9	303.06	11.48
		11.19	307.49	11.77
		11.44	309.13	12.02
		11.65	309.79	12.23
		11.89	305.98	12.47

		12.9	158.48	13.48
		5.64	0	6.22

Table B.5: Experimental results for specimen EPT14

Deflection [mm]	Load [kN]
0.00	-0.03
0.24	15.54
0.49	27.08
0.74	41.34
1.01	57.8
1.26	73.59
1.51	88.34
1.75	101.64
2.01	114.94
2.25	125.73
2.52	137.49
2.75	151.31
2.99	162.44
3.24	171.5
3.5	179.69
3.73	187.41
3.99	194.85
4.24	198.53
4.51	207.65
4.77	212.05
4.98	213.94
5.25	218.37
5.49	222.35
5.75	225.37
5.99	231.53
6.25	237.08
6.52	242.38
6.76	245.37
7	251.14
7.25	254.85
7.51	259.85
7.75	264
7.98	268.23
8.24	272.49
8.51	273.64
8.76	280.04
9.01	284.68
9.25	288.23
9.51	291.63
10	298.81

10.25	300.29
10.51	305.95
10.77	310.15
11	313.2
11.25	316.41
11.48	319.22
11.74	323.47
11.99	325.54
12.26	328.86
12.49	331.8
12.76	334.44
12.98	334.02
13.25	338.2
13.48	340.97
13.75	343.72
14	345.97
14.23	347.9
14.53	351.88
14.76	353.67
14.97	353.94
15.92	141.42
7.91	0

B.3   Group 2

Group 2 also consisted of four reinforced concrete beams. All beams were designed similar to Group 1 except for the spacing of the shear reinforcement which was 180 mm in Group 2 and 250 mm in Group 1. Beams were named EPT21, EPT22, EPT23 and EPT24. All beams except the first beam EPT21 were strengthened by external post-tensioning.

Filtered data obtained for the specimens EPT21, EPT22, EPT23 and EPT24 are summarised in Table B.6, Table B.7, Table B.8 and Table B.9 respectively.

Table B.6: Experimental results for specimen EPT21

Deflection [mm]	Load [kN]
0	0
0.5	19.57
0.8	28.06
1.1	38.19
1.5	51.29
1.6	54.12
1.7	56.95
1.8	60.03
1.9	62.31
2	64.86
2.1	68.61
2.2	70.91
2.3	73.02
2.4	75.13
2.5	77.13
2.6	80.24
2.7	82.4
2.8	85.4
2.9	87.23
3	88.95
3.1	91.42
3.2	94.25
3.3	95.61
3.4	97.03
3.5	99.11
3.6	100.05
3.7	101.74
3.8	104.6
3.9	105.77
4	107.77
4.1	109.93
4.2	110.82
4.3	113.01
4.4	115.48
4.5	117.29
4.6	118.15
4.7	120.23
4.8	122.86
4.9	123.95
5	125.64
5.1	126.17
5.2	128.05
5.3	128.22
5.4	130.11
5.5	125.5
5.6	128.36
5.7	133.05
5.8	135.58
5.9	137.63

6	138.99
6.1	140.32
6.2	142.13
6.3	143.79
6.4	145.15
6.5	147.01
6.6	147.4
6.7	149.92
6.8	151.01
6.9	152.39
7	154.17
7.1	154.95
7.2	156.59
7.3	158.78
7.4	159.61
7.5	160.66
7.6	163.41
7.7	163.02
7.8	165.69
7.9	166.02
8	167.91
8.1	168.1
8.2	170.66
8.3	171.04
8.4	172.9
8.5	172.93
8.6	174.76
8.7	175.6
8.8	177.34
8.9	178.32
9	179.87
9.1	180.56
9.2	182.51
9.3	182.95
9.4	182.04
9.5	181.92
9.6	183.06
9.7	184.64
9.8	185.81
9.9	186.42
10	188.56
10.1	189.2
10.2	190.08
10.3	191.64
10.4	192.14
10.5	194.02
10.6	193.8
10.7	195.3
10.8	195.86
10.9	197.05
11	196.52
11.1	197.6

11.2	195.99
11.3	196.41
11.4	195.86
11.5	192.14
11.6	191.75
11.7	191
11.8	187.42
11.9	187.72
12	187.2
12.1	185.86
12.2	186.5
12.3	184.45
12.4	184.7
12.5	182.98
12.6	182.12
12.7	181.98
12.8	177.9
12.9	164
13	167.49
13.1	168.96
13.2	170.82
13.3	171.93
13.4	170.96
13.5	171.13
13.6	170.02
13.7	169.35
13.8	166.22
13.9	165.47
14	164.83
14.1	162.44
14.2	162.11
14.3	160.17
14.4	159.58
14.5	159.14
14.6	156.28
14.7	156.31
14.8	152.51
14.9	152.23

Table B.7: Experimental results for specimen EPT22

Pre-Loading		Loading after post-tensioning	
Deflection [mm]	Load [kN]	Deflection [mm]	Load [kN]
0	0	0	0
1.8	35.96	0.25	11.16
2.05	40.71	0.51	17.68
2.29	45.23	0.74	23.28
2.55	51.26	1	28.22
2.82	56.75	1.25	34.14

3.05	62.16	1.5	39.19
3.31	68.99	1.74	43.96
3.54	74.54	2.01	49.37
4.01	85.98	2.25	53.73
4.26	92.22	2.5	58.06
4.49	98.63	2.77	62.39
4.74	104.35	3	66.64
5.01	108.71	3.26	71.41
5.24	113.37	3.52	76.21
5.49	118.59	3.75	80.35
5.74	122.22	3.98	85.42
5.99	123.25	4.25	90.03
6.25	127.63	4.51	94.83
6.51	131.66	4.77	100.13
6.75	135.29	4.99	104.6
6.99	139.32	5.25	109.38
7.26	142.76	5.76	119.95
7.49	146.34	6	125.06
7.72	150.34	6.26	129.64
8	153.78	6.5	135.21
8.3	158.55	6.75	139.27
8.52	162.02	7.01	145.01
8.74	164.63	7.26	149.51
9.03	169.32	7.52	154.14
9.26	172.87	7.76	157.97
9.48	175.9	7.99	161.94
9.74	179.28	8.28	165.58
10.01	182.2	8.52	168.63
10.24	184.89	8.76	171.02
10.49	187.47	9.01	172.27
10.75	190.52	9.24	170.57
11.02	192.94	9.73	165.88
11.25	194.85	9.99	162
11.52	197.21	12.14	130.88
11.77	199.52		
12.01	200.85		
12.27	202.18		
12.48	202.96		
12.73	202.9		
13	201.74		
13.26	197.96		
13.28	196.8		
13.55	184.58		

Table B.8: Experimental results for specimen EPT23

Pre-Loading		Loading after post-tensioning	
Deflection [mm]	Load [kN]	Deflection [mm]	Load [kN]
0	0	0	0
0.26	12.32	0.25	14.32

0.49	20.12	0.53	24.34
0.51	21.54	0.76	32.36
0.75	25.87	0.99	39.88
0.98	32.61	1.23	46.02
1.03	32.94	1.48	53.95
1.27	36.86	1.78	61.36
1.52	41.38	2.03	68.47
1.74	44.82	2.27	75.3
2.02	50.29	2.76	89.67
2.28	55.04	3.02	97.36
2.49	58	3.51	110.65
2.76	62.94	3.76	118.06
2.99	67.39	3.99	125.5
3.26	71.77	4.23	131.47
3.51	76.02	4.5	139.13
3.77	81.23	4.72	144.96
4.01	86.4	4.99	152.45
4.24	90.92	5.24	158.17
4.52	96.14	5.47	165.24
4.77	101.3	6.01	178.29
4.99	105.21	6.24	183.48
5.24	108.65	6.47	188.5
5.51	112.85	6.75	194.8
5.74	116.43	7.03	200.8
6	117.4	7.26	205.49
6.25	123.84	7.56	211.12
6.5	128	8.03	220.64
6.75	131.47	8.24	223.39
7.01	136.1	8.49	226.36
7.25	138.93	8.75	229.83
7.52	142.49	9.01	232.99
7.75	145.73	9.26	235.68
8.01	148.62	9.52	238.12
8.25	150.62	9.77	241.4
8.51	153.17	9.98	244.67
8.74	156.89	10.24	248.37
9	160	10.51	251.7
9.27	162.36	10.73	254.8
9.51	165.52	11.02	259.08
9.73	168.74	11.25	261.6
10.03	171.82	11.51	263.94
10.24	174.07	11.78	267.07
10.51	176.68	12.02	270.18
10.74	179.01	12.27	272.1
11	178.04	12.48	274.68
11.26	179.09	12.76	277.73
11.55	178.45	12.98	279.87
11.74	176.98	13.24	282
12	170.57	13.5	283.81
		13.76	285.75
		14.02	287.53

		14.25	288.61
		14.51	289.72
		14.73	291.02
		14.98	291.55
		15.23	292.49
		15.49	292.33
		15.74	292.63
		16.01	292.11
		16.27	291.88
		16.55	290.88
		16.74	288.86
		17	285.42

Table B.9: Experimental results for specimen EPT24

Deflection [mm]	Load [kN]
0	0
2.27	88.17
2.5	96.52
2.74	105.18
3.03	115.62
3.24	123
3.49	130.96
3.77	137.93
3.99	143.81
4.23	148.06
4.49	153.42
4.75	159.55
5.01	163.35
5.26	168.21
5.5	172.29
5.76	178.01
6.02	181.14
6.24	186.89
6.49	190.63
6.74	195.13
6.99	199.96
7.26	204.15
7.51	209.01
7.75	212.5
8	216.08
8.26	220.16
8.52	225.13
8.78	229.16
9.02	232.57
9.25	236.01
9.49	239.76

9.75	242.81
9.99	245.86
10.25	249.5
10.51	252.58
10.75	255.63
11	259.21
11.26	261.88
11.5	264.43
11.77	267.54
12	270.18
12.27	272.42
12.49	274.51
12.75	276.98
13.01	278.75
13.27	280.64
13.5	282.33
13.77	283.19
14	284.47
14.22	285.91
14.49	286.11
14.72	286.99
14.98	287.08
15.23	287.44
15.51	286.47
15.74	286.05
16.01	283.3
16.28	281.44
16.54	276.59
16.73	273.95
16.98	272.17
17.23	266.32

B.4   Group 3

Group 3 consisted of eight reinforced concrete beams. All beams were designed with the same dimensions as Group 1 and 2. 2-N24 bars were used as tensile reinforcement and 2-N16 bars were used as compressive reinforcement. R6 bars were placed at a spacing of 250 mm as shear reinforcements. Beams were named ECL31, ECL32, ECL33, ECL34, ECL35, ECL36, ECL37 and ECL38. All beams except the first beam, ECL31, were strengthened by external clamping. Specimens ECL32, ECL33, ECL34 and ECL35 were strengthened by vertical clamping.

Specimens ECL36 and ECL37 were strengthened by inclined clamping. Specimen ECL38 was strengthened by a combination of vertical and inclined clamping.

Filtered data obtained for specimens ECL31, ECL32, ECL33, ECL34 AND ECL35 are summarised in Table B.10, Table B.11, table B.12, table B.13 and Table B.14 respectively.

Table B.10: Experimental results for specimen ECL31

Deflection [mm]	Load [kN]
0	0
0.24	9.08
0.51	26.47
0.75	34.09
1.01	41.21
1.27	49.12
1.5	56.82
1.76	62.82
2.01	69
2.28	77.85
2.5	86.49
2.74	94.78
3	99.71
3.23	106.88
3.5	114.33
3.74	120.28
4.01	126.23
4.25	130.55
4.52	134.8
4.73	139.65
4.99	143.32
5.25	146.16
5.51	148.63
5.77	151.6
6.01	155.09
6.24	157.68
6.49	160.22
6.77	162.46
7.01	163.25
7.24	165.28
7.51	167.93
7.75	169.76
8	172.15
8.25	174.08
8.5	175.6
8.75	170.54

9	168.82
9.25	169.02
10.01	160.43

Table B.11: Experimental results for specimen ECL32

Pre-Loading		Loading after clamping	
Deflection [mm]	Load [kN]	Deflection [mm]	Load [kN]
0.00	0.00	0	0
0.40	7.19	0.52	22.48
0.61	10.79	1.01	34.2
0.81	14.37	1.59	47.09
1.06	18.56	2.01	56.98
1.29	23.54	2.2	61.84
2.05	36.10	2.41	67.2
2.50	45.26	3	81.74
3.01	54.33	3.19	86.93
3.20	56.33	3.37	92.01
3.49	61.24	3.58	97.45
3.70	65.33	3.82	103.18
4.02	73.26	3.99	108.03
4.21	76.33	4.22	113.24
4.51	81.02	4.41	118.71
4.70	83.97	4.62	124.2
4.99	90.33	4.81	129.13
5.20	93.54	4.99	133.63
5.50	97.88	5.23	139.28
5.70	101.01	5.4	142.76
5.99	106.30	6.01	155.52
6.25	113.17	6.21	159.67
6.49	116.04	6.42	164.29
6.76	120.77	6.59	167.7
7.01	125.37	6.81	171.77
7.52	133.07	6.99	174.72
7.99	135.82	7.06	175.89
8.20	134.65	7.17	177.54
8.50	136.43	7.29	177.08
8.90	136.94	7.5	181.56
9.29	140.45	7.74	186.8
9.50	141.59	8.05	191.8
10.03	144.67	8.19	193.81
10.24	144.57	8.55	199.2
10.47	144.11	8.71	202.05
10.75	141.82	8.98	206.37
10.81	141.90	9.19	209.12
10.85	136.33	9.41	212.52
		9.58	215.17
		9.81	218.5
		9.98	220.79
		10.22	224.58

		10.42	227.83
		10.6	230.32
		10.79	233.22
		10.99	236.02
		11.2	238.33
		11.41	241.15
		11.62	243.24
		11.81	244.99
		12.02	247.13
		12.2	249.42
		12.4	251.04
		12.61	253.08
		12.81	255.08
		12.97	255.95
		13.18	257.7
		13.35	258.85
		13.54	260.14
		13.73	261.08
		13.89	261.8
		14.01	262.13
		14.08	254.09
		14.2	242.19
		18.32	232.13
		18.5	229.69

Table B.12: Experimental results for specimen ECL33

Pre-Loading		Loading after clamping	
Deflection [mm]	Load [kN]	Deflection [mm]	Load [kN]
0	0	0	0
0.28	6.75	0.54	11.72
0.56	15.6256	0.79	16.89
0.6	17.02356	1	20.88
0.8	24.41	1.2	25.38
1	30.59	1.61	36.82
1.18	34.7	1.8	42.87
1.38	40.4	2	50.22
1.61	45.66	2.25	57.13
1.81	51.36	2.47	64.76
1.96	55.93	2.98	81.56
2	56.72	3.19	87.84
2.22	63.31	3.61	99.31
2.42	68.98	3.8	105.69
2.59	73.48	3.99	110.04
2.8	80.14	4.21	115.53
2.99	85.86	4.6	125.65
3.17	91.4	4.81	130.1
3.41	96.48	5.01	134.09
3.6	101.04	5.2	138.36
3.82	104.8	5.39	141.95

4	108.56	5.61	146.65
4.19	111.92	5.81	150.97
4.39	116.01	5.96	153.67
4.59	119.72	6.19	158.8
4.81	123.28	6.42	162.03
4.99	125.82	6.61	165.8
5.2	126.94	6.79	168.82
5.42	131.16	7.01	172.76
5.64	134.32	7.21	176.17
5.81	136.73	7.41	179.52
6.02	139.35	7.6	182.73
6.19	140.27	7.81	185.65
6.27	140.72	7.98	189.06
6.3	140.24	8.23	193.08
6.36	139.86	8.4	195.92
6.42	140.29	8.6	198.95
6.49	140.01	8.82	202.33
6.59	139.4	8.97	204.11
6.81	140.34	9.22	206.75
6.99	140.93	9.39	208.99
7.18	141.18	9.59	211.71
7.24	135	9.8	215.07
		10.02	218.04
		10.25	220.89
		10.6	225.72
		10.8	227.86
		10.99	230.04
		11.21	232.38
		11.42	234.08
		11.61	236.14
		11.8	238.05
		12	239.47
		12.24	241.79
		12.45	243.9
		13	248.09
		13.21	249.8
		13.42	251.32
		13.66	253.18
		13.99	255.62
		14.21	257.07
		14.57	259.51
		14.79	261.03
		15	262.28
		15.21	263.75
		15.38	264.7
		15.59	265.94
		15.82	267.77
		16.02	268.71
		16.19	269.63
		16.6	272.07
		16.8	273.14
		16.98	274.03

		17.2	274.89
		17.41	275.42
		17.6	275.42
		17.79	273.34
		18	273.62
		18.2	274.15
		18.44	274.92
		18.6	275.5
		18.83	276.01
		18.97	276.34
		19.2	276.72
		19.4	277.08
		19.6	277.51
		19.8	277.74
		20	277.97
		20.24	278.12
		20.49	278.48
		20.74	278.73
		21	278.78
		21.26	278.91
		21.51	278.88
		21.76	278.86
		22.01	278.63
		22.25	277.59
		22.52	277.41
		22.76	277.69
		23.01	277.94
		23.27	278.12
		23.51	278.09
		23.74	278.04
		24.01	277.89
		24.22	277.66
		24.52	277.28
		24.76	276.59
		24.99	276.01
		25.25	275.09
		25.35	274.08
		25.4	273.36
		25.4	260.81

Table B.13: Experimental results for specimen ECL34

Loading after clamping	
Deflection [mm]	Load [kN]
0	0
0.49	7.52
0.99	13.96
1.61	28.4
1.8	32.82
2	38.34

2.59	52.45
2.79	56.21
3	61.32
3.71	77.87
3.85	81.43
4	84.15
4.23	89.69
4.45	96.74
4.99	109.4
5.26	115.7
5.46	118.07
5.99	132.1
7.01	150.59
7.2	155.54
8.01	173.67
8.25	178.65
8.5	183.43
8.72	188.44
8.99	193.53
9.23	197.6
9.43	202.27
9.49	194.8
9.53	199.63
9.65	204
9.8	207.43
10	211.96
10.19	215.77
10.4	219.33
10.63	223.58
10.8	225.46
10.99	228.84
11.21	231.64
11.4	234.1
11.58	236.24
11.8	238.94
12	241.6
12.19	243.89
12.42	246.89
12.6	248.93
12.76	250.81
12.83	244.1
12.86	246.56
12.94	249.26
13.01	251.14
13.19	254.8
13.43	257.22
13.59	259.38
13.82	261.49
14	261.79
14.07	262.68
14.14	261.82
14.3	262.63

14.49	265.33
14.72	267.31
14.87	268.78
15.02	269.83
15.21	271.5
15.41	273.44
15.6	274.86
15.79	275.34
16.02	277.5
16.2	278.98
16.4	279.82
16.6	280.73
16.79	282.05
17.02	283.27
17.21	283.91
17.4	284.27
17.6	285.16
17.79	286.02
18	286
18.19	285.39
18.39	283.89
18.61	284.39
18.8	285.26
19	285.77
19.19	285.05
19.4	284.67
19.6	283.63
22	251.39

Table B.14: Experimental results for specimen ECL35

Loading after clamping	
Deflection [mm]	Load [kN]
0	0
0.1	5.75
0.2	7.22
0.4	9.79
0.61	11.7
0.8	14.09
1	16.99
1.25	21.59
1.48	24.88
1.74	30.11
2	31.38
2.22	34.38
2.41	37.83
2.6	42.41
2.8	45.54
3	49.12
3.2	53.8

3.4	57.23
3.59	60.16
3.82	65.29
4.01	68.57
4.21	73.51
4.4	78.34
4.59	84.46
4.84	88.17
5	93.87
5.2	99.39
5.39	104.37
5.58	110.14
5.8	113.9
6.01	118.68
6.19	121.51
6.4	125.35
6.6	128.62
6.82	132.13
6.99	135.77
7.21	140.19
7.41	143.85
7.59	147.13
7.8	150.97
8	154.48
8.2	157.1
8.45	159.79
8.62	163.51
8.8	166.74
9	170.5
9.2	174.06
9.39	177.08
9.59	179.8
9.82	183.67
9.99	187.02
10.2	190.99
10.4	194.22
10.61	197.4
10.8	200.6
11	203.83
11.19	206.73
11.4	209.4
11.59	211.89
11.8	215.58
12.01	218.78
12.2	220.89
12.41	223.33
12.6	225.92
12.84	228.67
13	230.35
13.21	233.22
13.4	235.13
13.6	237.14

13.79	239.17
14	240.47
14.19	242.3
14.39	242.96
14.59	243.36
14.81	243.19
15.01	243.11
15.24	242.91
15.49	242.8
15.74	243.06
15.99	243.64
16.26	244.48
16.49	245.09
16.75	245.91
17.01	246.36
17.25	246.95
17.49	247.33

Filtered data obtained for the specimens ECL36 and ECL37 are summarised in Table B.15 and Table B.16 respectively.

Table B.15: Experimental results for specimen ECL36

Pre-Loading		Loading after clamping	
Deflection [mm]	Load [kN]	Deflection [mm]	Load [kN]
0.00	0.00	0	0
0.10	1.99	0.2135	3.05
0.21	4.10	0.42	6
0.42	7.99	0.61	7.53
1.03	19.99	0.8	13.93
1.32	26.36	1	17.59
1.41	28.71	1.2	22.68
1.60	35.12	1.42	27.13
1.82	40.76	1.6	31.81
2.01	46.05	1.82	36.84
2.20	51.51	2	41.59
2.40	57.34	2.2	46.42
2.61	61.48	2.41	51.87
2.81	66.97	2.6	55.76
3.00	72.39	2.8	59.7
3.22	76.66	2.99	63.97
3.41	80.60	3.2	68.47
3.61	86.42	3.4	71.85
3.80	91.15	3.61	77.19
4.00	94.96	3.79	81.71
4.19	99.82	4.01	87
4.40	104.37	4.21	91.35

4.61	108.85	4.4	95.85
4.80	112.68	4.59	100.43
5.01	116.40	4.81	105.36
5.21	118.68	5	110.11
5.40	122.52	5.22	115.17
5.61	125.85	5.4	119.16
5.80	126.95	5.59	124.02
6.00	130.00	5.8	129.16
6.21	132.95	6	133.55
6.42	135.74	6.19	137.8
6.61	138.62	6.41	142.17
6.82	141.29	6.59	146.24
7.01	143.50	6.79	149.67
7.21	145.89	7	153.05
7.41	147.87	7.19	156.77
7.60	149.88	7.39	159.33
7.80	152.04	7.58	162.31
8.00	153.97	7.79	165.16
8.22	155.96	8	167.77
8.40	157.99	8.2	170.55
8.60	159.24	8.4	172.63
8.81	161.27	8.61	174.56
9.01	162.52	8.8	176.47
9.20	163.66	9	178.66
9.43	164.27	9.19	180.64
9.47	163.81	9.41	182.55
9.49	160.00	9.61	184.05
		9.81	186.05
		10.01	187.43
		10.19	188.88
		10.4	190.55
		10.59	192.11
		10.81	193.78
		11	194.39
		11.2	195.89
		11.41	197.47
		11.6	198.74
		11.8	199.81
		11.99	201.23
		12.19	202.76
		12.39	204.26
		12.6	205.61
		12.81	206.9
		13	208.12
		13.19	209.09
		13.4	210.36
		13.6	211.5
		13.79	212.34
		13.99	212.88
		14.2	213.26
		14.42	212.98
		14.5	211.35

		14.52	209.34
		14.61	198.61
		14.82	182.09
		14.99	177.89

Table B.16: Experimental results for specimen ECL37

Pre-Loading		Loading after clamping	
Deflection [mm]	Load [kN]	Deflection [mm]	Load [kN]
0	0	0	0
0.128	2.01	0.25	3.23
0.321	5.06	0.48	10.71
0.44	7	0.75	15.46
0.64	9.46	1	19.33
0.81	12.82	1.25	23.67
1.01	16.96	1.49	28.2
1.2	20.01	1.75	33.87
1.4	24.94	2	39.01
1.58	28.63	2.25	44.4
1.8	32.65	2.51	49.76
2.01	37.63	2.75	55.58
2.2	41.55	3	60.84
2.39	44.8	3.21	65.6
2.58	48.51	3.41	70.56
2.8	53.52	3.6	75.03
3.03	58.05	3.8	78.67
3.22	62.14	3.99	82.63
3.42	65.9	4.2	87.57
3.6	69.62	4.41	91.23
3.79	73.66	4.6	96.16
4.02	78.31	4.79	100.1
4.19	81.26	5	104.14
4.42	85.84	5.2	108.54
4.61	90.06	5.39	112.53
4.82	93.41	5.6	116.78
5	97.45	5.8	120.77
5.2	101.4	5.98	125.17
5.4	104.12	6.2	129.11
5.6	107.83	6.4	133.18
5.64	105.54	6.6	136.28
5.67	107.07	6.8	140.07
5.8	109.05	7	143.78
5.98	112.05	7.2	148.08
6.04	109.25	7.39	151.51
6.06	110.98	7.59	155.91
6.21	112.86	7.81	159.59
6.41	116.29	8.01	163.66
6.61	119.37	8.2	167.04
6.81	122.12	8.39	171.44
6.98	124.35	8.6	175.61

7.13	126.44	8.8	179.04
7.13	122.6	8.99	182.75
7.15	121.99	9.21	185.32
7.15	124.71	9.4	189.24
7.21	126.64	9.6	192.95
7.4	130.68	9.8	196.25
7.6	131.32	10.01	199.69
7.78	134.29	10.19	203.04
8	135.59	10.4	206.6
8.19	139.56	10.42	206.78
8.41	142.61	10.61	209.37
8.59	144.46	10.79	212.37
8.8	147.52	11	215.91
9.01	150.16	11.2	219.09
9.22	151.84	11.4	223.18
9.22	150.26	11.6	225.95
9.23	149.04	11.81	229.46
		12	231.75
		12.12	232.99
		12.17	232.08
		12.26	226.69
		12.41	224.35
		12.6	223.28
		12.79	222.44
		13	222.14
		13.19	221.96
		13.39	222.06
		13.59	222.97
		13.78	224.07
		14	225.16
		14.21	226
		14.4	226.86
		14.59	227.55
		14.79	226.84
		15.01	226.28
		15.2	224.55
		15.39	221.7
		15.6	220.86
		15.79	220.69
		15.99	220.46
		16.19	220.36
		16.4	219.21
		16.59	217.97
		16.82	215.91
		17.01	212.17
		17.21	210.21
		17.4	209.63
		17.6	208.66
		17.8	208.61
		18	208.38
		18.2	207.62
		18.4	207.42

		18.61	206.75
		18.78	202.84
		18.75	199.74

Filtered data obtained for the specimens ECL38 is summarised in Table B.17.

Table B.17: Experimental results for specimen ECL38

Pre-Loading		Loading after clamping	
Deflection [mm]	Load [kN]	Deflection [mm]	Load [kN]
0	0	0	0
1.03	23.16	1.01	15.94
1.19	25.88	1.2	21.53
1.4	30.89	1.41	28.3
1.59	35.84	1.6	33.15
1.79	40.01	1.81	38.69
1.99	44.79	2	43.78
2.2	49.98	2.2	48.41
2.39	54.86	2.38	52.45
2.59	60.23	2.62	57.15
2.8	65.26	2.8	61.78
3	70.75	3	66.61
3.2	76.35	3.21	70.88
3.39	80.74	3.41	76.19
3.6	86.74	3.6	81.48
3.8	91.22	3.8	85.91
4	96.94	4.01	90.76
4.2	102.41	4.21	96.53
4.41	107.44	4.4	101.9
4.6	111.1	4.6	105.92
4.8	116.24	4.79	110.8
4.99	120.1	5	116.21
5.03	120.84	5.2	121.91
5.07	121.07	5.39	127.4
5.1	121.19	5.61	132
5.2	122.36	5.8	137.34
5.41	126.1	6	142.7
5.59	129.89	6.21	147.46
5.79	134.21	6.41	152.44
6	138.18	6.6	157.17
6.2	141.58	6.79	163.07
6.39	141.74	7.01	167.54
6.59	144.99	7.19	172.7
6.8	148.86	7.41	177.15
7	152.44	7.61	181.45
7.2	155.13	7.81	186.08
7.41	157.88	8.02	190.2
7.59	160.07	8.19	193.86

7.79	161.21	8.39	197.44
8	163.55	8.59	200.9
8.19	165.97	8.8	204.87
8.41	169.07	8.98	208.2
8.6	171.18	9.2	210.89
8.8	173.08	9.4	214.07
8.99	174.99	9.6	217.12
9.19	177.23	9.8	220.04
9.4	179.82	9.99	222.41
9.6	182.34	10.21	224.54
9.82	184.96	10.4	226.63
10	186.69	10.61	228.84
10.22	188.92	10.81	231.56
10.26	188.97	11.01	233.14
10.28	187.42	11.18	235.2
10.38	184.93	11.4	236.7
10.55	184.35	11.6	238.63
10.6	181.3	11.79	240.21
		11.98	242.06
		12.08	242.55
		12.32	231.54
		12.39	231.56
		12.6	235.17
		12.67	233.82
		12.67	232.38
		12.71	230.06
		12.7	230.04

B.5   Experimental Data – Graphical Format

B.5.1 Change in Post-tensioning Force (Group 2)

Effect of shear crack on the behaviour of externally post-tensioned reinforced concrete beam also can be illustrated by the change in the post-tensioning force during loading process. This is discussed in Chapter 4 with by comparing the change of post-tensioning force among Group 1. As explained in Chapter 4, the behaviour of Group 2 specimens also very similar to that of Group 1 as shown in Figure B.2.
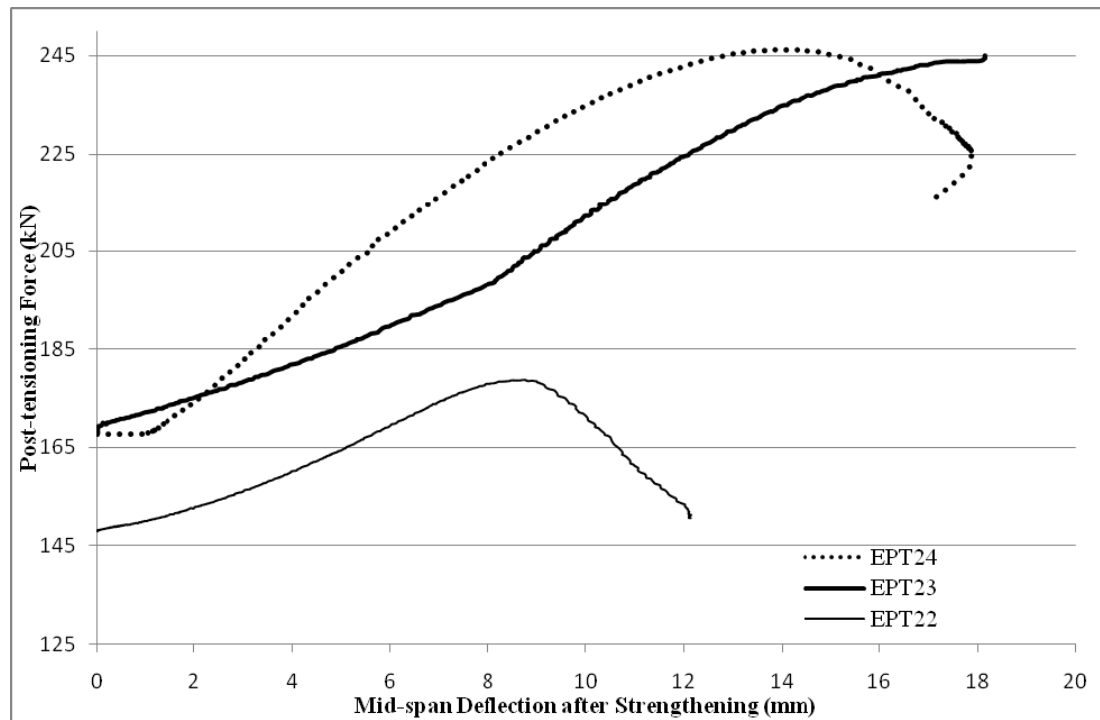
Figure B.2. Increase in external post-tensioning force with deflection of the beams (Group 2)

B.5.2 Change in External Clamping Force (Group 3 – Specimens with Inclined Claming)

In Group 3 specimens also a very similar behaviour was observed in first 5 specimens (control beam and the specimens with vertical clamping) as in Group 1 and Group 2, which is discussed in Chapter 4. However, in specimens with inclined clamping (ECL36 and ECL37) the variation of the strain in external clamping bars (Figure B.3) was much different from the first 5 specimens due to premature failure (detail of the failure is explained in Chapter 5).
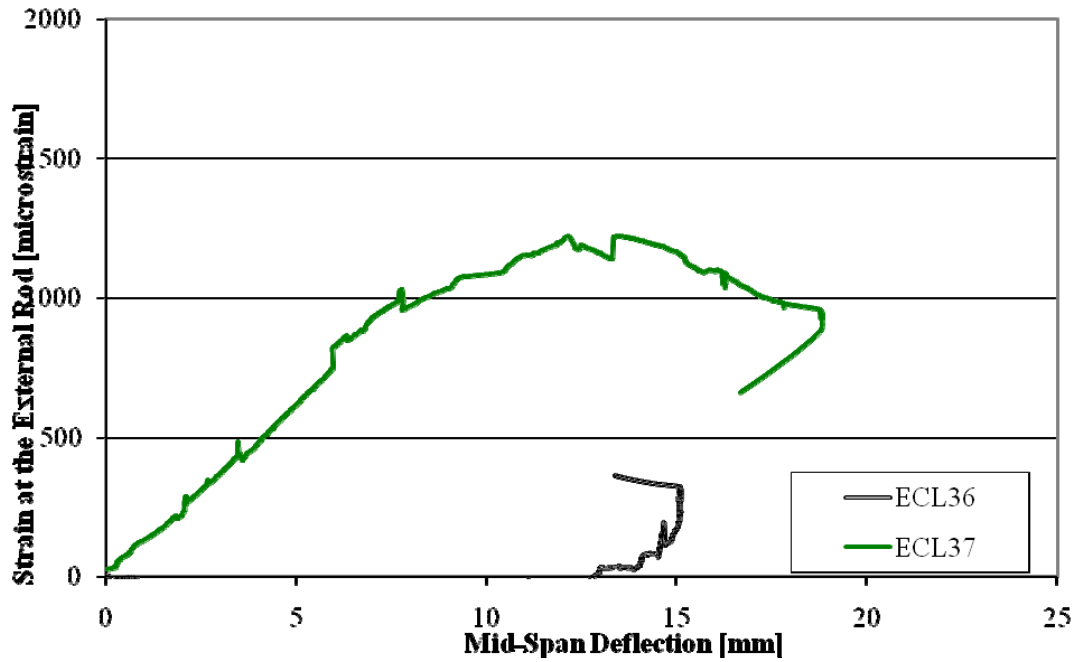
Figure B.3. Variation of strain in the external clamping rods of specimens with inclined clamping

B.5.3 *Change in Strain in Reinforcement during Loading*

In this section the strain variation in the shear reinforced bars are given. As discussed in the main thesis, in all specimens the shear reinforcement reached yielding point and in most cases failed during loading.

Figure B.4 shows the strain variation in the shear reinforcement (SR1) of Group 1 specimens. It can be noted that these shear reinforcements reached yielding strain and failed during the experiment. The strain variation of cracked or repaired specimens was not provided as either one of the shear reinforcement in that specimen failed during the preloading process and, therefore, no data is available for that particular case.
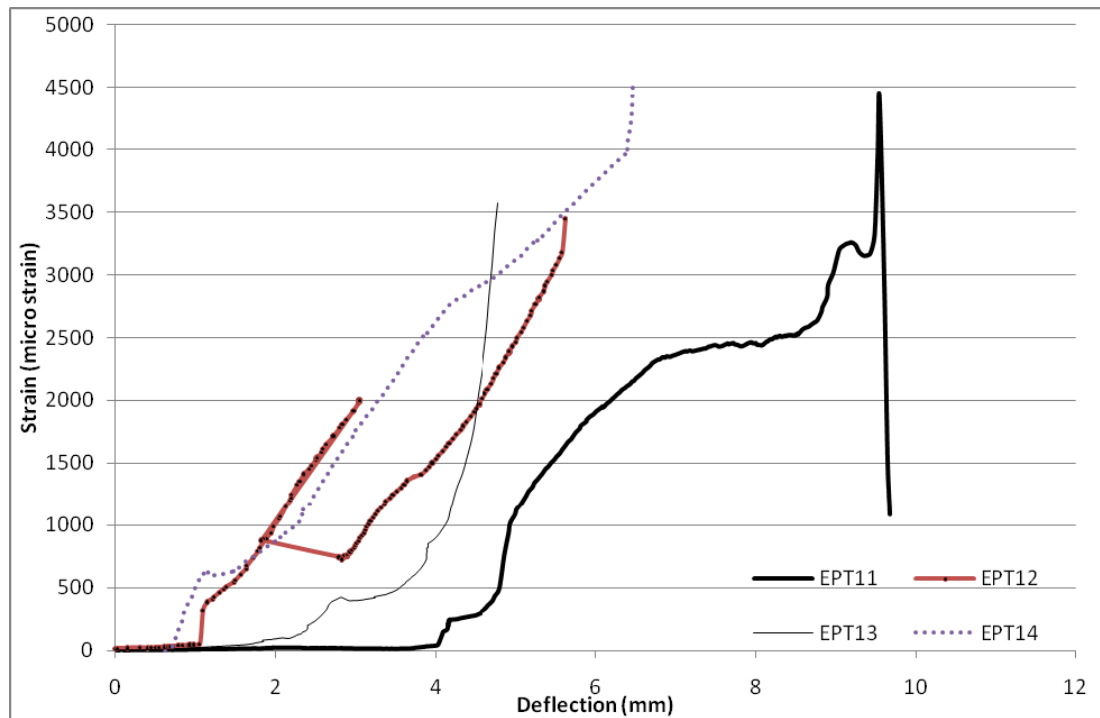
Figure B.4. Variation of strain in the shear reinforcement (SR1) of Group 1 specimens

Similarly the strain variation in the shear reinforcement (SR1) of Group 2 is shown in Figure B.5. A similar behaviour can be observed in Group 2 also.
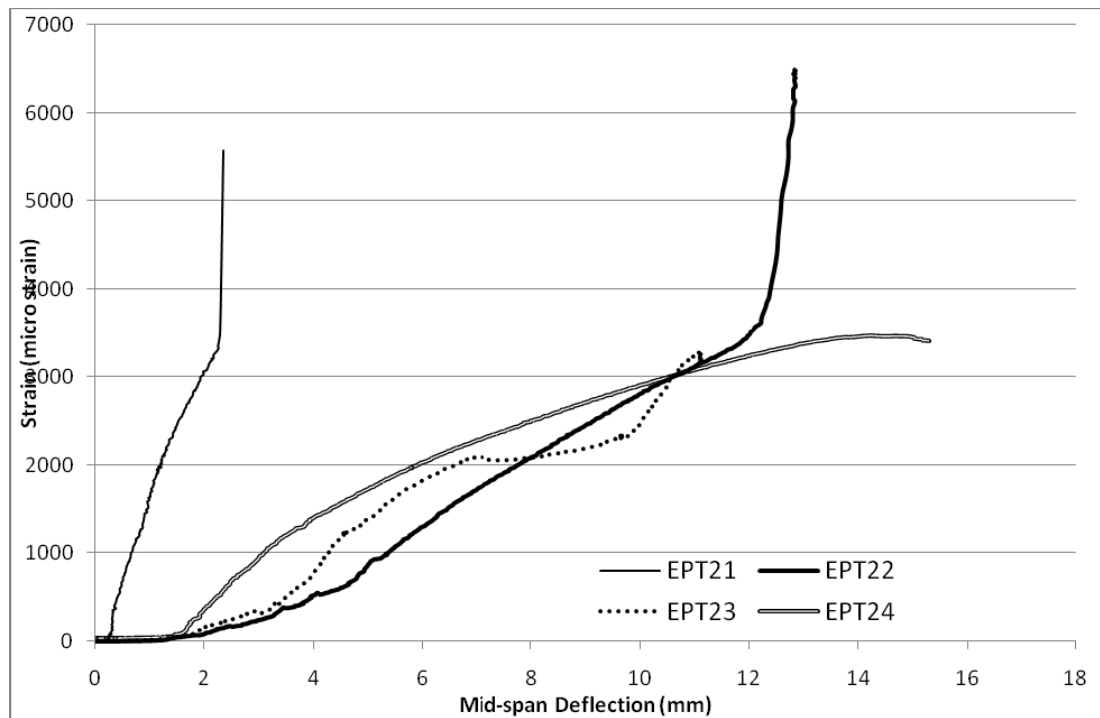

Figure B.5. Variation of strain in the shear reinforcement (SR1) of Group 2 specimens

A slight variation can be noted among the specimens in both groups due to difference in the concrete strength (capacity of the specimen).

On the other hand, the strain in longitudinal reinforcement bars (either compressive or tensile reinforcement) was less than the yielding strain of those bars. The variation of the strain in longitudinal bars of Group 1 and Group 2 are shown in Figure B.6 and Figure B.7, respectively.
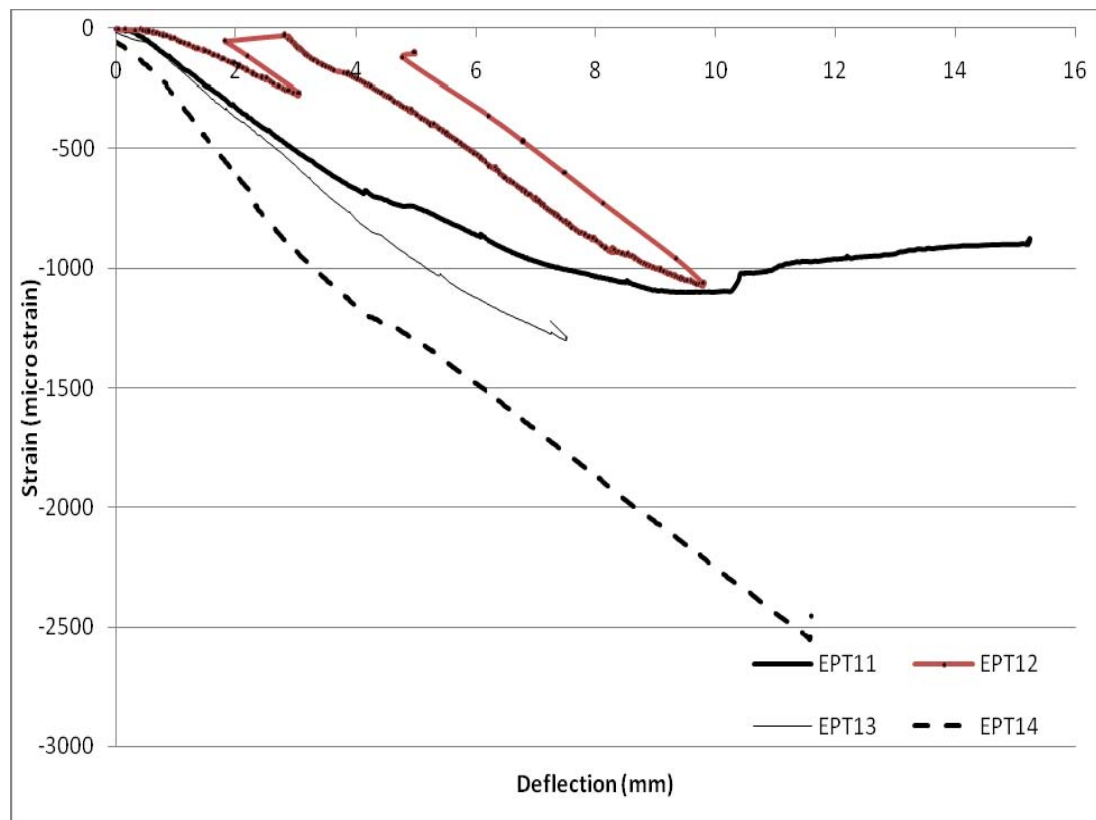
Figure B.6. Variation of strain in the compressive reinforcement of Group 1 specimens
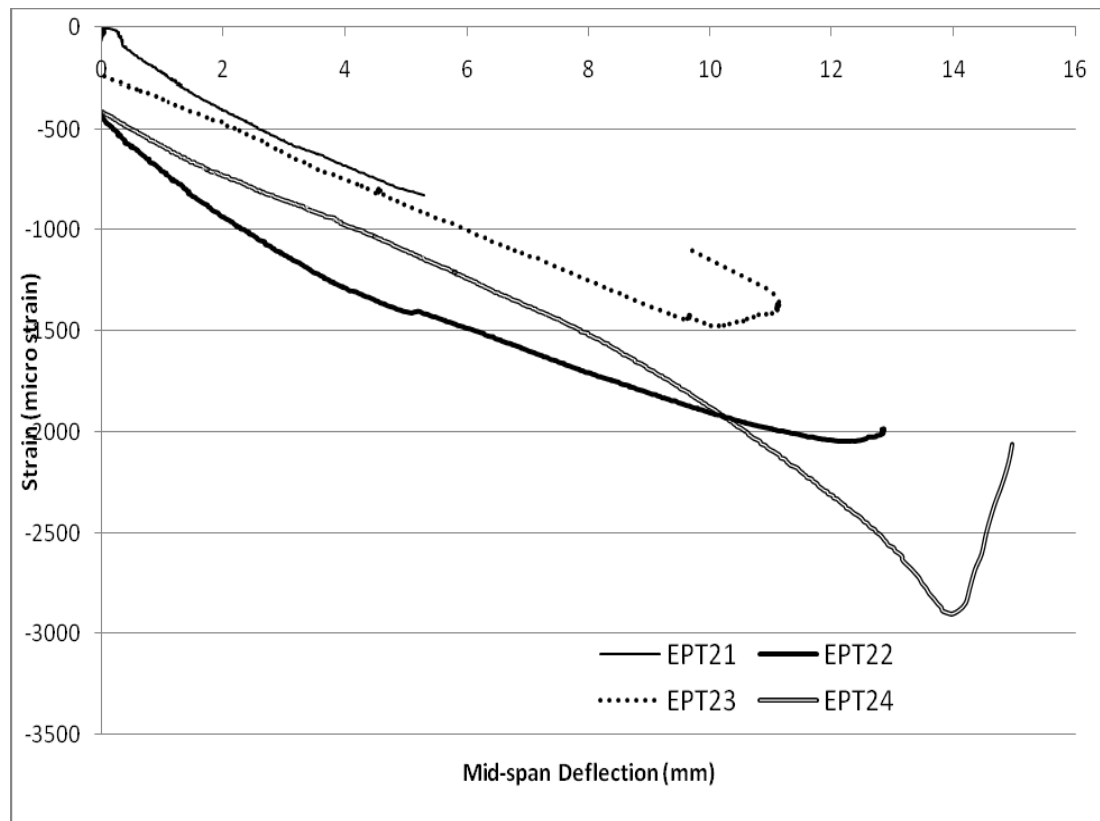
Figure B.7. Variation of strain in the compressive reinforcement of Group 2 specimens

<div align="right">

Appendix C

ADDITIONAL DATA OF PREVIOUS INVESTIGATIONS

(Supplement to Chapter 2)

</div>

C.1   Material Properties

In this appendix the three sets of experimental data reported by Aravinthan and Heldt (2005), Aravinthan and Suntharavadivel (2007) and Khaloo (2000) are given in detail. These data were used to calculate the capacity of the corresponding specimens and the capacities are reported in Chapter 2 (Section 2.3.3). Major parameters of the specimens tested by these researchers are summarised in Table C.1.

Table C.1: Specimen details of RC beam strengthened by external post-tensioning

Specimen	Dimension b×D [mm]	Shear Span	Shear R/F ratio	Remarks
RB1	350-400×250 (tapered)	2L/3	R6@250 mm	Bridge bent caps (Aravinthan et al. 2005)
RB2(a)				
RB2(b)				
RB3				
RCB1	300×150	750 mm	R6@250 mm	Rectangular beams (Aravinthan et al. 2007)
RCB2				
RCB3				
RCB4				
1	80×150	L/4	0.0097	The beams strengthened after cracking (Khaloo 2000) L=1800 mm
2		L/4	0.0097	
3		L/4	0.0145	
4		L/4	0.0145	
5		L/4	0.0097	
6		L/4	0.0097	
7		L/4	0.0097	
8		L/4	0.0145	
9		L/4	0.0097	
10		L/4	0.0145	
11		L/4	0.0097	
12		L/4	0.0145	
13		L/6	0.0097	
14		L/6	0.0097	
15		L/6	0.0145	
16		L/6	0.0145	
17		L/6	0.0097	
18		L/6	0.0145	
19		L/6	0.0097	
20		L/6	0.0145	
21		L/4	0.0145	
22		L/4	0.0145	
23		L/4	0.0145	
24		L/4	0.0097	

<div align="right">

Appendix D

APPLICATIONS OF THE STRUT-AND-TIE MODEL

(Supplement to Chapter 5)

</div>

D.1 General

The strut-and-tie model was developed on the basis that concrete is strong in compression (compression struts) and steel is strong in tension (tension ties). The concept of this model is explained in Chapter 5 (Section 5.2.1). A comparison of strut-and-tie model predicted crack with the experimental results is given in this appendix.

D.2 Strut-and-tie Model for the Simply Supported Beam

Strut-and-tie model was developed in a 2500 mm long reinforced concrete beam with four-point loading as shown in Figure D.1. In order to compare the effect of external post-tensioning in the crack pattern, the following two cases were considered.

- Reinforced concrete beam without any post-tensioning (control beam)

- Reinforced concrete beam with post-tensioning
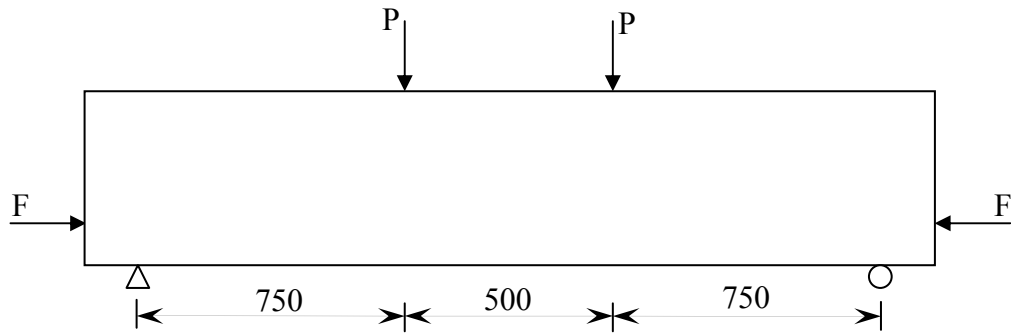
Figure D.1. Simply supported prestressed concrete beam

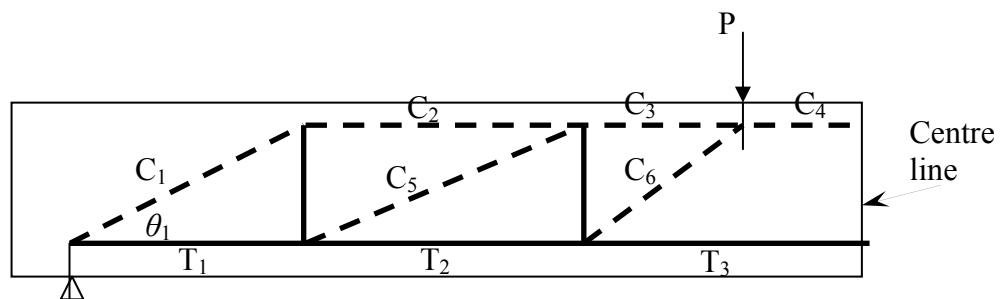Based on the loading arrangements, the strut-and-tie model for the control beam is shown in Figure D.2.

Figure D.2. Strut-and-tie model in non-prestressed beam

As per definition of B- and D- regions, the angle θ_1 is approximately 41.2^0. The detail of calculation is given below.

$$Tan\ \theta_1 = \frac{d}{D} = \frac{263}{300} = 0.876$$
$$\theta_1 = 41.24^0$$

Similarly, the strut-and-tie model of post-tensioned beam is shown in Figure D.3. It has no tension chord at the bottom of the beam (Schlaich et al 1987).
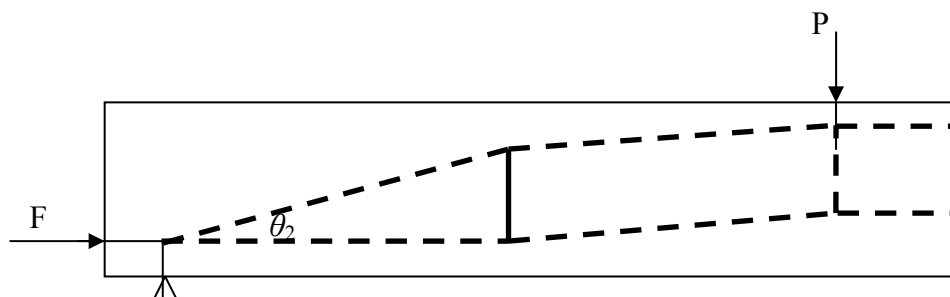
Figure D.3. Strut-and-tie model in prestressed beam (Schlaich et al 1987)

In this case the angle θ_2 is highly depends on the values F and P. However, it can be noted that the angle θ_2 is less than angle θ_1 to satisfy the internal equilibrium.

As the strut-and-tie model provides a rational approach by representing a complex structural member with an appropriate simplified truss model, there is no single, unique strut-and-tie model for most design situations encountered. For the purpose of this study, the above strut-and-tie models were further simplified as shown in Figure D.4.
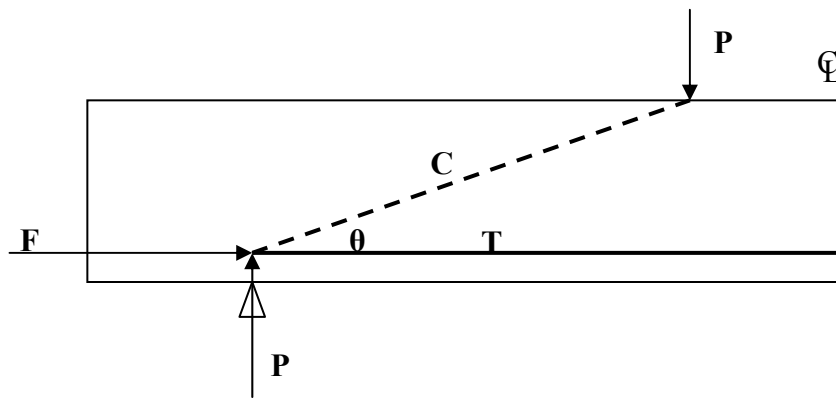
Figure D.4. Simplified Strut-and-tie model in prestressed beam

Based on the experimental results, the crack inclination angle (θ), for the Group 1 and Group 2 specimens are summarised in Table D.1.

Table D.1: Crack inclination angle (θ) predicted by simplified strut-and-tie model

Specimen	Crack Inclination Angle, θ (deg)	
	With Post-tensioning Force	Without Post-tensioning Force
EPT11	N/A	26.6
EPT12	N/A[*]	26.6
EPT13	20.1	N/A
EPT14	18.2	N/A
EPT21	N/A	23.6
EPT22	N/A[*]	23.6
EPT23	18.9	N/A
EPT24	16.7	N/A

* No new crack developed (initial crack re-opened during loading)

The crack inclination angle is reduced by the action of the external post-tensioning force. That means the crack in a post-tensioned reinforced concrete beam will be much flatter than crack in a reinforced concrete beam without any external post-tensioning. This pattern was observed in the specimens tested in this project as explained in Chapter 4. It was clearly observed in epoxy repaired beam as shown in Figure D.5. From this, it can be noted that the strut-and-tie model predictions match well with the experimental results.
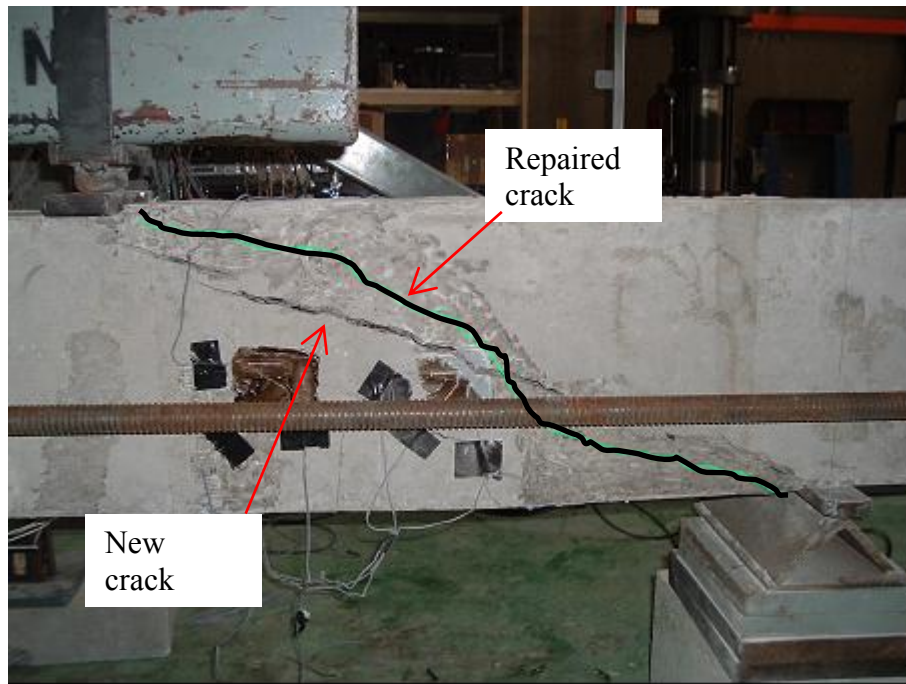
Figure D.5. Failure of EPT13 (Post-tensioned after epoxy repaired)
* Repaired crack is highlighted

References

Schlaich, J., Schaefer, K., and Jennewein, M. (1987). "Toward a Consistent Design of Structural Concrete." *PCI Journal*, 32(3), 74-150.

<div align="right">

Appendix E

PREDICTION OF SHEAR CRACKS

(Supplement to Chapter 6)

</div>

E.1 General

In this Appendix attempted to predict the shear crack in a reinforced concrete beam with and without post-tensioning force. These results will be then compared with the crack pattern used in finite element model as well as the experimental observation.

E.2 Prediction of Shear Cracks Using Computer Program

There are a number of approaches available to predict the shear crack in a reinforced concrete beams. In this appendix the computer program called "Response-2000" developed by Evan Bentz et al. (2001) based on the modified field compression theory (Vecchio, F. J., and Collins, M. P. 1986).

A reinforced concrete beam with cross section 150×300 mm was used in this analysis. Loading and support conditions were given very similar to that used in the experimental program. Input cross section is shown in Figure E.1.
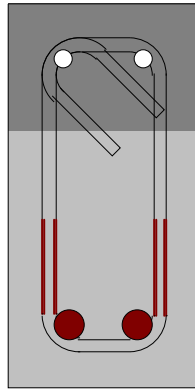
Cross Section

Figure E.1. Cross section of the reinforced concrete beam

E.3   RC Beam without External Post-tensioning

The crack diagram of a reinforced concrete beam without external post-tensioning is given in Figure E.2.
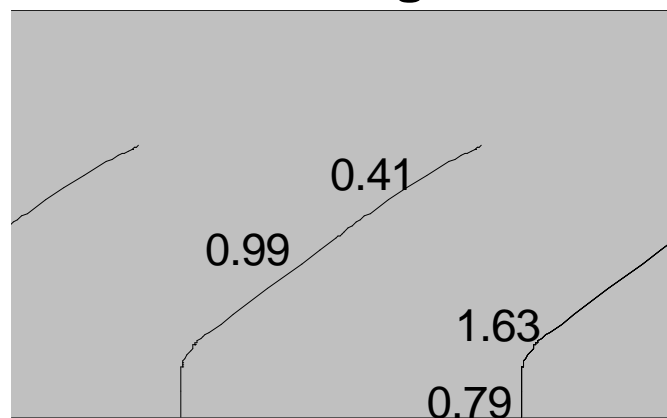
Crack Diagram

Figure E.2. Analytical results of a reinforced concrete beam without external post-tensioning

E.4   RC Beam with External Post-tensioning

The crack diagram of a reinforced concrete beam with external post-tensioning is given in Figure E.3. In this program external post-tensioning was applied as an axial force with a moment (due to the eccentricity of the applied post-tensioning force in the experimental program) to the cross section.

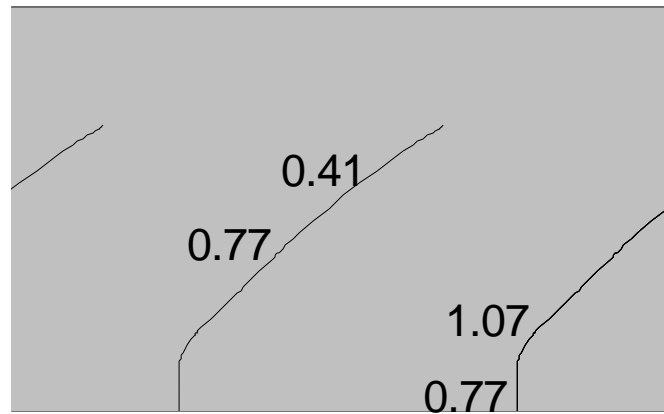# Crack Diagram

0.41

0.77

1.07

0.77

Figure E.3. Analytical results of a reinforced concrete beam with external post-tensioning

From Figure E.2 and Figure E.3and it can be noted that the shear cracks are almost straight lines in the critical regions. It is also noted that the crack width and the inclination of the crack were slightly reduced when external post-tensioning was applied. This result is very similar to the experimental observations discussed in Chapter 4. Even though a number of cracks were predicted in this analysis, some of them were not observed since the Response-2000 is developed based on a simplified strut-and-tie model that may not always match with the experimental results. However, it can be noted that the sum of the maximum crack widths are nearly the same as that observed during the experiment.

References

Bentz, E. (2001). "Response-2000." Toronto, Canada.

Vecchio, F. J., and Collins, M. P. (1986). "The Modified Compression-Field Theory for Reinforced Concrete Elements Subjected to Shear." *ACI Journal Proceedings*, 83(2), 219-231.